Aspects on the Gas
Generation and Migration
in Repositories for
High Level Waste
in Salt Formations

GRS

Aspects on the Gas Generation and Migration in Repositories for High Level Waste in Salt Formations

André Rübel
Dieter Buhmann
Artur Meleshyn
Jörg Mönig
Sabine Spiessl

July 2013

Abstract

In a deep geological repository for high-level waste, gases may be produced during the post-closure phase by several processes. The generated gases can potentially affect safety relevant features and processes of the repository, like the barrier integrity, the transport of liquids and gases in the repository and the release of gaseous radionuclides from the repository into the biosphere. German long-term safety assessments for repositories for high-level waste in salt which were performed prior 2010 did not explicitly consider gas transport and the consequences from release of volatile radionuclides.

Selected aspects of the generation and migration of gases in repositories for high-level waste in a salt formation are studied in this report from the viewpoint of the performance assessment. The knowledge on the availability of water in the repository, in particular the migration of salt rock internal fluids in the temperature field of the radioactive waste repository towards the emplacement drifts, was compiled and the amount of water was roughly estimated. Two other processes studied in this report are on the one hand the release of gaseous radionuclides from the repository and their potential impact in the biosphere and on the other hand the transport of gases along the drifts and shafts of the repository and their interaction with the fluid flow.

The results presented show that there is some gas production expected to occur in the repository due to corrosion of container material from water disposed of with the backfill and inflowing from the host rock during the thermal phase. If not dedicated gas storage areas are foreseen in the repository concept, these gases might exceed the storage capacity for gases in the repository. Consequently, an outflow of gases from the repository could occur. If there are failed containers for spent fuel, radioactive gases might be released from the containers into the gas space of the backfill and subsequently transported together with the gas flow of non-radioactive gases.

The travel time of the gases in the mine strongly depends on the boundary conditions like gas production rate and gas volume in the mine. Therefore, gas generation, its transport and potential consequences have to be regarded in detail in future safety assessments, preferentially by considering two-phase flow of the gases in the long-term safety assessment codes. To do so, the according codes and a data basis for the two phase flow parameters of salt grit have to be developed in the future.

Table of contents

1   Introduction

In a deep geological repository for high-level waste, gases may be produced during the post-closure phase by several processes. The generated gases can potentially affect safety relevant features and processes of the repository, like the barrier integrity, the transport of liquids and gases in the repository and the release of gaseous radionuclides from the repository into the biosphere. The most important gas generation process is the anaerobic corrosion of iron which is emplaced in large amounts as waste container material. Additionally, microbial degradation of organic matter and radiolysis may contribute to the gas generation.

The anaerobic corrosion of iron and most of the other gas generation processes depend on the availability of water, which is consumed during the processes and whose amount is expected to be limited in a repository for high level waste in salt[1]. The prerequisites for gas generation are usually given for both, the normal, undisturbed system evolution of the repository as well as for disturbed evolutions which cannot be ruled out. The system evolution however, influences the gas production rate and/or the absolute amount of gases generated and therefore also the resulting consequences.

While the radioactive gases are of relevance due to their potential radiological consequences in case of the existence of a gas pathway to the biosphere, non-radioactive gases act as carrier gas for transporting radioactive gases and might also be important because of their potential pressure related impacts on the engineered barrier system and the geological host formation. Mitigating these various issues to be regarded presents the designer with a possible conflict of goals: While radioactive gases are subject to the strategy of confinement, non-radioactive gases may need to be dissipated to minimize the pressure build-up in the repository system. Options that can be taken into account to resolve this issue are the storage of the non-radioactive gases in the repository system or minimisation of gas production by design – e. g. by choice of container materials.

German long-term safety assessments for repositories for high-level waste in salt which were performed prior to the preparation of this report, did not explicitly consider

---

[1]   The information given in this report applies to high-level radioactive waste repositories in salt formations for which the short term "waste repository" is used in the following.

gas transport and the consequences from release of volatile radionuclides. First attempts to do so are done within the "Vorläufige Sicherheitsanalyse Gorleben (VSG)" /LAR 13/ to which the work presented here served as additional input.

In this report, selected aspects of the generation and migration of gases in repositories for high-level waste in a salt formation are studied from the viewpoint of the performance assessment. The selected aspects are:

− the availability of water in the repository, in particular the migration of salt rock internal fluids in the temperature field of the radioactive waste repository towards the emplacement drifts,

− the release of gaseous radionuclides from the repository and their potential impact in the biosphere and

− the transport of gases along the drifts and shafts of the repository and their interaction with the fluid flow in a two-phase flow process.

The listed topics are discussed in the following three chapters of the report. The fifth chapter summarizes implications for integrated performance assessment.

2　　　Brine migration in rock salt formations

Rock salt is envisaged as potential host rock for repositories for high-level radioactive waste in Germany. The safety concept for such repositories /MOE 12/ is based on the containment of the radionuclides in a part of the salt host rock formation, the so called isolating rock zone (ewG)[2]. One essential pillar of the containment concept is to prevent or at least to minimise the contact of water with the waste for different reasons:

−　Prevent the mobilisation of the radionuclides and also the transport in the liquid phase from the waste container and/or the matrix.

−　Minimize the generation of gases resulting from the corrosion of the steel waste containers or the degradation of organic material to

- prevent high gas pressures that potentially jeopardize the integrity of the salt rock barrier and

- minimize the generation of non-radioactive gases which may act as a carrier gas for gaseous radionuclides (see chapter 2).

Therefore, it is aimed for minimising the gas production by minimising the availability of water in the repository.

Three potential sources of water have to be taken into account in a repository for high-level waste in rock salt, which are:

−　**Brine inflow from the overburden:** Two requirements are given in the safety concept of a waste repository in salt to avoid a relevant impact of fluid inflow from the overburden on the long-term safety. The first one is that the envisaged salt formation itself shows no potential flow paths for brines from the overburden into the ewG.

The second one is that the shaft and drift seals prevent the fluid inflow in the short-term, while in the long-term, mined spaces in the repository which are backfilled with salt grit close by salt creep so that the compacted salt grid has a permeability low enough to avoid significant water inflow to the waste emplacement sites. Both

---

[2]　In German: ewG = "einschlusswirksamer Gebirgsbereich"

requirements have to be demonstrated as part of a long-term safety assessment of a future waste repository.

– **Emplacement of moisture along with the waste or the backfill:** The emplacement of liquid wastes is not foreseen in the German concepts of radioactive waste repositories. However, small amounts of water might be emplaced as moisture along with the waste itself or with the backfill. Especially the latter can be of importance due to its large amount and the fact that a small moisture content of the salt grit cannot be completely avoided. As part of the safety concept for a waste repository in salt it is planned to at least minimise the water emplaced in the repository by using salt grit as dry as possible in areas close to the emplaced waste.

An emplacement drift with a mean cross section area[3] of about 15.8 m^2 is backfilled with an amount of 238 000 kg of salt grit per meter of drift length[4]. With an initial water content[5] of the salt grit of 0.02 %$_{wt}$, an amount of 4.42 kg of emplaced H_2O is calculated per meter of drift length. Investigations in /SCO 98/ suggest that this water can be consumed by corrosion at a rate[6] of 0.2 kg·a^{-1}.

– **Migration of brine from the host rock to the waste:** Although salt is often denoted as a "dry" rock, small amounts of brine are a ubiquitous part of the natural occurring material components to be found in salt deposits. The Hauptsalz of the Staßfurt series[7] (z2HS) of the Gorleben salt dome for example has a water content of 0.0164 %$_{wt}$. Multiple experiments applying a thermal load on the salt rock have shown that at least part of this water might be released from the host rock to the emplacement sites.

The first two of the three mentioned water sources can be avoided or at least minimised in a future waste repository by a proper investigation of the host rock or by de-

---

[3] A representative section of the emplacement drift consists of a 2.63 m long part with a cross section of 17 m^2 and a 5.46 m long part where the cross section is reduced by 2 m^2 due to the container.

[4] The following values are used for the estimation: The density of rock salt is 2 165 kg·m^{-3} and the initial porosity of the salt grit backfill is 35 %, resulting in an initial salt grit density of 1 400 kg·m^{-3}.

[5] The assumed water content of 0.02 %$_{wt}$ for the salt grit is close to those of the salt rock itself. This requires that the salt grit is not stored for long time and has to be regarded as lower boundary value.

[6] The water consumption rate was calculated from a measured corrosion rate of 2 μm·a^{-1}, a surface of a Pollux container of 30 m^2, a density of iron of 7 800 kg·m^{-3} and a consumed amount of water of 0.43 kg$_{H2O}$/kg$_{Fe}$.

[7] In the following the term "Hauptsalz" is used shortly for the Hauptsalz of the Staßfurt series (z2HS).

sign. The importance and potential implications resulting from the migration of brine in the host rock of a repository for high-level radioactive waste in salt are discussed in the following chapter of this report.

Many different laboratory and in-situ experiments as well as theoretical considerations have been carried out to assess the amount of water in salt rock and its potential migration mechanisms; most of them during the 1970's and 80's. This chapter summarises the – to our point of view – most important results of these studies and tries to give an estimation for the brine migration to be expected in a potential repository at the German Gorleben site.

The different types of water naturally occurring in salt rock formations are described in the following section. The second section discusses the different types of migration processes and finally in the third section the information is adopted to the situation at the German Gorleben site. Due to the large amount of relevant literature, the references section also gives additional literature not cited in the text, but which is useful for further background information.

2.1 Types of internal water in rock salt formations

As mentioned before, water is part of the natural material content of a salt rock body. The water can be present in different physical and chemical states which are described in the following. It has to be noted that the actual types of water occurrences in a salt rock body is very site specific. Not all types of water are necessarily present at every site and the overall water availability can also vary over a large scale. Usually, the overall water content of bedded salt is higher than in a salt dome. The different types of water are:

–   **Hydrated minerals:** Besides the water-free types of salt like halite (sodium chloride, NaCl) or sylvite (potassium chloride, KCl), there also exist some types of salt minerals that are hydrated and therefore contain more or less amount of water according to their mineral formulae.

Important examples for these types of minerals are in order of increasing water content: kieserite, polyhalite, carnallite and bischofite. The water is bound in the

mineral structure and is not released under natural conditions[8]. However, all water containing salt minerals have a specific critical temperature of stability; when heated above this temperature, the mineral starts to dehydrate. The critical temperature is dependent on the pressure and is given in table 2.1 at atmosphere pressure for the mentioned minerals along with their mineral formulae.

Thermal output of the high level waste forms emplaced in salt rock increases the rock temperature. However, the dehydration of salt minerals and the subsequent release of the water to the emplacement sites are to be avoided. Therefore, two measures are possible against the dehydration of salt minerals.

The first possibility is to keep a sufficient distance between the emplacement areas and layers with high content of hydrated salts with low dehydration temperature. At the Gorleben site, the emplacement of the waste is foreseen in the Hauptsalz in the central part of the salt dome, which consists to more than 95 % of halite and some anhydrite or more seldom, polyhalite /BOR 08/. Carnallite is found in specific strata in the outer parts of the salt dome (e. g. z3LS). A sufficient safety distance is foreseen in the repository concept to prevent the dehydration of the carnallite.

The second possibility is to limit the amount of emplaced waste per volume of salt rock in such a way that the thermal load of the salt rock is limited. The German safety concept for a repository for high-level waste in salt limits the maximum temperature in the salt rock to a value of 200 °C. This limit is accounted for in the repository layout and ensures that there is no dehydration of polyhalite and kieserite.

It is assumed that the measures taken in the repository concept will prevent the dehydration of hydrated salt minerals in a potential high-level waste repository at the Gorleben site. Therefore, this type of water is not further considered in the following.

− **Intracrystalline water** (fluid inclusions): Water in rock salt is denoted as intracrystalline water, if the water volume is fully surrounded by one single salt grain. This type of water is also called fluid inclusion in the literature and in the following text.

Fluid inclusions are usually several tens of micrometres in size, but can reach up to millimetre size. According to microscopic examinations /JOC 81a/, fluid inclu-

---

8 One possibility how the hydrated water might be released is the contact with a solution which is undersaturated by the respective mineral and a subsequently dissolves the mineral. Since this is expected only under disturbed evolution scenarios of the repository, this case is not considered in the following.

sions usually are not equally distributed in the salt rock, but are found in accumulations. Fluid inclusions can be distinguished in three different types according to the type of fluid contained:

- fully filled with liquid,

- filled with a combination of liquid and gas or

- fully filled with gas.

The last type mentioned is not of further interest in this context. The migration of fluid inclusions is described in section 2.2.1.

− **Intercrystalline water** (brine filled "pores"): The water in rock salt in the following denoted as intercrystalline water is the small amount of water residing between different salt grains.

A thin film of water can be found on salt grain surfaces. Classical porosimetry measurements with mercury injection and gas adsorption suggest a mean pore size of a few nanometres for the examined salt rock samples /DEL 97/. It has been a subject of discussion, whether that film of water is interconnected like it is in a porous medium and whether transport can occur in this pore space or not. While the successful carrying out of porosimetry measurements already show a connectivity of at least part of the pore space, considerations on the dihedral angle in halite crystals and the effect on the pore connectivity suggest that „a water content of 9 – 46 ppm is sufficient to wet virtually all grain boundaries" /TER 05/, /LEW 96/.

Measurements of the self-diffusion of the water in the pore space /FRI 00/ and measurements of its helium content /RUE 00/ further suggest, that a diffusion of the water and substances dissolved in the pore water of rock salt is possible with a low diffusion coefficient[9] in the order of 10^{-11} m$^2 \cdot$s^{-1}. This value is also in the range of values indirectly derived in /WAT 02/ from the electrical impedance of halite under confining pressure. The diffusion coefficient was estimated to depend on the thickness of the intercrystalline water film layer to be 10^{-13} to 10^{-11} m$^2 \cdot$s^{-1} for a thickness ranging from 1 to 10 nm.

---

[9] The self-diffusion of water does not imply that an effective transport of other substances is possible in this water film. First, the diffusion coefficient was found to be a very low value. Second, the diffusing of substances other than water or helium might be hindered by interaction with the charged salt surface and third, the low porosity of the salt only allows for a very small mass flux.

The migration of intercrystalline water is described in section 2.2.2.

– **Large volume brine reservoirs:** Besides the rather finely distributed water occurrences described before, most salt rock bodies here and there also contain large volume brine reservoirs.

In the Gorleben salt dome, several brine reservoirs have been found from which brine has drained with volumes ranging from 10 to 160 m^3. The actual sizes of the brine reservoirs were derived from pressure tests to be even higher. Maximum values of up to a few 1 000 m^3 were estimated /BFS 02/. All large volume brine reservoirs found in Gorleben up to date, were located in specific strata, i. e. the Hauptanhydrit, Mittlere Orangesalz (Gorlebenbank) and the Anhydritmittelsalz. No brine reservoir has been found so far in the Hauptsalz, which is foreseen for the emplacement of the waste. According to the repository concept, a sufficient safety distance is foreseen between the emplacement areas of the repository and those strata where large volume brine reservoirs have been found. Therefore, those brine reservoirs are not discussed in detail in the following, but a few remarks are made at the end of the chapter 2.2.1 on the migration of fluid inclusions.

The determination of the water content of salt rock and the classification into one of the listed categories is a task with many potential pitfalls /ROE 81/. The most common method for the measurement of the water content is thermo-gravimetry, i. e. the loss of weight of rock samples is determined at elevated temperatures. Since it is possible to release all water from a salt rock sample by using very high temperatures, care has to be taken to stepwise increase the temperature in a way as not to release hydrated water or at least to notice that. Furthermore, the sample should not be disturbed in a way that no distinction can be made between inter- and intracrystalline water (e. g. by crushing the sample).

Other methods used are the Karl-Fischer titration /JOC 81a/, which is not able to distinguish between intra- and intercrystalline water and the diffusive exchange with tritium /FRI 00/, which only accounts for intercrystalline water. The following discussion will show that in most cases a distinction between intra- and intercrystalline water is not crucial for the estimation of the amount of water that might migrate towards emplaced radioactive waste.

It has to be mentioned that the experimental determination of the water content from rock samples only shows a snap-shot of a changing distribution in time. This especially

is true for the proportion of intra- and intercrystalline water. The application of stress and thermal load on rock salt can lead to a significant recrystallization of the salt grains including a grain boundary movement /URA 86/. The grain boundary movement can lead to two concurring processes depending on the movement velocity; this the formation of new fluid inclusions from intracrystalline water as well as the release of fluid inclusions into the grain boundaries /SHM 10/.

Tab. 2.1   Water containing salt minerals

Name	Chemical formula	Critical temperature at p = 0.1 bar [°C]	Reference
Kieserite	$MgSO_4 \cdot H_2O$	280	/JOC 81b/
Polyhalite	$K_2Ca_2Mg(SO_4)_4 \cdot 2\,H_2O$	230 – 280	/ROT 86/, /JOC 81a/
Carnallite	$KMgCl_3 \cdot 6H_2O$	80 – 170	/ROE 81/
Bischofite	$MgCl_2 \cdot 6H_2O$	155 – 220	/JOC 80/

2.2   Migration processes for water in rock salt

This section describes the potential migration mechanisms for intra- and intercrystalline water and briefly also for large brine reservoirs. The main aspects can be summarised shortly as follows:

Intercrystalline water migrates either as liquid if a hydraulic force is applied or as vapour if the water is evaporated. The hydraulic forces resulting in a migration in the liquid phase can be either due to the thermal expansion of the water and/or the rock salt or by other changes in the principal stress in the salt rock.

The migration in the vapour phase requires a thermal input high enough to effectively evaporate the intercrystalline water. Fluid inclusions migrate if a temperature gradient is applied to the salt rock. They migrate short distance to the next grain boundary and are released into the intercrystalline water. Any further migration will mainly follow the same path as for intercrystalline water initially present.

In a high-level waste repository, the main mechanism relevant on the long-term is likely the migration of intercrystalline water in the vapour phase. This mechanism is limited to

the first several hundred years after the waste emplacement, when the temperatures are elevated (thermal phase). Some short term effects might result from migration in the liquid phase due to the fast temperature increase close to the waste directly after its emplacement. Fluid inclusions will be released to the intercrystalline pore network and migrate there. No distinction between inter- and intracrystalline water has to be made to estimate potential long-term water inflow into an emplacement area for high-level waste.

2.2.1 Migration of fluid inclusions

Many different experiments have shown that fluid inclusions are moving in a thermal gradient field, e. g. /ROE 80/, /OLA 84/ and that this movement might be relevant under conditions expected in the vicinity of a high-level waste repository in salt. As mentioned above, two types of fluid inclusions are relevant here, filled with brine or filled with brine and gas, while the former type seems to be the more common. The migration behaviour of those two types of fluid inclusions differs in a way that filled fluid inclusions completely filled with fluid migrate towards the thermal source, while the ones filled with a gas/fluid mixture tend to migrate in the opposite direction.

The principal cause for the migration is the temperature dependent solubility of salt in water and the temperature difference at both sides of the fluid inclusion. The theory of the transport process was invented in the 1970's /ANT 71/ and further developed in the 1980's at the Batelle Institute /OLA 80/, /OLA 84/, /MCC 87/. It seems to be well understood and is widely accepted. The process steps during migration of fluid inclusions completely filled with fluid are as follows:

1. Dissolution of salt at the warmer surface of the fluid inclusion due to the increased solubility.

2. Migration of the dissolved salt through the inclusion towards its cooler side due to the concentration gradient in the brine.

3. Crystallisation of the transported salt at the cooler site at supersaturation.

As this process is continuing as long as the temperature gradient exists, the brine inclusion will slowly migrate through the salt grain towards the heat source.

In fluid inclusions partly filled with gas, there are two concurring processes. The first one is as described above and the second one is as follows: Due to the higher water vapour pressure at the hot side of the inclusion, water is evaporated there, and is condensed on the colder side. The evaporation of brine at the hot side results in a precipitation of salt, there. If the fraction of the gas volume is greater than 10 %, the overall process is driven by the comparably fast vapour transport in the gas phase. In that case, the fluid inclusion is moving away from the heat source.

The migration velocity v of a fluid inclusion completely filled with fluid is described by the following equation /OLA 80/:

$$v\rho_s = \frac{D}{L}(C_s^h - C_s^c) - \sigma D C_s^m \nabla T \qquad (2.1)$$

with

ρ_s density of the salt rock (2 165 kg·m^{-3}),

C_s salt concentration in the inclusion at the hot side (superscript h), cold side (superscript c) and mean concentration in the inclusion (superscript m),

σ Soret coefficient (-2·10^{-3} °C^{-1} for NaCl brine at 50 °C),

L dimension of the fluid inclusion in direction of the thermal gradient,

D diffusion coefficient of the salt in the brine (2.6·10^{-9} m^2·s^{-1} for NaCl brine at 50 °C),

∇T temperature gradient in the brine.

This formula assumes an instantaneous dissolution and crystallization of the brine at the hot side and the cold side, respectively. As this assumption is not true, kinetic terms are added for different kinetic relationships in /OLA 84/. Besides the temperature gradient itself, other parameters do influence the inclusion velocity, most of them by affecting either the salt solubility or the effective temperature gradient across the fluid inclusion. The most important parameters are:

– Absolute temperature: due to an increase of the solubility, the fluid inclusion velocity increases with temperature.

– Inclusion size: due to changes in the effective temperature gradient, large fluid inclusions tend to move faster than small inclusions.

However, there exists a criterion depending on the fluid inclusion size and its migration velocity, that if exceeded, the liquid inclusion disintegrates into several smaller ones /ANT 73/. This is supposed to be due to the difference in the thermal gradients in the centre and the edges of the fluid inclusion.

– Shape of fluid inclusion relative to the temperature gradient: the orientation of the fluid inclusion determines the effective temperature gradient.

Fluid inclusions tend to change their shape during movement. Both, flattening in a plane normal to the temperature gradient /CLI 72/ as well as elongation in direction to the temperature gradient /ROE 80/ has been observed.

– Dissolved solids in the fluid inclusion: the dissolved solids affect the solubility.

– Crystal orientation and dislocations in the crystal lattice: these two parameters may add an additional transport resistance to the fluid inclusion.

In principle, there exist limits in the size of the fluid inclusion and in the temperature gradient, that cause the movement of the brine inclusion to stop, if the actual values fall below one of the limits. The existence of such a limit is evident from the fact that fluid inclusions do exist in salt rock bodies despite the natural geothermal temperature gradient. However, the actual values for these limits are hard to predict. It will be assumed in the following that the movement of the fluid inclusions does take place under the conditions relevant in a high-level waste repository during the thermal phase.

Results from migration experiments /LAM 80/ as well as theoretical considerations about the grain boundary tension /JEN 79/ show that the migration will slow down, or even fully stop when the fluid has moved into a grain boundary. Therefore, it can be assumed that nearly all fluid inclusions will finally end up in the intercrystalline water, if the thermal gradient exists for a sufficiently long time.

Different laboratory experiments have been carried out to study the transport velocity of fluid inclusions in single salt crystal samples. An overview of some of the results for halite is given in table 2.2 in terms of the maximum migration velocity in centimetres per year for a thermal gradient of one degree per centimetre. The experimental results have to be treated with some care, since the actual boundary conditions like the applied thermal gradient differ quite much. Nevertheless, those results give a good overview for the range of the velocities to be expected.

The data obtained from Bradshaw & Sanchez /BRA 68/ has been used by Jenks /JEN 79/ to obtain an exponential fit function, which was used quite often in later numerical modelling studies. The function was fitted to give an approximation of the upper boundary of the experimental values. According to this function, the fluid inclusion velocity v in centimetres per year is given by:

$$v = \nabla T \cdot 10^{0.00656 \cdot T - 0.6036}$$
(2.2)

with

T temperature of the salt [°C],

∇T temperature gradient in the salt [°C/cm].

As can be seen from table 2.2, the values given by Bradshaw are much higher than those obtained by other authors and therefore, the function given by Jenks might overestimate the fluid inclusion velocity considerably. Additionally, the data by Bradshaw shows a wide range of scatter, which results in the Jenks function to be highly undetermined. From our point of view we agree to the statement in /ROE 82/ that the formula given by Jenks has neither a theoretical basis nor is it based on data that is appropriate to yield an empirical relationship. Therefore, the formula from Jenks should not be used[10].

The data given in table 2.2 shows that even if the lowest values are taken into account and a nominal salt grain size of 1 cm is assumed, all fluid inclusions will be swept out of the salt grain into the intercrystalline water after a few tens of years[11]. From this fact it follows that the exact knowledge about the migration behaviour of intracrystalline water through salt grains (i. e. over a distance of a few centimetres at maximum) is of low relevance for the knowledge about the total long-term brine migration towards the emplaced high-level waste in a repository.

---

[10] The formula given by Jenks sometimes even has been used to model water movement over distances larger than the grain size. This should not be done in no case, since the Jenks formula applies only for intracrystalline water. Any agreement of numerical modelling using Jenks formula and laboratory migration experiments of water in bulk rock salt samples is only by chance.

[11] As mentioned above, the migration of grain boundaries on the other hand may result in the formation of new fluid inclusions.

In the following it will be assumed that all fluid inclusions are released from the grains into the intercrystalline space during the thermal phase. Since the migration of the intercrystalline water (see next section) is faster than those of the intracrystalline water, this is a conservative assumption with regard to the migration velocity.

Tab. 2.2   Maximum fluid inclusion velocities in rock salt as function of temperature

Reference		Temperature [°C]	Velocity [cm·y^{-1} / °C·cm^{-1}]
Bradshaw	/BRA 68/	85	0.5
		115	2.9
		160	2.3
		190	4.4
		200	6.8
		240	7.6
Olander	/OLA 80/	50	0.01
		100	0.06
Roedder	/ROE 80/	100	0.8
		150	1.1
		200	0.9
Olander	/OLA 84/	65	0.04

Remark: Some of the data was derived by metering from figures in the given literature. Therefore, the values can only be taken as rough indication.

As mentioned before, there also exist large volume brine reservoirs in salt rock formations. At the Gorleben site, those brine reservoirs are only found in distinct strata which are at least 50 m away from the planned emplacement areas. No literature information was found about models or not even principle ideas on the migration of such reservoirs in the temperature gradient field. Although these large volume brine reservoirs reside in open fissure networks and are therefore inter-, not intracrystalline water, it is imaginable that the principle transport mechanism described for very small brine inclusions is also an option for large scale reservoirs, i. e. the dissolution of salt on the hot side of the reservoir and the crystallization at the cold side.

If we assume the transport process to be valid for large scale reservoirs, we can use equation 2.1 to give an estimate for their migration velocity. If we further assume a brine reservoir of 1 m in diameter, a mean rock temperature at the location of the brine

reservoir of 60 °C and a temperature gradient of 1 K·m^{-1}, we obtain a mean solubility[12] of NaCl of 324,5 kg·m^{-3} and a solubility gradient of 0.24 kg·m^{-3}. Using the other parameter values as given above, we obtain a migration velocity of the brine reservoir of 3.4·10^{-5} m·a^{-1}. It is obvious that this migration velocity is completely irrelevant, even on the long-term scale[13].

2.2.2 Migration of intercrystalline water

The water residing in the intercrystalline pore space can be transported in two different phases, either as liquid or as vapour, if the brine is evaporated during the thermal phase of the repository. In that case, the transport is driven by water vapour pressure gradients, i. e. gradients of the water vapour concentration. The transport of water as liquid occurs due to hydraulic gradients in the brine, which can also result without applying a thermal load. Both transport processes are described in detail in the following:

Migration in the liquid phase

The transport of brine in the liquid phase usually happens due to hydraulic gradients in the brine itself. According to the Darcy law, the brine flow is proportional to the hydraulic gradient[14]. For the situation regarded here, the hydraulic pressure gradients in the brine can result from two different reasons which are either an external force transmitted by the rock matrix due to elastic or plastic deformation or an internal force due to an expansion of the fluid.

An external stress applied to the rock matrix can result in an elastic or plastic deformation, which further results in a compaction of the pore space. Due to the creep behaviour of the salt rock, the pressure of the brine in the interconnected pore space is

---

[12] According to /GEV 81/, the solubility L of NaCl in water in [‰$_{wt}$] is given as a function of temperature T in Kelvin by the formula $L = 32.161 - 0.05071 \cdot T + 0.000106 \cdot T^2$.

[13] One might notice that this value is lower than the ones given in table 2.2, which seems to contradict the statement that larger fluid inclusions should move faster. This is because although the temperature gradient as driving force is increasing linearly with the size, the time needed to transport the solutes from one side to the other by diffusion increases quadratic with size. Therefore, there exists a critical size; if exceeded, the fluid inclusion will start to move slower with increasing size.

[14] It is most likely that the Darcy law is not valid for rock salt, because a strong interaction between the transported fluid and the rock matrix surface, so the assumed linearity between the pressure gradient and the transport velocity is not valid.

closer related to the stress in the salt rock than in other porous media, where the stiffness of the rock matrix transmits only a portion of the applied force on towards the pore water. Two types of models are used to describe the water flow resulting from external stress applied to the rock matrix:

−   The first type of model is a model of either elastic or plastic compaction. The resulting water flux is equivalent to the change in pore volume which is furthermore governed by rock properties and the geometry of the pore space. An overview of some equations for the deformation for different pore geometries is given in /SCH 86/.

−   The second type of model is the stress-gradient model and the resulting transport is described in /SHE 82/. Under the assumption that the fluid pressure in the pores is equal to the rock stress, a gradient in the rock stress leads to a hydraulic gradient and a water flow. The cause of the stress in the salt rock can be either due to mechanical reasons, like a change in the superimposed load or mining activities, or due to a thermal input and a resulting expansion of the salt rock.

The thermal expansion applies not only to the rock matrix itself, but to an even greater extent to the brine in its pore space. Figure 2.1 shows the change of the specific volume of rock salt and saturated NaCl brine compared to their specific volume at 50 °C according to data given in /GEV 81/. It can be clearly seen that the effect of the thermal expansion for the brine is much stronger than for the rock salt itself. Therefore, it is concluded that the thermal expansion of the brine is more relevant for the transport of the brine than the thermal expansion of the rock salt.
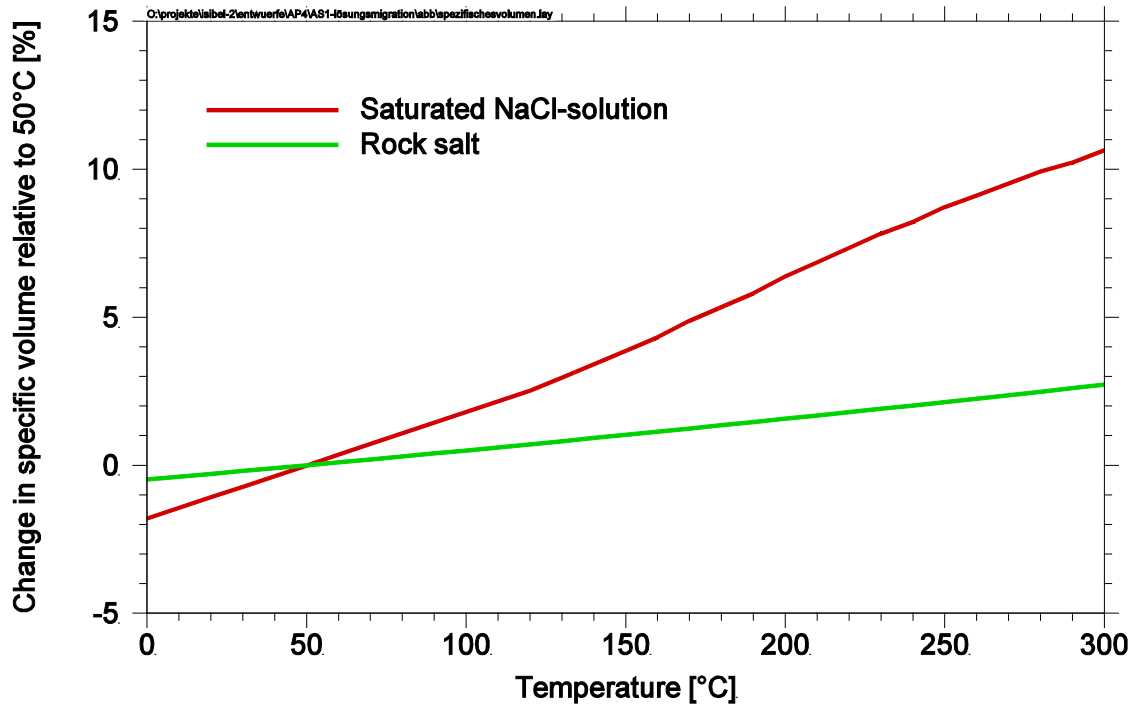
Fig. 2.1   Change in the specific volume of saturated NaCl brine and rock salt rela-
tive to their specific volume at 50 °C

Laboratory and in-situ experiments in which a thermal load has been applied to rock
salt have shown increased rates of extruding water during the transient phases of heat-
ing and even more pronounced during phases of cooling down (e. g. /HOH 80/). The
results from modelling of the transient phases of such experiments suggest that the in-
creased outflow of brine is due to the flow in the liquid phase. During the heating phase
the increase of the outflow is likely due to the expansion of the pore water as discussed
above and during cooling phase it is due to mechanical stress changes in the rock salt.
The latter however applies only to a fast cooling down in laboratory experiments and is
not expected under repository conditions. In /SCH 86/, a good agreement has been
found between the short-term water extrusion from heated rock salt during the heating
phase and a model taking into account the thermal expansion of the water.

Although the water migration as liquid during the transient phase of the heating of the
rock salt is important to explain increased flow rates observed in experiments, it seems
to be of lower relevance when considering the total amount of water flowing in from the
salt rock formation into an emplacement site on the long-term scale. Some experi-
mental evidence for this statement will be given in section 2.2.3. The most relevant
process for the long-term mass flux of water is most likely the migration of water in the
vapour phase which is described in the following.

Migration in the vapour phase

If the thermal load applied to the rock salt will elevate its temperature to above 100 °C, it is likely that water will evaporate at the rock salt surface of the emplacement drift or borehole, since the salt grit in the emplacement area is initially unsaturated and at atmospheric pressure. The water vapour will be transported along the water vapour pressure gradient from the salt rock into the drift and the evaporation front will progress deeper into the rock salt body.

The driving mechanism of this process is the gradient in the water vapour pressure between the evaporating front and the emplacement area, and the process can continue as long as the water vapour pressure in the emplacement area is low. While /SCH 86/ argued that the process will stop as soon as the pore volume in the salt grit is low, it is assumed that the process will continue as long as corroding material exists in the emplacement area that consumes the inflowing water vapour. The corrosion process is acting as water vapour sink that preserves the pressure gradient.

A mathematical description of the evaporation front model was developed by Hadley in /HAD 82/ and /HAD 80/. The flux of the water j is given by:

$$j = -nD_k \frac{N_A}{RT} \frac{\partial p}{\partial z} - \frac{k}{\mu} p \frac{N_A}{RT} \frac{\partial p}{\partial z} \tag{2.3}$$

with

n	porosity,
D_k	Knudsen diffusion coefficient,
N_A	Avogadro number,
R	gas constant,
T	temperature,
p	vapour pressure of the water,
k	permeability of the rock salt and
μ	viscosity of the fluid.

The first term in equation 2.3 denotes the diffusive transport and the second one the advective transport. Due to the very low permeability of the salt rock, the advective term can be neglected compared to the diffusive one. Due to the very small pore size and the low density of the water vapour, the diffusion process is expected to be of the

Knudsen type, i. e. the transport process is determined by the collision of the water molecules and the pore wall rather than by the water molecules with each other[15]. The application of this model to laboratory and in-situ experiment was found to result in a good agreement of the model results with the experimental results for the water outflow from heated salt /HAD 81/, /SCH 86/.

It is most plausible that this transport process is responsible for the long-term water migration from heated rock salt bodies and therefore it was applied for the following estimating calculations. One reason to concentrate on this transport mechanism is that it is the only one of the considered mechanisms that is able to transport the brine over long distance and its driving force is maintained over the relevant time span of about 1 000 years. Another reason is that the good agreement between experimental data and modelling results.

2.2.3 Results from selected experiments

This section very briefly describes the layout and results of a few laboratory and in-situ experiments which were found to be important for an evaluation of the relevance of the different transport mechanisms. It has to be noted that although the different processes described in the preceding sections result in water migration in different phases, the presented experiments all determine the water release by freezing water from the vapour phase. Therefore, the determined amount of water is pure water. Due to this procedure it unfortunately can't be concluded from the chemical composition of the water, which one was the most relevant transport process.

Salt-Block-II laboratory experiment

The Salt-Block-II experiment was a large-scale laboratory experiment conducted around 1980 and its layout, experimental and modelling results are described in /HOH 80/, /HAD 81/. In the experiment, a rock salt cylinder of 1 m in diameter and height was heated through a central borehole while the temperature at the outer boundary was controlled by water cooling.

---

[15] In strict terms, this means that the free particle path is larger than the mean pore size.

This experiment is of special interest in so far, as the model developed for the water migration in the vapour phase for a small-scale laboratory experiment /HOH 79a, HOH 79b/ was also used with the same set of parameters to model the results from the Salt-Block-II experiment, yielding reasonable results. Therefore, the modelling of the Salt-Block-II experiment has shown that the upscaling of the water vapour migration model seems to be valid – at least in that case. Some of the Salt-Block-II experimental results and its modelling are shown in figure 2.2. It can be seen that the modelling utilising the vapour migration model shows a reasonable fit to the experimental data. Results obtained for the migration of fluid inclusions according to Jenks equation are also plotted in figure 2.2. It is obvious that this model data is not able to describe the experimental results.
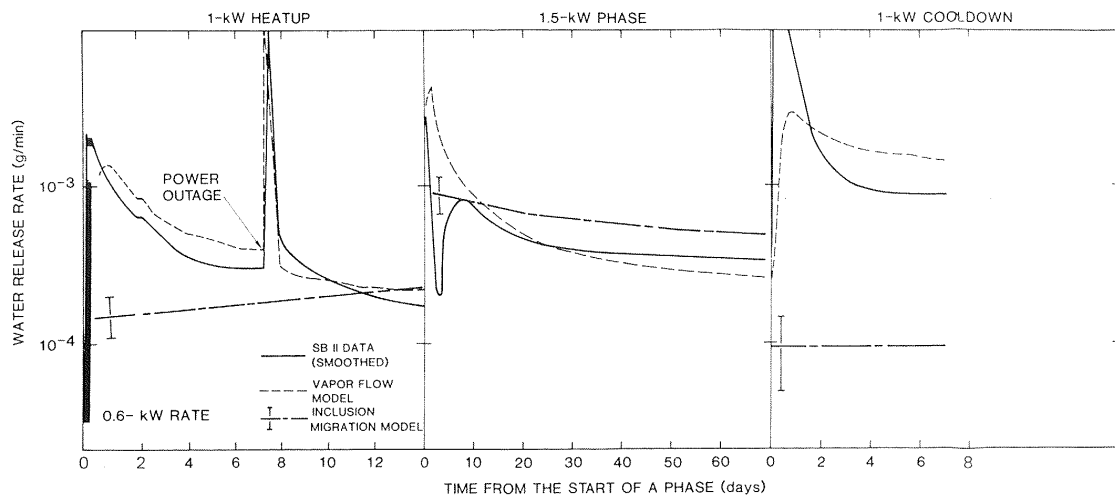
Fig. 2.2   Experimental and modelling results of the Salt-Block-II experiment /SHE 82/

TV5 – in-situ test at the Asse mine

The in-situ experiment "Temperaturversuch 5" (TV5) was carried out in the Asse salt mine at the beginning of the 80's. The layout and the experimental results are described in detail in /ROT 86/. A heater of about 3 m in length was placed into a borehole of about 7 m in length. The initial diameter of the borehole was 0.28 m. The electrical power of the heater was increased stepwise during the experimental duration of 300 days. The temperature in the rock was measured at different locations in the salt rock and a comparison with the results from a thermo-mechanical model has shown an excellent agreement (see figure 2.3).

20

The inflow of water from the salt rock to the borehole was determined by flushing the borehole 10 times a day with a helium atmosphere and freezing the water vapour in a cold trap. Figure 2.4 shows the inflow rate and the cumulated inflow of water into the TV5 borehole. As some of the water was believed not to come from the salt rock, but from other sources, the cumulated mass was corrected down by 100 g for the modelling. The corrected data is shown as open circles in figure 2.4. The shaded areas in figure 2.4 denote the different steps in the heater power. It is clearly visible that an increase in the heater power results in an immediate response in the inflowing rate. After the fourth increase of the heater power after about 180 days, the temperature exceeded 200 °C at the salt rock surface. At least part of the water released afterwards is believed to stem from dehydration of polyhalite. Therefore, the modelling of the temporal evolution of the water inflow was only performed for the first 150 days.

An intensive modelling of the water inflow has been performed in /SCH 86/ using different models including vapour diffusion, Darcy flow, matrix compaction, stress gradients and thermal fluid expansion. The best fit to the experimental data was obtained from the vapour diffusion model under the consideration of some thermal expansion of the fluid (see figure 2.5). Using only pure vapour diffusion (line PKO in figure 2.5) in the model, the general trend of the inflow rate is in good agreement, but the initial increase after changing the heater power is underestimated. A better agreement is found if the thermal fluid expansion of the brine is regarded (shown as lines $c_a = a$ in figure 2.5, where a is a parameter giving the effectiveness of the thermal expansion of the brine). However, for the cumulated amount of water retrieved from the borehole, the consideration of the thermal expansion is of low importance as can be seen in the lower part of figure 2.5. This supports the statement given above that for a proper estimation of the long-term fluid inflow, the water vapour diffusion model is sufficient.
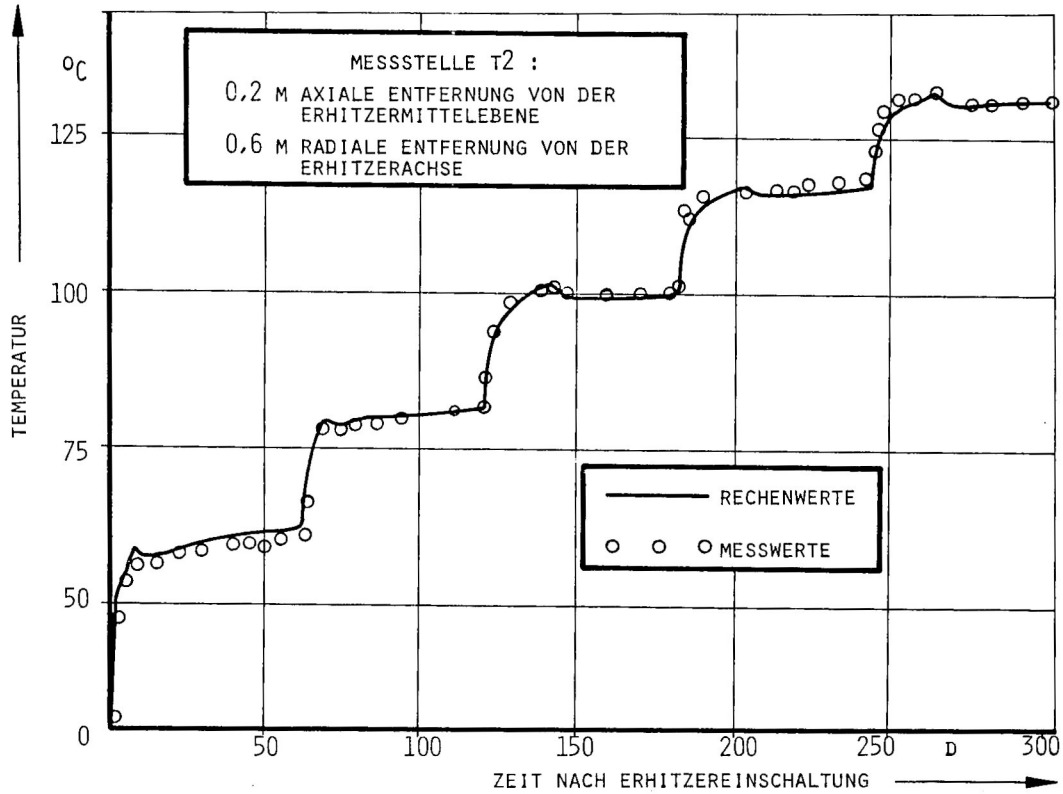
Fig. 2.3   Temperature evolution in 0.6 m radial distance to the borehole /SCH 86/
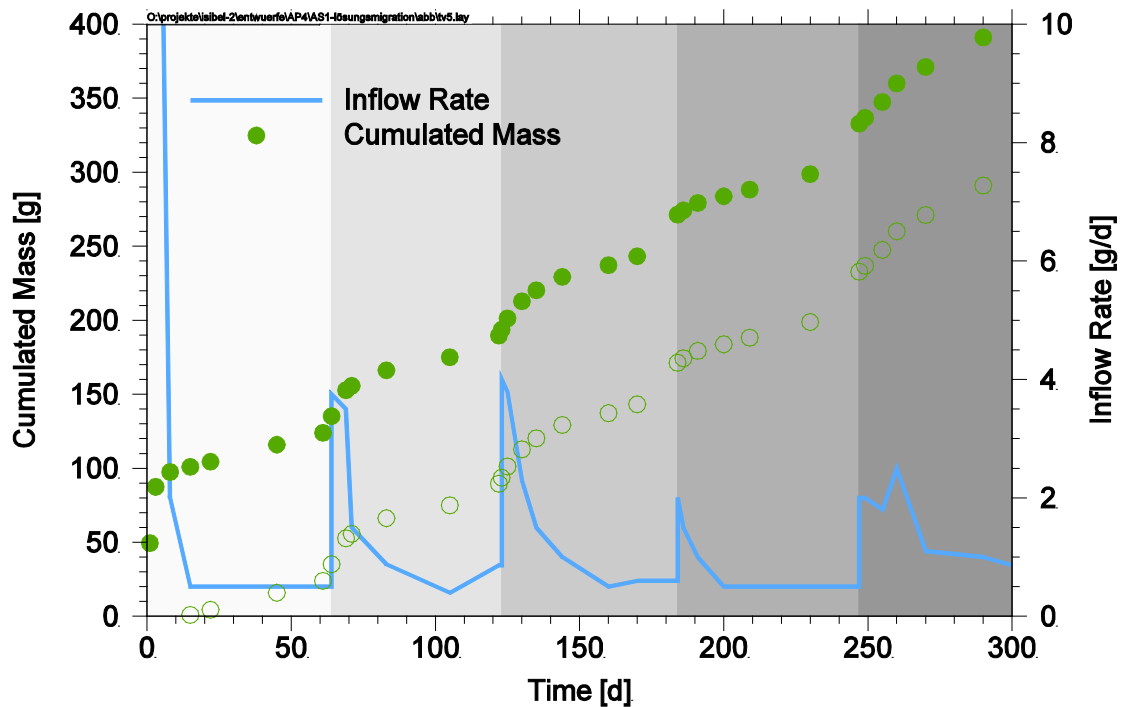
Fig. 2.4   Water inflow rate and cumulated mass during the TV5 experiment

(The background shading denotes different steps of heater power)

22
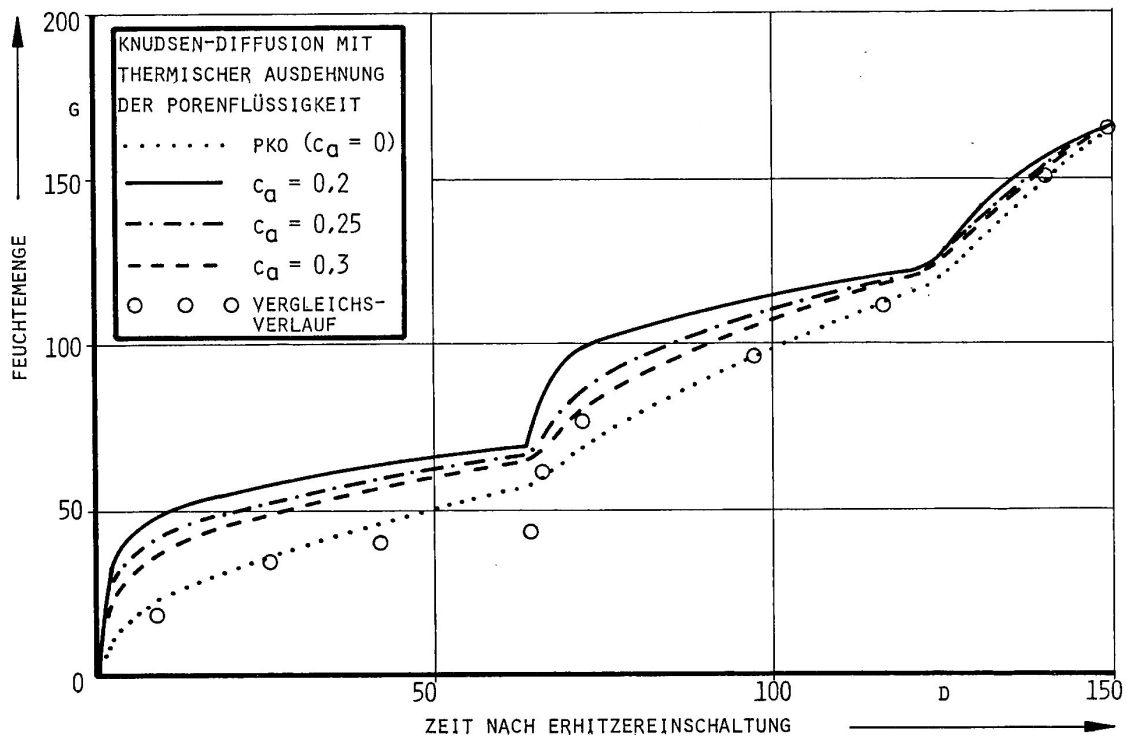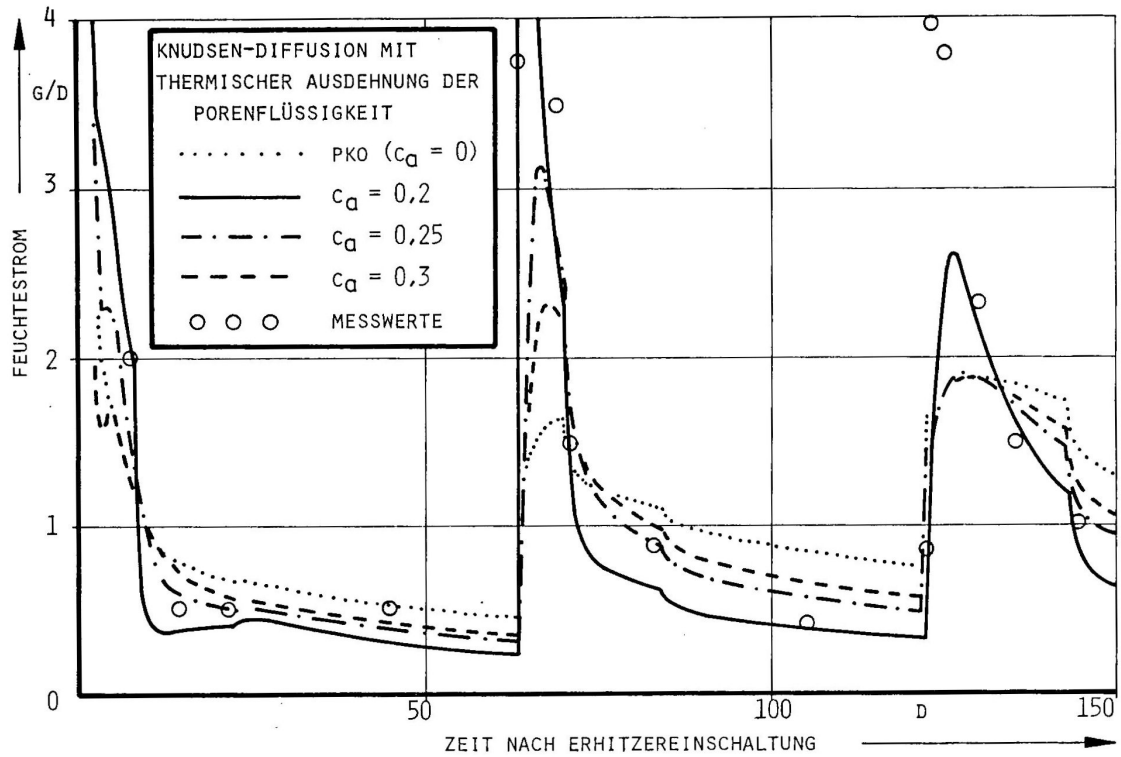
Fig. 2.5 Modelling of the temporal evolution of brine inflow (upper figure) and integrated brine volume (lower figure) for the TV5 borehole /SCH 86/

(Dots denote the corrected experimental data, while the lines represent different modelling results)

Brine Migration Test – in-situ test at the Asse mine

The Brine Migration Test (BMT) was a large-scale in-situ experiment carried out in the frame of a German-U.S. cooperation during the first half of the 1980's in the Asse mine. A detailed description of the experimental procedure and the results are given in /ROT 88/. The experiment consisted of four test sites, arranged about 15 m apart from each other in one line at the bottom of the same access gallery. Each site consisted of a borehole array with guard heaters around one central borehole containing a Co-60 source. The central borehole had a diameter of 0.43 m and a length of 5 m. The heater power was controlled to get a maximum salt rock temperature at the central borehole wall of 210 °C for the two inner test sites (BMT 2 and BMT 3). The water flowing into the central borehole was caught using a cold trap as in the TV5 experiment. The water inflow to the borehole was modelled in the same way as for the TV5 experiment /SCH 86/. A good agreement with the experimental data was found using an adapted water content of the rock salt of 0.01 compared to 0.04 used for the modelling of the TV5 experiment (figure 2.6). This demonstrates the good transferability of the model from one to another experimental location.
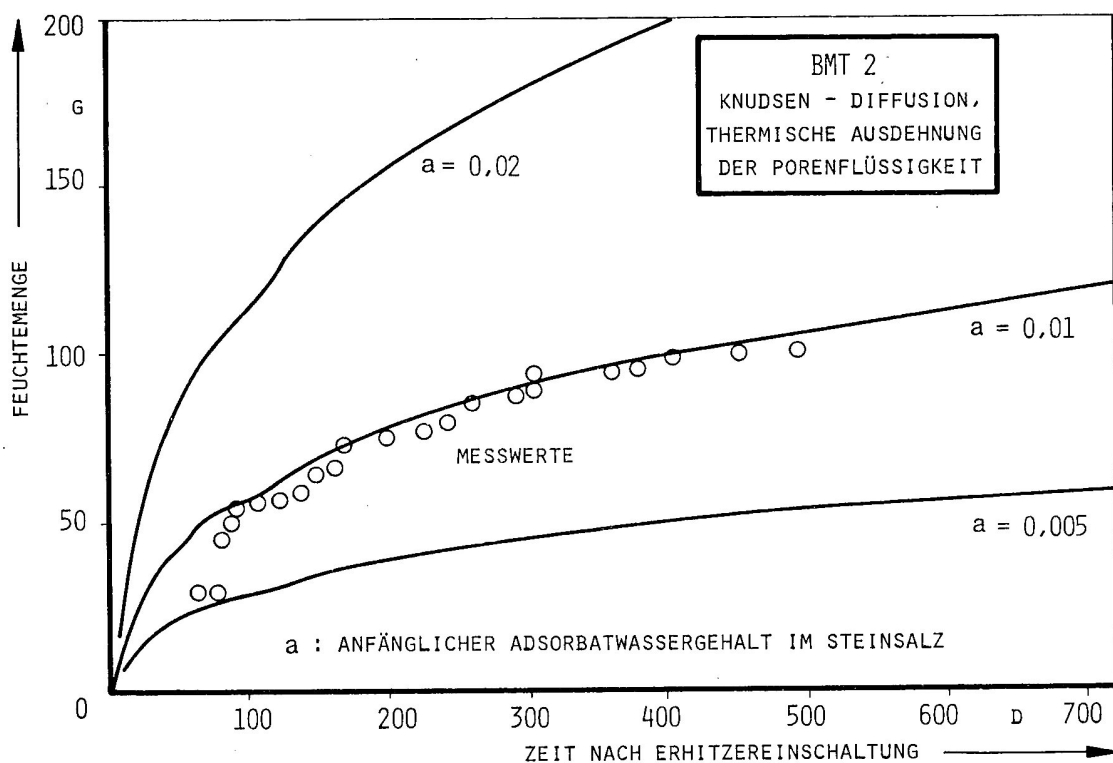
Fig. 2.6   Modelling of the water volume flown into borehole BMT 2 /SCH 86/

(Dots denote experimental data, while lines represent modelling results)

24

2.3 Estimation of water migration into a HAW borehole

The model of water vapour diffusion described in equation 2.3 in principle allows a detailed modelling the water migration towards an emplacement area for a specific location. However, neither the information needed for such a model is currently available for a specific high-level waste repository in Germany (like detailed geometry, temperature field, distribution of water content, diffusion coefficient etc.) nor is it clear in the end whether the model describes the water migration process sufficiently well for a very detailed modelling without pretending a non-existent accuracy. Because of these reasons, in the following a very rough estimate is presented for the expected water inflow into a HAW borehole.

The first question of interest is quite simple: Which amount of water is potentially available around the emplacement borehole? For a borehole with an inner radius of 0.215 m and a mean water content in the salt rock of 0.0164 %$_{wt}$ /SAN 01/, the available amount of water per metre borehole length is given according to equation 2.9 and the results are shown in figure 2.7 as a function of the distance to the borehole wall. With a borehole to borehole distance of 20 m, a maximum amount of 100 litres of water is available per metre of borehole length.
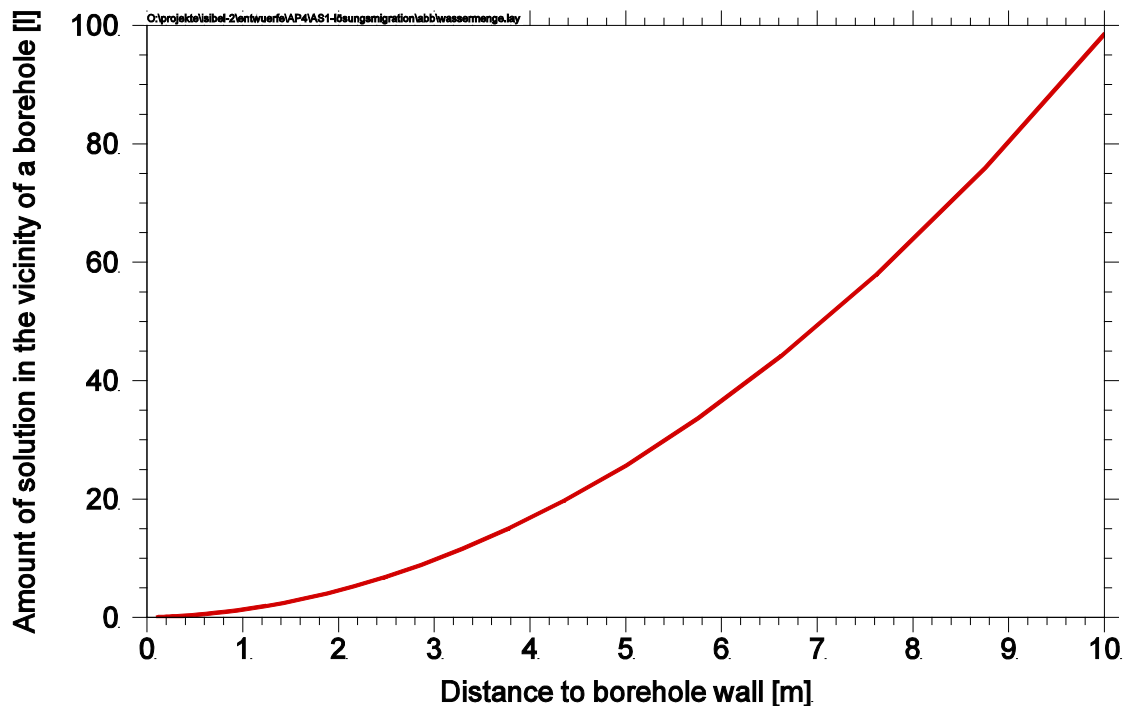
Fig. 2.7 Amount of water available in the vicinity of a HAW borehole per metre of borehole length as a function of distance to borehole wall

However, it is not expected that the evaporation front will be penetrating to such a depth into the salt rock formation. The thermal phase of the waste repository is limited to some hundreds years and the migration process will stop as soon as the temperature decreases to a level significantly below 100 °C. The penetration depth of the evaporation front, which is expected to be limited by the comparably slow diffusion process, is roughly estimated in the following. Using the parallel pore model, the Knudsen diffusion coefficient D_k of the water vapour in the pore is given by /CUS 97/:

$$D_k = \frac{2}{3} r \bar{v}$$
(2.4)

where the mean velocity $\bar{v}$ is given according to the Maxwell-Boltzmann distribution by:

$$\bar{v} = \sqrt{\frac{8RT}{\pi M}}$$
(2.5)

with

r pore radius [m],

R gas constant (8.314 J·K^{-1}·mol^{-1}),

T temperature [K],

M molar mass of water (18·10^{-3} kg·mol^{-1}).

For an estimated mean pore size[16] of $r = 2 \cdot 10^{-9}$ m and a temperature of 100 °C (373 K), the Knudsen diffusion coefficient $D_k = 8.83 \cdot 10^{-7}$ m^2·s^{-1} is obtained. Finally, the effective diffusion coefficient in a porous medium is given by

$$D_{eff} = n \cdot D_k \, .$$
(2.6)

With a porosity[17] of $3 \cdot 10^{-4}$, an effective diffusion coefficient of $D_{eff} = 2.65 \cdot 10^{-10}$ m^2·s^{-1} is calculated[18].

---

[16] The mean pore size was estimated by visual inspection of the pore size distribution function plotted in /DEL 97/.

[17] The porosity was calculated from a mean water content measured for the Hauptsalz at the Gorleben site of 0.0164 %$_{wt}$ /SAN 01/ and densities for the salt brine of 1 200 kg·m^{-3} and for the rock salt of 2 165 kg·m^{-3}, respectively.

The diffusion into a plane sheet can be calculated as a function of the distance from the source x and the time t from /CRA 79/

$$C(x,t) = C_0 \cdot erfc\left(\frac{x}{2\sqrt{Dt}}\right),$$ (2.7)

where C_0 denotes the initial concentration at the source. The distance x at which the concentration of the diffusing substance is about half the initial concentration at the source is about[19]

$$x \approx \sqrt{Dt} .$$ (2.8)

This distance is used in the following as an estimate for the penetration depth of the evaporation front. Finally, the pore volume V of a cylinder barrel around a borehole of the radius r_i and an outer radius $r_a = r_i + x$ is:

$$V = \pi (r_a^2 - r_i^2) \cdot n .$$ (2.9)

From the formulas given above, the penetration depth and the amount of water vapour flowing into a borehole can be estimated as a function of time. It has however to be mentioned that the calculated results show a quadratic dependence on the assumed water content of the salt rock – which is a value of high uncertainty.

First, we want to test this formula for the BMT in-situ experiment (see section 2.2.3). For a water content[20] of 0.02 %$_{wt}$, a time of 660 days, an inner radius of r_i = 0.215 m and an effective length of the borehole of 1.85 m, we estimate a water inflow of 134 grams, which is in a good agreement with experimental values of 114, 100 and 137 grams measured in the BMT 2, 3 and 4 boreholes.

---

[18] This value is almost identical to the value obtained in /SCH 86/ by numerical modelling of the TV5 in-situ experiment (D = 2.64·10^{-10} m^2·s^{-1}) and one order of magnitude higher than the one obtained from modelling the BMT in-situ experiment (D = 2.16·10^{-11} m^2·s^{-1}).

[19] The deviation from the correct value is less than 5 %.

[20] The water content is the mean value from 10 pre-test measurements on core samples (data in /ROT 88/ p. 229). All other parameter values of the BMT are taken from the list in /ROT 88/ p. 261.

Second, we estimate the water inflow into a borehole with vitrified waste. Using a mean water content of 0.0164 %$_{wt}$ and a borehole radius of 0.215 m, we receive results as plotted in figure 2.8 on a double logarithmic scale and in figure 2.9 on a linear scale. Within 700 years[21], the penetration depth is estimated to be 2.4 m and the amount of inflowing water to be about 6.3 kg or litres per metre of borehole length. If we assume a bandwidth of a factor of two for the estimated penetration depth of the evaporation front, the lower and upper limits for the amount of inflowing water equals 1.8 kg and 23 kg, respectively. About the same range of values is found, if the water content is varied by a factor of two.

The calculation of the given values for the penetration depth assumes that the water in the host rock can be evaporated with identical efficiency independent from the penetration depth. This assumption neglects that in the undisturbed rock, the boiling point of the water might be increased due to high pressures. If the evaporation front is not able to penetrate the undisturbed rock salt and therefore stops at the EDZ-boundary, the amount of water would be limited by the thickness of the EDZ to about 1 kg per metre of borehole length, if the EDZ reaches about 1 m deep into the rock formation. On the other hand, the penetration of the evaporation front might lead to an extension of the disturbed zone deeper into the rock. Since this question cannot be assessed from the performed experiments, the values for the calculated amount of water have to be regarded as a conservative estimation regarding this question.

It is not expected that the amount of inflowing water will affect the integrity of a waste container by corrosion. An amount of 6.3 kg of water is able to corrode 14.7 kg of iron, resulting in a gas production of 7.9 Nm^3 of hydrogen (see also chapter 3.2). A waste container with a diameter of 0.43 m has a specific surface of 1.35 m^2 per metre. Under the assumption of surface corrosion, a consumption of 14 kg will result in a loss of only 1.4 mm of the container surface. The according bandwidth is 0.4 to 5.1 mm. Compared to this number, the wall thickness of high-level waste containers is at least several centimetres[22]. CSD-V-containers for vitrified waste on the other hand that are not con-

---

[21] The timespan was estimated from temperature design calculations performed for the SAM study /BUH 91/. According to this data (control point 19), the temperature at the surface of the emplacement borehole for vitrified high-level waste exceeds 100 °C after less than 10 years, reaches a maximum of about 170 °C after about 70 years and falls again below 100 °C after about 700 years.

[22] The wall thickness of the BSK-3 spent fuel waste container of the type from 2008, which was not planned to withstand the rock pressure, was 40 mm /BOL 08/

structed to withstand rock pressure have a wall thickness of 5 mm and therefore a considerable amount of these containers can be corroded by the inflowing water.
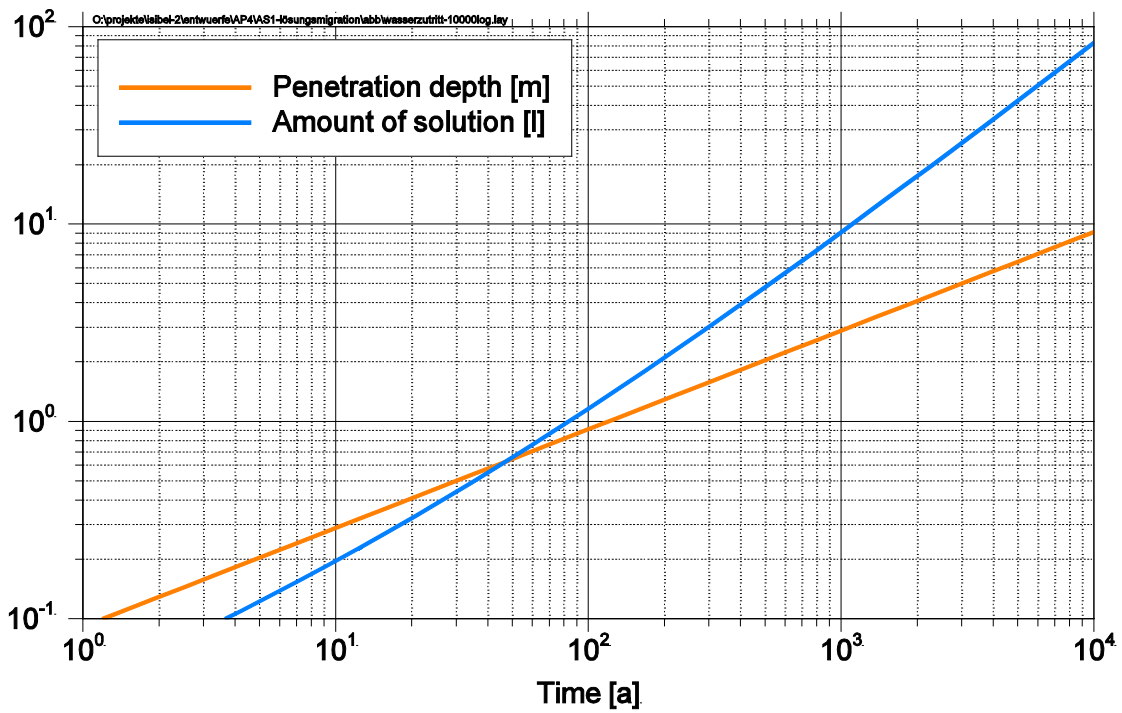
Fig. 2.8   Inflow of water vapour into a HAW borehole as a function of time (log-log scale)
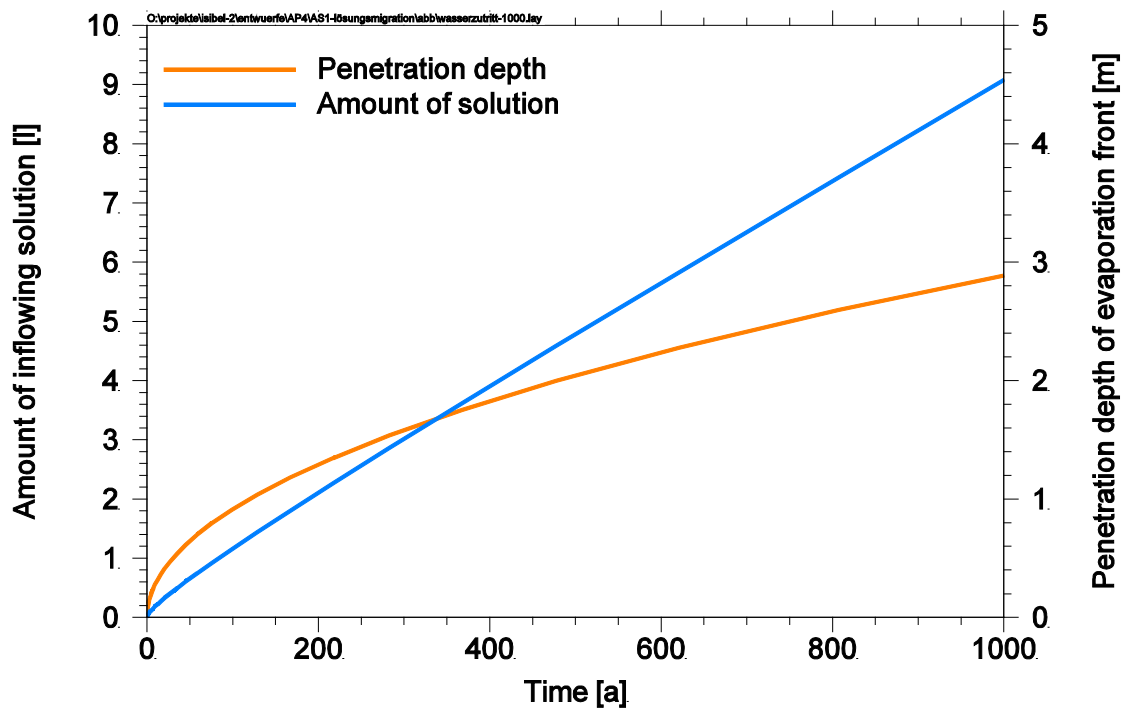
Fig. 2.9   Inflow of water vapour into a HAW borehole as a function of time

2.4   Résumé

In this chapter, the state of knowledge about the fluid migration in salt rock due to thermal load from radioactive waste was summarised and assessed. The most important aspects can be summarised in the following three statements:

1.   Intracrystalline water, i. e. fluid inclusions, migrates along the temperature gradient up to the next grain boundary where it is released into the intracrystalline pore space. Fluid inclusions can also be taken up by the intercrystalline water by grain boundary movement, which on the other hand may also create new fluid inclusions depending on the movement velocity. For areas close to head generating waste, it is conservatively assumed that the intracrystalline water is completely released from the salt grains into the intercrystalline pore space within several tens of years. An exact description of this process is not relevant for the long-term evolution of the repository system.

2.   Intercrystalline water is evaporated at the boundary of the intact salt rock to a drift or borehole as soon as the temperature exceeds the boiling point of the water. Due to the water pressure gradient, the evaporated water is transported into the drift or borehole by diffusion. If corroding substances are accessible in the respective drift or borehole, the water is consumed by corrosion and the water vapour pressure gradient is maintained[23]. Since more and more water is evaporated at the boundary to the fully saturated salt rock, an evaporation front is slowly migrating into the salt rock body. The process stops as soon as the temperature falls below the boiling point of the water again, or the water vapour pressure in the drift or gallery rises, so the pressure gradient is levelled out. No knowledge exists, how deep the evaporation front can move into the salt rock formation (see also below).

3.   Additional driving forces for the migration of the intercrystalline water are the thermal expansion of the pore water and the rock salt matrix as well as mechanical stress of the matrix. Although these processes are of importance for short term fluid migration during transient phases of temperature and stress, the contribution to the absolute amount of water released from the host rock is not relevant on the long-term. This effect has to be taken into account when modelling short-term experiments, but can be neglected for issues of long-term behaviour.

---

[23] The generated hydrogen gas does not hinder the water vapour transport, since this is a diffusive process, only depending on the water vapour pressure, not the absolute pressure.

Using plausible assumptions for the situation at Gorleben, a rough estimate of the amount of water vapour that is transported into an emplacement borehole for vitrified HAW yields about 6.3 kg per metre of borehole length, with an estimated bandwidth ranging from 1.8 to 23 kg per metre of borehole length. Until now it is unclear whether the evaporation front can penetrate deeper into the salt rock than the extent of the EDZ. If not, the amount of water would be limited by the thickness of the EDZ. For an EDZ thickness of 1 m, an amount of only 1 kg water per metre of borehole length is estimated for the situation given above.

3 The release of gaseous radionuclides and their relevance for the potential radiation exposure

One task of long-term safety assessments for deep geological repositories for nuclear waste is to determine the future radionuclide fluxes released from the repository and the potentially resulting radiological consequences for the population. The main attention during these assessments is usually paid to the release of radionuclides that are dissolved into the water in the repository and that are subsequently transported up to the biosphere in the dissolved state. Nearly all of the radionuclides disposed of in the repository can only be transported that way, including the long-lived and highly radio-toxic actinides. However, there are a small number of radionuclides that may exist at least partially in gaseous form in the repository and that can be released via a gas pathway.

Present-day long-term safety assessments for repositories for low-level waste have shown that the gaseous radionuclides may contribute significantly to the potential future radiation exposure e. g. /BEC 09/. Radiocarbon has turned out to be the most relevant radionuclide in that assessment. However, waste repositories for high-level waste have very different characteristics with regard to waste properties like radionuclide inventory, waste packaging and repository concept. Therefore, the results for the assessment of a low-level repository cannot be simply applied to assessments for high-level waste repositories in salt.

In a radioactive waste repository, large amounts of non-radioactive gases are potentially produced by the anaerobic corrosion of the radioactive waste itself, or its packaging, which are heavyweight steel containers in the case of high-level waste. The latter mainly results in the production of hydrogen. Additionally, air is trapped in the mine with closure, which also contributes to the amount non-radioactive gases. These large amounts of non-radioactive gases can act as carrier gas for the much smaller amount of radioactive gases existing or being produced in the waste. Due to their small amount, the radioactive gases themselves are unlikely to be released from the repository in gaseous form without being transported by a carrier gas. The gas production of non-radioactive gases from the container corrosion however requires the presence of water which is consumed by the corrosion process.

The principal safety concept for a high-level waste repository in salt is the safe containment of the waste in the salt formation. The convergence of the rock salt results in the compaction of the crushed salt backfill down to a low permeability. The low permeability should provide the separation of the waste from the geosphere by excluding, or at least considerably delaying contact of the waste with water. Due to the given facts, it was unclear whether the release of gaseous radionuclides – especially radiocarbon – from a waste repository in salt can occur and whether there is any relevance for the potential radiation exposure of future populations.

The work presented in this chapter is giving fundamental considerations to allow the strategic planning on future research or repository concepts. The first section deals with the inventory and source-term of radioactive gases. The second section studies the generation of non-radioactive gases which can act as carrier for the radioactive gases and therefore enhance the release of radioactive gases from the repository. The generation of gases is strongly coupled to the availability of water for the corrosion of container materials. Therefore, this subject is also addressed in this section. The third to fifth sections discuss the release of radioactive gases from the repository, to the geosphere and the biosphere. Finally the sixth section estimates the potential radiation exposure resulting from the volatile radionuclide release.

3.1   Source term of gaseous radionuclides

Besides the large amount of non-radioactive gases, a small amount of radioactive gases is being produced in a repository for high-level waste. The radioactive gases are either present in the gas phase of the spent fuel element or will be produced as soon as the waste gets in contact with water. The latter is most notably true for carbon dioxide and methane which contain radiocarbon. C-14-containing gases can be produced from the contact of the fuel elements or hull material with water. Briefly, the process can be described as follows: C-14 is found in the oxide film of the hull, at least partly in the form of zircaloy carbides. In case of contact with water, these are converted to short-chain organic compounds and finally transferred to C-14-containing gases. There are uncertainties in the exact process at various steps which is described in more detail in what follows.

3.1.1 Carbon-containing gases

Radiocarbon has a half-live of 5 730 years and is produced in nuclear power reactors by neutron absorption by carbon, nitrogen or oxygen which are present – mainly as impurities – both in the structure materials and the fuel. The highest effective cross sections for the formation of C-14 are for the reactions (in the given order) $^{14}N(n,p)^{14}C$, $^{13}C(n,\gamma)^{14}C$ and $^{17}O(n,^{4}He)^{14}C$ /NCRP 85/. The first reaction dominates the production of C-14 by far, due to the different concentrations of the source isotopes. The concentration of nitrogen impurities was determined e. g. by /DAV 79/ to vary from 3 to 50 $\mu g \cdot g^{-1}$ with a mean value of 25 $\mu g \cdot g^{-1}$ in the fuel itself and values of the same order of magnitude for zircaloy material. The resulting C-14 production is about $4 \cdot 10^{8}$ Bq/GWd for LWR oxide fuel and up to a factor of ten higher for the hull material.

The C-14 concentration in the radioactive waste is usually calculated by fuel burn-up simulations. Calculations performed by the GRS with the OREST code /PEI 11/ result in a C-14 inventory 40 years after unloading from the reactor of about $3.7 \cdot 10^{10}$ Bq/t_{SM} for BWR and PWR fuel elements with a burn-up of 50 and 55 GWd/t_{SM}, respectively. These values are in a reasonably good agreement with the values given above. Two container options have been recently taken into consideration for spent fuel in Germany. The first option is the Pollux-container holding about 5.3 t_{SM} and the BSK-3-container holding about 1.6 t_{SM}[24]. The data for the Pollux container is taken as example in the following, but however, no final decision has yet been made on actual container design.

The C-14 inventory produced in the waste is distributed over different compartments of the spent fuel element, i. e. the uranium-oxide fuel itself, the cladding and the structural materials. The latter two can be subdivided into the zircaloy or steel material in the inner part and a zirconia-oxide film of 40 to 80 μm thickness in the outer part /JOH 05/. The oxide film is formed during reactor operation and is typically of porous structure.

With respect to the radionuclide release behaviour, the uranium-oxide fuel can be roughly subdivided into two compartments. The first is the matrix, which comprises the uranium oxide grains from which the radionuclides are released very slowly. The sec-

---

[24] The given values correspond to 30 BWR or 10 PWR fuel elements for each Pollux and 9 BWR or 3 PWR fuel elements for each BSK-container. Each fuel element contains about 0.177 t_{SM} or 0.525 t_{SM} for BWR or PWR fuel elements, respectively.

ond is the so-called instantaneous release fraction "IRF", which comprises all areas from which radionuclides can be easily released, like the gap and the rim and grain boundaries. The different compartments of a fuel rod are shown in figure 3.1.
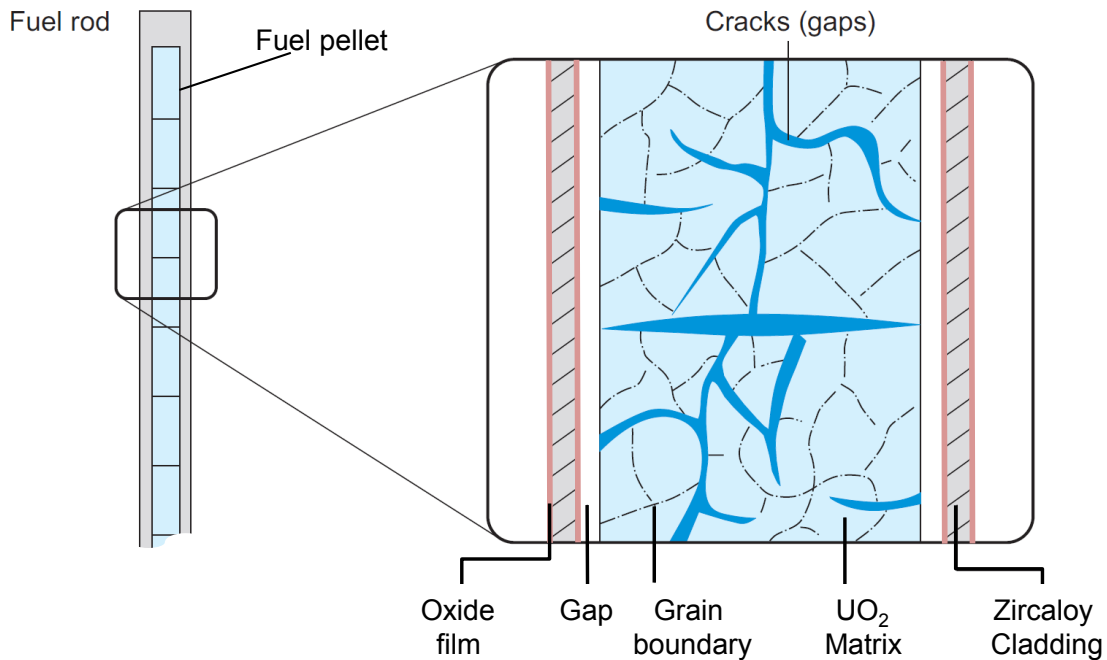
Fig. 3.1 Compartments in the spent fuel element (after /NAG 02/)

The distribution of the radionuclide inventory into the different compartments of the waste depends on the radionuclide regarded. On the basis of values given in /JOH 97/ and /JOH 05/, Nagra has made a compilation for all safety relevant radionuclides in /NAG 02/. For C-14 from BWR fuel they come to the following conclusions:

–   54 % of the total inventory resides in the fuel, while the other

–   46 % reside in the metal parts.

And finally, the IRF is

–   10 % for the fuel and

–   20 % for the metal parts.

The latter is also in a good agreement with the findings presented by Tanabe in /TAN 09/. According to /JOH 05/, the C-14-IRF is independent from the burn-up of the fuel. For a C-14-inventory of a Pollux container of $1.93 \cdot 10^{11}$ Bq, these values result to a radionuclide inventory distribution as given in table 3.1.

Tab. 3.1   Distribution of radiocarbon inventory into different compartments of the spent fuel in one Pollux container

Compartment		Fraction [%]	Inventory [10^{10} Bq]
Fuel Matrix	Matrix (uranium oxide)	48.6	9.39
	IRF (gap, grain boundaries)	5.4	1.04
Cladding	Zircaloy	36.8	7.11
	Zirconia (IRF)	9.2	1.78
Sum		100	19.32

The release behaviour of the C-14 is different for each compartment. The release behaviour from the cladding has been studied by /TAN 09/ with measurements for the hull of PWR and BWR spent fuels over a time-span of one year.

The release from the zircaloy and metal parts has been shown to be congruent with the slow corrosion rate of the material. For the leaching conditions used in the experiments with simulated groundwater corresponding to a granitic environment[25], a period required to leach all C-14 from the hull waste of 20 000 years was estimated. For a NaCl-saturated brine, as expected in a repository for high radioactive waste in salt, the corrosion of the zircaloy might occur with a rate of 0.1 to 0.5 $\mu m \cdot a^{-1}$ /GRA 00/, /KUP 00/ suggesting release times which are by a factor 2 to 10 shorter[26] than those determined in the experiments by Tanabe. However, not data exists, yet which fully correspond the expected repository conditions.

For the oxide film, the release was found to occur much faster and a minimum time of 400 years was estimated to leach all C-14 /TAN 09/. There is no data available on the effect of the solution composition on the dissolution of the oxide film. However, in analogy to the corrosion of the zircaloy it is likely that the dissolution of the oxide film is faster in highly saline brines.

There are some experiments which suggest that the release of C-14 from the oxide films and the zircaloy is possible by diffusion at elevated temperature without the pres-

---

[25] The experiments were carried out with a test solution composition corresponding to a sea-water derived groundwater that has reacted with cement (chloride concentration of 0.6 $mol \cdot l^{-1}$).

[26] These numbers are calculated considering a cladding tube of 1 mm wall thickness.

ence of water /SMI 93/. A comparison between different atmospheric conditions showed that oxygen seems to be a prerequisite in this case /KOP 90/, /KON 94/. In the presence of atmospheric air, the observed release fraction is in the range of $2 \cdot 10^{-4}$ to $4 \cdot 10^{-3}$ within 8 h for temperatures of 100 °C and 200 °C. Under the assumption that these release rates prevail for long times, most of the C-14 would be released into the gas phase in the storage container after a few years, already prior to the final disposal in the repository and the volatile part might be removed in case of the waste being re-packaged before disposal from storage to disposal containers.

The release from the uranium-oxide fuel matrix is expected to occur at the same very slow rate of the matrix dissolution within hundreds of thousands or even several millions of years /POI 05/. Therefore, nearly all of the C-14 residing in the fuel matrix will have decayed in the matrix before being released. The C-14 inventory of the gap is expected to be in non-volatile, but easily accessible form /JOH 05/ and the release was found to occur within several years when the fuel gets in contact with water /JOH 97/.

Different studies have tried to investigate the chemical form of the radiocarbon released from the hull material. While the exact chemical form is still unclear, it seems most probable that the majority of the radiocarbon is in organic form (see e. g. /YAM 99/ for zircaloy and /DEN 97/ for carbon steel). While Sasoh has found a fraction of organic C-14 of 66 to 75 % /SAS 04/, Tanabe has found even higher fractions of 80 to 100 % /TAN 09/. According to Tanabe, the carbon compounds are in organic, but not gaseous form. Therefore, it is recommended to presume that all C-14 released from the hull material is in organic form.

After being released from the hull in organic form, the C-14-containing compounds may be transferred into gaseous form by at least two different processes. The first one is the microbial degradation of the organic matter which is a usual process taken into account for low- and intermediate level wastes (see e. g. /MOR 01/). However, there is quite some uncertainty about the exact microbial reactions taking place in a repository since these are highly dependent from various boundary conditions, like the presence and the type of substrates, microbial fauna and additional key nutrients /ROD 03/. All these boundary conditions are often ill defined in a waste repository due to the variability in the waste composition or geochemical conditions. Despite this uncertainty about the participating reactions, their gaseous products are known: the carbon containing gases being formed by microbial activity are either carbon dioxide or methane.

A second process which degrades organic components into carbon bearing gases in a repository for high level waste types is radiolysis. A decomposition of longer organic molecules (formic acid, formaldehyde, methanol…) to carbon dioxide and water by γ−radiation has been observed by /NOH 04/[27]. It seems most likely that this effect also occurs for other radiation types. While the decomposition efficiency seems to depend on the organic compound concentration, there is only low influence by the dose rate[28]. The overall decomposition efficiency determined by /NOH 04/ ranged from 0.1 up to 10 % for an organic compound concentration of 10^{-7} mol·l^{-1} to 10^{-5} mol·l^{-1}. Below a concentration of 10^{-7} mol·l^{-1} no further decrease of the decomposition efficiency was observed.

Finally, it has to be concluded that all the C-14 present in the IRF may be mobilised in gaseous form within a few hundred years. Until now it is unclear whether it is a prerequisite or not that the waste gets in contact with water to release the C-14 into volatile form. The volatile C-14 released within rather short term makes about 15 % of the total C-14 inventory emplaced with the spent fuel or, equivalently, about $2.9 \cdot 10^{10}$ Bq per Pollux container[29]. Additionally, the C-14 inventory of the cladding of $7.1 \cdot 10^{10}$ Bq will be released into volatile form with a somewhat slower rate. Conservatively it has to be assumed that these C-14-inventories are initially in organic form and are converted after their release into C-14-containing gases, i. e. carbon dioxide and methane.

3.1.2   Other Gases

There are other radionuclides than C-14 which might be released from the waste in gaseous form. These are the so-called fission gases, mainly krypton and xenon, produced during the burn-up of the fuel and which are – in contradiction to C-14 – in gaseous form right from the start. These noble gases have no dose relevance and are therefore not considered further.

---

[27] These experiments were carried out using a Co-60 gamma radiation source with a dose rate ranging from 0.3 to 200 Gray per hour.

[28] The experiments have shown no effect of the dose rate on the decomposition efficiency for a dose rate ranging from 0.1 to 10 Gy/h. The actual does rate expected under repository conditions is however at least one order of magnitude lower than the lowest value used in the experiments.

[29] This is equivalent to an amount of $1.2 \cdot 10^{-2}$ moles or a volume of $2.7 \cdot 10^{-4}$ Nm³.

Besides the noble gases, there are other radionuclides present in the gap of the fuel element that might at least partially form gaseous compounds. According to /JOH 05/, volatile radionuclides in the gap are Cl-36, Cs-137, Cs-135, I-129 and Se-79 and these are the only potential candidates for gaseous release. Due to its short half-life, Cs-137 has no relevance, here. The inventory of the other radionuclides in the gap and grain boundaries of the fuel elements of one Pollux container is given in table 3.2 for a burn-up of the fuel of 48GWd/t$_{SM}$. The given values increase depending on the radionuclide by about a factor of 1.2 up to 4 if the burn-up is increased to 60 GWd/t$_{SM}$. Slightly higher fractions are also found if the rim regions of the fuel are accounted for, too.

Tab. 3.2   Fraction of volatile radionuclides per Pollux container with spent DWR elements, 40 years after removal from the reactor

Nuclide	Inventory /PEI 11/ [Bq]	Fraction in gap and grain boundaries /JOH 05/ [%]	Inventory in gap and grain boundaries [Bq]	Inventory in gap and grain boundaries [mol]
Cl-36	$5.72 \cdot 10^9$	10	$5.72 \cdot 10^9$	$1.30 \cdot 10^{-2}$
Se-79	$1.40 \cdot 10^{10}$	2.1	$2.95 \cdot 10^8$	$1.45 \cdot 10^{-3}$
I-129	$8.66 \cdot 10^9$	4	$3.46 \cdot 10^8$	$4.11 \cdot 10^{-1}$
Cs-135	$1.79 \cdot 10^{11}$	2.5	$4.48 \cdot 10^9$	$6.76 \cdot 10^{-1}$

In principle, all of these elements are able to form gaseous compounds, however, the fraction of these radionuclides present in gaseous form is expected to be in general very low. The reason for this statement is that all of these elements are either already present in very soluble form, like it is the case for caesium and iodine which are mainly present as CsI /JOH 97/, or are highly reactive and form high soluble compounds by chemical reaction, like chlorine.

Nevertheless, especially for iodine a small portion might be present in the form of I$_2$ in the gap of the fuel element. Iodine partition coefficients between air and aqueous solutions have been measured for different types of solution, temperatures and pH ranges in the context of assessing the release of iodine by reactor accidents, but not in the context of direct disposal. These investigations therefore might have to be reassessed. The determined values show a wide range over many orders of magnitude: "*Their values are very sensitive to temperature, iodine concentration, pH, presence of other compounds, capable of reacting with chemical species, involved in iodine equilibrium*" /EC 82/. Tables for partition coefficients determined by theoretical calculations

/PAR 70/ for 80 °C and a pH of 8.0 yield iodine-water partition coefficients of around 80 for an iodine concentration in the liquid of 1 mol per cubic metre of solution; i. e. 1/80th of the iodine inventory might be found in the form of I_2 in the gaseous phase. However, for a more realistic estimation of the I_2 concentration in the gas phase, partition coefficients would be needed taking into account in the presence of other chemical elements than just water and iodine. This is especially true for caesium, as CsI is expected to be the dominant species of iodine.

For chlorine, no investigations exist about the existence of a gaseous fraction in the container, but this is assumed to be very unlikely due to high reactivity of Cl_2 gas. The same applies to selenium (as SeH_2) and caesium. It is therefore assumed that I_2 is the only gas that might be found in the container in a potentially relevant amount.

3.2 Container corrosion and generation of non-radioactive gases

The container corrosion is an important process with regard to the release of the radioactive gases from the repository for two reasons. First, the radioactive gases cannot be released from the container before it fails from corrosion (or from other cause). Secondly, the corrosion process is providing large amounts of non-radioactive gases. This is described in more detail in the following.

The very small absolute amount of a few moles per Pollux container of radioactive gases in a waste repository could easily be stored in the pore space of the backfill material and would never be released from the repository if no additional driving force existed like the generation of non-radioactive gases or the compaction of the backfill. The small amount of radioactive gases mingles with the large amount of non-radioactive gases which subsequently act as transport media[30]. Therefore, the generation of non-

---

[30] This effect is used for example in gas-chromatography, where a non-reacting carrier gas is used to transport a very small amount of gas to be analysed.

radioactive gases is of major interest for the estimation of the potential radiation exposure resulting from radioactive gases[31].

Non-radioactive gases in a waste repository are the trapped air in the repository and hydrogen being generated by the container corrosion. The production of other gases, which are generated by the degradation of organic material like the polyethylene neutron absorbers in the Pollux containers, are neglected in the following due to their comparably small amount and slower production rate[32].

After the oxygen in the repository is used up by aerobic corrosion processes, the corrosion of the metal parts of the container progresses under anaerobic conditions by conversion of iron into iron(II)oxide and finally into magnetite. A prerequisite of this conversion is the availability of water. To corrode 1 kg of iron, 0.43 kg of water is used up and 0.535 Nm³ of hydrogen is produced.

The corrosion behaviour of TStE355-steel, which is foreseen to be used for the spent fuel containers was studied for different temperature ranges and different solution compositions by /SMA 95/, /SMA 99/. For an unlimited availability of the water, the corrosion rate at 90 °C was determined to be about 5 $\mu m \cdot a^{-1}$ for NaCl- und 70 $\mu m \cdot a^{-1}$ for MgCl$_2$-solutions[33]. Although the maximum temperature can be higher, the temperature of 90 °C is representative for late times when the earliest additional intrusion of water can be expected. Using a corrosion rate of 5 $\mu m \cdot a^{-1}$ and a container surface[34] of about 30 m^2, the corrosion of one Pollux container results in a gas production of

---

[31] It has however to be noted that a release of gases from the repository under some circumstances can also be expected from the trapped air alone, even if no additional gases are generated. In a completely backfilled mine with a backfill porosity of 35 %, the pressure of the trapped air rises from atmospheric pressure to a pressure of 3.5 MPa, while the porosity of the backfill reduces to 1 %. This pressure already slightly exceeds for example the hydrostatic pressure at the salt surface at the Gorleben investigation site. Therefore, in that case, all gases that would be produced from amounts of water initially emplaced with the waste could potentially result in an equivalent gas flow from the mine.

[32] This is not necessarily true if other waste types than spent fuel, vitrified waste and type C and B wastes from reprocessing are emplaced. These waste forms will however most probably be stored in another area of the repository. The release of gases from these waste types will have to be assessed separately.

[33] Corrosion of TStE355 steel in NaCl-rich brine at 150 °C was determined to be about 16 $\mu m \cdot a^{-1}$. In comparison to that, 15MnNi6.3 steel (material number 1.6210), which is also suggested as candidate container material, has shown about 7 times higher corrosion rates under the same conditions /SMA 95/, /SMA 02/.

[34] The diameter of a Pollux container is 1.542 m and its length is 5.462 m.

0.626 Nm³·a^{-1} (28 moles per year) while 0.5 kg of water and 1.17 kg of iron are consumed[35]. To fully corrode the inner TStE-cask of the Pollux container with a thickness of 0.16 m, about 30 000 years are needed[36]. For magnesium-rich brines, other materials or higher temperatures, the quantities of produced matter can be accordingly higher and the corrosion duration shorter. However, in the following we hold on the assumption of a corrosion rate of 5 μm·a^{-1} and a corresponding consumption of water of 0.5 kg per container.

Comparative studies on the corrosion of TStE355-steel at 170 °C with MgCl$_2$-rich brine in the liquid phase and the vapour phase have shown that a vapour phase is able to maintain the corrosion process, but the corrosion rate was found to be lower by a factor of 20 /SMA 95/. On the other hand, direct measurements of the hydrogen production rate from the corrosion of the container material in naturally dry salt grit at 90 °C contradict this statement and yield comparable corrosion rates for the corrosion through the vapour phase and the liquid phase of about 2 μm·a^{-1} /SCO 98/.

For a waste repository in rock salt, the availability of water is limited under all expected conditions. The water present in the repository, owing to the emplacement of the waste and backfill or being released from the host rock is comparably small, and will corrode only a thin layer of the container surface (see chapter 2). A container failure is therefore only expected, if one of the following conditions is true:

1. There is an additional inflow of water from the overburden that brings enough water to fully corrode the containers. This is not expected in the reference scenario due to the low permeability of seals in early times and of the compacted backfill in later times.

2. Pitting corrosion occurs. Pitting corrosion is not expected for corroding steels. A higher probability for this process is expected for stainless steels, since the passivation layer which is responsible for the low corrosion rates is not able to reform under reducing conditions.

---

[35] A density for iron of 7 800 kg·m^{-3} is used.

[36] No credit is taken from the outer cask made from cast iron which is interspersed with the neutron absorbers.

3. There are initial defect containers. The presence of initial defective container cannot be fully ruled out, but has a low probability. Studies by SKB /SKB 03/ have resulted in a probability for the presence of undetected defects during the container manufacturing process of one defect container out of 1 000 emplaced containers.

Since the availability of water is crucial for the corrosion process, the inflow of water from the overburden into a waste repository in salt was using the LOPOS code. The simulations were carried out along the lines used for the VerSi project /RUE 10a/ and are described in Annex A.1. The most important results are the following:

- For the expected evolution, an inflow of external waters from the overburden through the shaft and drifts up to the emplacement areas is not expected before some 10 000 of years.

- If a storage volume for brine and gases is foreseen in the infrastructure area made from non-compactable backfill an additional retardation of the brine inflow for some 100 000 years might be achieved.

- The inflow rate of water into the emplacement drifts might be sufficient to corrode from 8 up to 56 waste containers simultaneously in the first emplacement field, which holds 288 containers in total.

It has to be noted that the results are highly depending on the repository layout and parameter selection and are only illustrative. Other scenarios might be of relevance that have not been regarded in these simulations and which might lead to other results.

3.3 Release of gases from the repository

The transport of the gases in the repository depends on the saturation state in the drifts. As long as the backfill is partly unsaturated, the generated gases may be transported according to the relative gas permeability of the backfill. If the backfill is fully saturated, part of the liquid phase has to be displaced, before gas transport is starting. At early times, a partly unsaturated state is expected. At late times at least parts of the repository mine might be saturated due to inflowing brine and brines from other sources. At this point in time, the porosity of the salt grit in the drift is already close to or at its final compaction state, i. e. porosity. The movement of the brine into an unsaturated drift has been studied in /BUH 09/, /RUE 10/. According to the results from simulations for unsaturated flow, the brine is moving through the drifts of the repository as a

sharp front. Ahead of the front, the saturation is close to the initial state and where the front has already passed by, the saturation in the drift rises to about 100 %.

As soon as the inflowing brine gets in contact with the containers, it is partly used up by corrosion and gas production. As the gas pressure in the emplacement drift rises, the produced gases partly displace the water from the saturated drifts and are transported along the gas pressure gradient towards the shaft and are finally released into the overburden. The so-called two-phase flow process allows the simultaneous flow of brine into the emplacement drift and release of gas out of the repository. The two-phase flow parameters for highly compacted salt grid were unfortunately not available at the time of writing. The principal process can be identified from simulations performed in /KUE 99/ and presented in chapter 4.

The simulations in /KUE 99/ regard a gas release of about 40 Nm^3 per year[37] from a 100 m long initially unsaturated emplacement drift into a 300 m long, initially saturated access drift. In contrast to the expected conditions in the repository, the backfill of the drift regarded in these simulations is non-compactable and of high porosity and permeability. However, the principal sequence of events is expected to be similar for a drift backfilled with salt grit. The saturation versus distance resulting from the two-phase flow is shown in figure 3.2. In this case, the saturation in the emplacement drift rises with time, while the one in the access drift lowers. After about 500 years, a steady state evolves and the final saturation is between 80 and 90 % in the whole system. The mean travel time of the gas from the waste to the end of the drift is about 125 years.

---

[37] See section 3.2 for expected gas production rates and corrosion rates for comparison.
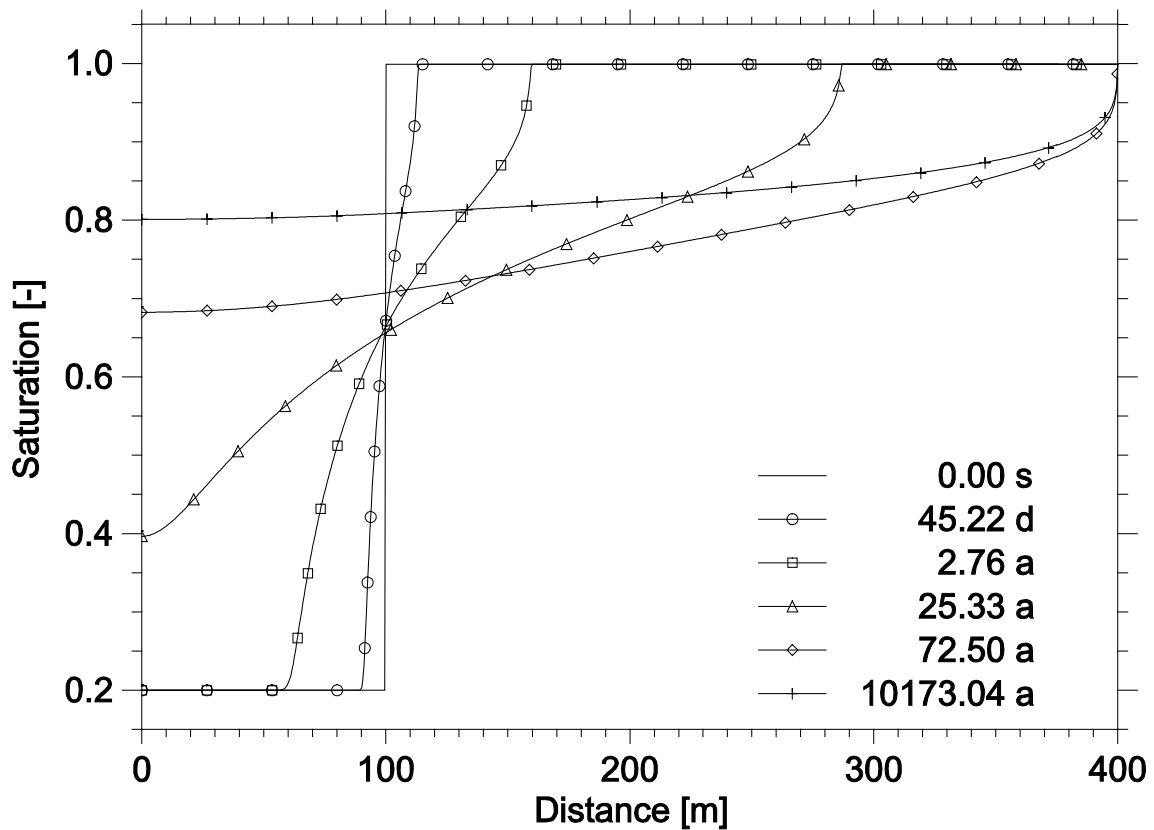
Fig. 3.2 Water saturation in a drift from two-phase flow by gas production in the left-most 100 m /KUE 99/

For some main issues which are of interest here, similar results are expected for simulations using more realistic parameters for the backfill, as is also shown in chapter 4, so that the following evolution of a gas pathway is predicted:

−   The gas production leads to a partial desaturation of the access drift and seal and the formation of a contiguous gas pathway from the waste up to the shaft, or even to the interface to the overburden. It is expected that the saturation in the drift shows lower values, the higher the gas production rates and the lower the porosity of the salt grit (see also results in chapter 4).

−   The desaturation stops at a saturation state at which the respective gas permeability is just as high as needed to dissipate the produced gases.

−   A steady state between gas production and gas transport is evolving with time, if the gas production rate is constant.

−   The time needed to establish the steady-state highly depends on the porosity of the backfill and the gas production rate and can range from several thousands to hundred thousand years depending on the parameter values (see also chapter 4).

- In steady-state, the travel time of the generated gases from the emplacement area to the geosphere can easily be calculated from the ratio of the gas production rate and the gas volume in the mine.

- Due to the low solubility of hydrogen in water[38], the brine in the repository is expected to be saturated with hydrogen within a short time. The concentration, i. e. the partial pressure of the radioactive gases in the hydrogen gas is rather low. Therefore, according to Henry's law, only a small portion of the gaseous radionuclides might be dissolved in the pore water of the backfill in the repository.

- Sorption of Hydrogen on the backfill or on other materials is expected to be low, but however, hydrogen might be consumed e. g. by microbial activity.

After a failure of a waste container, the described evolution implies that the volatile radionuclides released from the container are transported along the drifts in the gas pathway together with the non-radioactive gases that stem from corrosion processes. Depending on the gas production rate, the gases potentially can be transported up to the geosphere. If the gas production persists, a steady state may evolve between gas production and gas transport. In this case, the time span for the transportation of gaseous radionuclides within the repository is expected to be negligible compared to the half-life of the radionuclides considered.

3.4   Transport in the geosphere

As soon as the gas is released from the shaft of the repository, different possibilities exist for the further transport of the gases in the geosphere, which are discussed in detail in /BEC 09/. The first one is the transport of the gases in gaseous form up to the atmosphere, the second one is that the gases are dispersed and dissolved in the groundwater and lastly a combination of both.

The volume of the groundwater flow is highly depending on the hydrogeological situation in the overburden of the repository and can range from a few 10 000 m^3 up to several 100 000 m^3 per year. Irrespective of the real situation at a site, the minimum

---

[38] The solubility of hydrogen in water is about 0.8 moles·m^{-3}. If the water volume in the repository is assumed to be 10 000 m^3 at maximum, this volume can be fully saturated with the hydrogen generated from the corrosion of one container within less than 300 years.

groundwater flow sometimes conservatively assumed in safety assessments is 15 000 $m^3 \cdot a^{-1}$, which is the minimum amount of water needed by a small group of people for food production. The values assumed for the groundwater flow in previous safety assessments for generic repositories in salt in Germany range from 19 700 to 117 000 $m^3 \cdot a^{-1}$ in /BUH 91/ or is 48 000 $m^3 \cdot a^{-1}$ in /KEE 05/.

The absolute amount of gases released from the repository for high level waste in salt is quite low. According to the values given in section 3.2, the approximate range of the amount of gas expected to be released is from 224 to 1 600 moles per year[39]. In relation to the groundwater flow, this amount of gas can be easily dissolved in the groundwater, even if the minimum groundwater flow is assumed. Therefore, it is likely that the gases are dissolved and transported in the groundwater, rather than being released directly into the atmosphere.

As mentioned in section 3.1, C-14 produced in and released from the repository in gaseous form is either in the form of carbon dioxide or methane. The methane can be converted in the groundwater to carbon dioxide by microbial oxidation following the reaction /HAN 96/

$$CH_4 + 2\,O_2 \rightarrow CO_2 + 2\,H_2O + 883 \text{ kJ/mol}, \qquad\qquad (3.1)$$
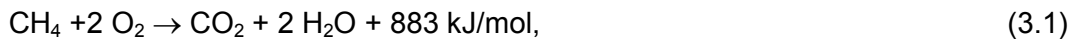
if oxygen is present in the groundwater. Therefore, it is assumed that all radiocarbon present in the groundwater is found in the chemical form of carbon dioxide.

3.5   Dose conversion factor

The dose conversion factor quantifies the annual radiation exposure (dose), which results from the use of groundwater contaminated with a given radionuclide concentration. The use of the groundwater implies both, direct uptake of the water and indirect uptake via the food chain. Therefore, the calculated dose conversion factor is strongly dependent on the consumption habits assumed for the population and the biosphere model applied. The dose conversion factors determined in /PRO 02/ are in compliance

---

[39] These numbers are calculated under the assumption that the number of containers that are corroding simultaneously and contributing to gas production is 8 at minimum and 56 at maximum and each container contributes 28 moles per year to the gas outflow.

with German regulations /AVV 90/ and include the following exposition pathways for their calculation:

(1) consumption of contaminated drinking water,

(2) consumption of fish from contaminated lakes,

(3) consumption of plants irrigated with contaminated water,

(4) consumption of milk and meat from cattle, which were watered and fed with contaminated fodder and

(5) exposure due to habitation on the contaminated land.

In the end, the conversion to the committed effective dose per unit intake of a given radionuclide is done on the basis of the ingestions dose coefficients published by /ICRP 96/. The resulting dose conversion factors for the radionuclides of interest here are listed in table 3.3.

The derivation of the ingestion dose coefficient of C-14 in /ICRP 89/ is based on the assumption that the ingestion of carbon occurs in the form of proteins, carbohydrates and fats. In these forms, the C-14 is completely taken up by and uniformly distributed in the body. This is surely true, if the carbon is ingested with products from the food chain as considered by the exposition pathways (2) to (4) from the list above. In these cases, the carbon has a long turn-over time in the body of about 37 to 40 days /NCRP 85, ICRP 89/. It is processed in the citric acid cycle and oxidized to CO_2, which is finally exhaled. During this process the C-14 is incorporated in all body tissues.

A somewhat different situation might be true, if the C-14 is ingested in the form of dissolved CO_2 with the drinking water. In this case, the ingested carbon is only slightly participating in the citric acid cycle and the turn-over time in the body is rather short, as can be deduced from experiments described in /ICRP 68/: "*Intravenous injection of labelled bicarbonate into two people, and measurement of exhaled radioactive carbon dioxide for 6 hr […] gave an apparent half-life of retention of 73 min.*". The situation for ingestion of dissolved carbon dioxide therefore might be more closely to the one ob-

served for the inhalation of carbon dioxide, than for the ingestion of carbohydrates and similar foods[40].

From these examinations it could be concluded that the use of the ingestion dose coefficient for the ingestion of drinking water with dissolved carbon dioxide overestimates by far the actual resulting dose. However, the total radiation exposure and the dose conversion factor are dominated by the exposition pathways (2) to (4), due to the high enrichment factors of carbon in the food chain. The direct uptake of drinking water only plays a very minor role for the overall dose conversion factor of C-14. Therefore, these considerations only apply if the ingestion of drinking water is regarded as the only or main exposition pathway and the dose conversion factor given in table 3.3 is used in the following.

Tab. 3.3   Dose conversion factors (DCF) in [Sv/a / Bq/m^3] /PRO 02/

Radionuclide	DCF
C-14	$4.6\cdot10^{-8}$
Cl-36	$3.5\cdot10^{-8}$
I-129	$5.6\cdot10^{-7}$

3.6   Estimation of potential radiation exposures

In this section, the results discussed in the preceding sections are summarised to draw a scenario of the processes leading to the release of radioactive gases from the repository for high level waste in a salt formation. Based on this scenario, the potential radiation exposure of the future populations is roughly estimated.

Scenario description

The water initially emplaced in the repository with the waste or backfill plus the water coming from the host rock lead to some container corrosion and gas generation, and do only affect the container integrity if pitting corrosion occurs. The gas production stops as soon as the water is consumed. The initially produced gases and the trapped

---

[40] For comparison: The dose factor for inhalation of C-14 containing CO_2 is $6.2\cdot10^{-12}$ Sv$\cdot$Bq^{-1} /BMU 01/.

air lead to a gas pressure build-up in the repository. The convergence of the mine openings due to the creeping of salt rock leads to a compaction of the backfill, a decreasing pore space and a further gas pressure increase. The maximum gas pressure in the repository is close to the hydraulic pressure at the top of the shaft[41].

Water is slowly flowing into the repository through the shaft and the flow rate is controlled by the permeability of the seals and the backfill[42]. The amount of water in the repository might be large enough to reach the waste containers in the emplacement area closest to the shaft and the container corrosion and gas production starts again. The arrival of the water in the emplacement drifts is expected to take at least several ten thousands of years. It is assumed that the backfill reaches a final porosity and the convergence stops before this point in time. The inflow rate determines how many waste containers corrode simultaneously and whether the corrosion progress is controlled by the corrosion rate or the inflow rate. The produced hydrogen gas leads to a partial water desaturation in the access drifts and is subsequently transported by two-phase flow through the drifts to the shaft and exits the repository. After some time, a steady state develops with respect to gas production and gas flow resulting in a constant gas flow from the emplacement areas, through the drifts and out of the repository. The pore water in the repository will be saturated by the hydrogen gas. For a constant pore volume, the time to develop the gas stream from the repository is depending on the gas production rate and the volume of the pore space in the repository[43].

Some thousands up to a few ten thousand years – depending on the solution composition and the temperature – after the contact of the containers with the inflowing water, some containers will start to fail due to the progressing corrosion and water vapour or liquid water if available sufficiently will intrude into the containers. C-14-containing organic compounds in the waste are converted in a multi-stage process into methane or carbon dioxide. Besides the produced carbon-containing gases, small amounts of other

---

[41] plus an eventual existing gas entry pressure

[42] The script for the repository evolution drawn in these paragraphs is based on the assumption that there exists a connected pore space and a permeability for liquid and gas transport in the compacted salt grit that allows for a Darcy-type flow, even at low porosity. However, there is still a lack of knowledge about the behaviour of salt grit and the value of its permeability at low porosity. If the assumption will turn out to be not true in the future, the specified evolution will differ fundamentally and the drawn conclusions are not correct.

[43] A retardation of the gas release could be achieved by gas storage in the mine. One possibility to store the gases in the mine could be the use of non-compactable backfill in the emplacement drifts /RUE 04/.

radioactive gases, especially I_2, may exist in the container. The radioactive gases are released from the container into the continuous stream of hydrogen corrosion gas and are transported within the gas stream up to the geosphere[44]. In case this continuous gas stream from the repository has already evolved before the container failure, the transport-time from the container up to the geosphere is determined by the ratio of the gas production rate and the accessible non-saturated pore volume and is not expected to significantly retard the release of the radioactive gases from the repository. If the containers fail at an early time, e. g. due to pitting corrosion or initial defects, and the steady state of the gas stream has not yet evolved at this point in time, an additional retardation of the gas release is expected until the gas flow has fully established.

The absolute amount of gases released from the repository is comparably low. Therefore, the gases are expected to be dissolved completely in the groundwater in the geosphere. The use of the contaminated groundwater can lead to a potential radiation exposure of the population.

Estimation of potential radiation exposure

Based on the scenario described above and the values given in the preceding sections, the potential radiation exposure of the future population is estimated. The radiocarbon is assumed to be released within 400 years from the IRF and within 1 000 years from the cladding after the container failure, yielding a mean initial release rate after container failure of $1.74 \cdot 10^{-3}$ per year[45]. The transport time in the mine and the geosphere is conservatively neglected. The amount of gases released per year are completely dissolved in an overburden groundwater flow of 20 000 m^3 per year. This water is afterwards used by the population causing a radiation exposure. The potential radiation exposure prevails as long as radiocarbon containing gases are released from the repository, which is after 1000 years under these assumptions. Annual doses are calculated using the dose conversion factors given in table 3.3.

---

[44] The dissolution of radioactive gases in the pore water in the mine is expected to be negligible due to the low partial pressure of the respective gases in the hydrogen gas stream and the low amount of water in the mine.

[45] The radiocarbon inventory 40 years after removal from the reactor is $2.8 \cdot 10^{10}$ Bq for the IRF and $7.1 \cdot 10^{10}$ Bq for the cladding per container (see table 3.1).

Due to the relatively short half-life of C-14, the calculated radiation exposure is highly depending on the time of the start of the release. Therefore, in figure 3.3, the potential annual radiation exposure is plotted as a function of the release start. The blue shaded area gives the expected bandwidth resulting from the uncertainty about the numbers of container affected simultaneously. The dashed lines give the extreme bandwidth for the case that either only one or all containers in one emplacement area are affected.

Figure 3.3 shows that the release into the groundwater must not start before about 40 to 55 000 years[46] for a maximum annual radiation exposure[47] to stay below $1 \cdot 10^{-5}$ Sv·a^{-1}. This retardation time can be either achieved by a late release of the radioactive gases from the containers or by a long travel time of the gases in the mine.

Comparing this time to the onset time of the container contact with the inflowing brine as given in table A.1, and keeping in mind the time necessary for a full corrosion of the container and the time needed to establish a steady state gas flow from the repository (see also chapter 4), one can be confident, that the contact of the water with the waste container will occur late enough to ensure that the C-14 decays sufficiently before the release starts. This is especially true, if non-compactable backfill is used in parts of the mine, delaying the water inflow and the gas release. However, from this assessment it is also evident that the possibility of a relevant release of C-14 from the repository cannot be ruled out a priori and has to be demonstrated depending on the repository concept.

---

[46] A ten times higher conversion rate of the C-14 would result in a ten times higher potential radiation exposure. In this case, the container must not fail before about 60 000 to 75 000 years.

[47] The given value corresponds to the maximum additional effective dose rate given in /BMU 10/ for a probable repository development. The value for a less probable development is by a factor of ten higher.
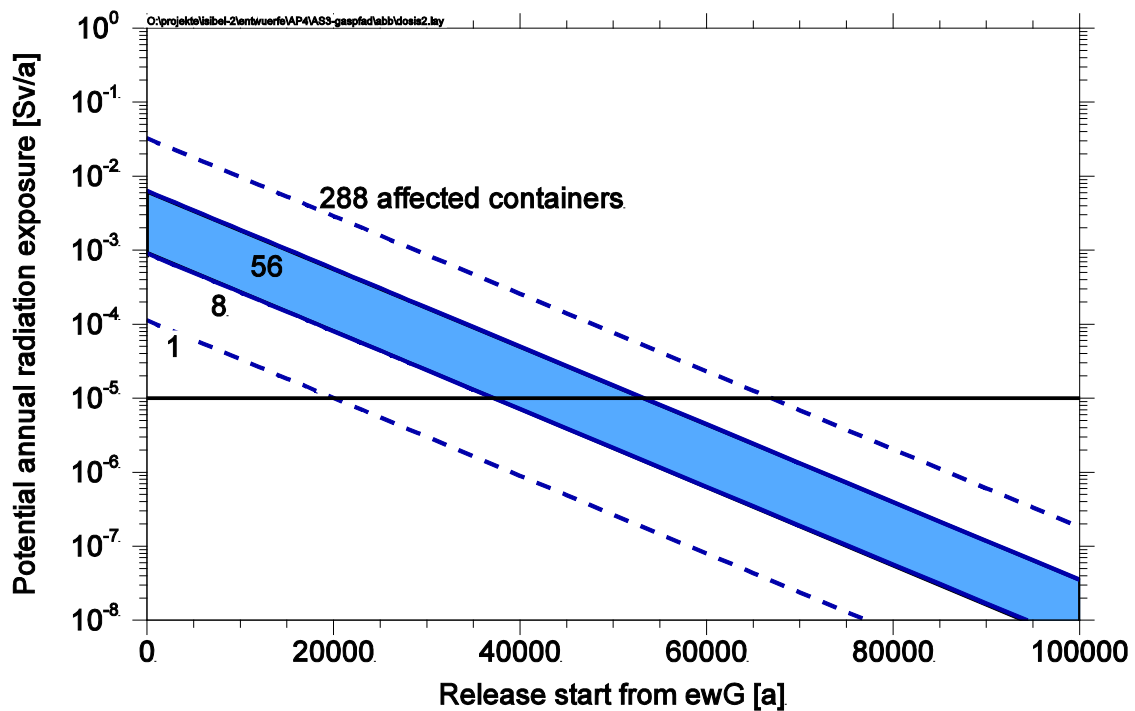
Fig. 3.3   Estimated radiation exposure from release of gaseous C-14 as a function of the container failure time for different numbers of containers affected

As discussed in section 3.1, a few radionuclides might potentially exist in gaseous form, but are believed to be dissolved rapidly in the brine due to high reactivity and solubility. However, it has to be kept in mind, that some of these radionuclides have a long half-life and might contribute to the dose even if the fraction of the radionuclide in gaseous form is very small. This issue is discussed on the example of I-129, which is the most relevant of the radionuclides mentioned.

The I-129 inventory in one container according to table 3.2 is $8.66 \cdot 10^9$ Bq from which 4 % reside in the gap and grain boundaries /JOH 05/. According to the considerations discussed in section 3.1, there is a probability that parts of the IRF fraction might exist in the gaseous form of I_2. An exemplary fraction of one per mil[48] is used in the following[49]. It is very unlikely that all fuel rods stored in one container will release their gases at once, so that an exemplary release period of 10 years is assumed during which the

---

[48] This estimation results from the assumption that 90 % of the iodine is in the form CsI and that 1 % of the remaining 10 % are in gaseous form. This assumption is however not supported by any evidence, but is only exemplary.

[49] i. e. $4 \cdot 10^{-5}$ of the total inventory

gaseous iodine is released into the hydrogen gas stream. Applying all other assumptions like for radiocarbon, this leads to a potential annual radiation exposure of $1 \cdot 10^{-6}$ Sv·a^{-1} per container. Due to the long half-life of I-129, this value is more or less independent of the onset time of the release. Due to the short release time span assumed, a simultaneous failure of multiple containers is quite unlikely.

However, if processes might exist, that lead to the failure of multiple containers within a short time span, the estimated potential radiation exposure is higher by the number of containers involved. One of such potential processes can be, for example, the mechanical failure of the containers due to the rock pressure, if types of containers are used which are not designed to withstand the rock pressure[50]. In this hypothetical case, a release can even occur without a sufficient amount of water available to fully corrode the containers. This consideration emphasises the importance of the use of containers that withstand the rock pressure.

3.7   Résumé

In this chapter, the principal relevance of a release of gaseous radionuclides from a repository for high level waste in a salt formation has been discussed on the basis of existing literature. From this information, the following conclusions can be drawn:

−   No release of gaseous radionuclides has to be expected if the waste containers stay intact.

−   If the containers fail, a potential radiation exposure might result from release of C-14 and I-129 through the gas pathway.

−   The question whether a release of radioactive gases from the repository might occur is linked to the question whether the waste container gets in contact with a significant amount of water. For the release of C-14 itself, it is an open question, whether the contact of the waste with water is a prerequisite for the transformation of the C-14 into gaseous form or not.

---

[50] At the time of writing, all types of containers considered for the disposal of spent fuel in Germany are designed to withstand the rock pressure due to regulatory requirements for a potential future recovery of the waste form from the repository /BMU 10/.

- A carrier gas is needed to transport the radioactive gases out of the repository. This might be either trapped air compressed by the convergence process and/or gases from corrosion and degradation processes.

- Due to the relatively short half-life of C-14, the impact of the release of C-14 can be lowered by delaying its release, i. e. the contact of the waste with water or the retardation of the gases in the mine by storage.

- The strategy to lower the potential radiation exposure by delaying the release does not work for I-129 due to its long half-life.

- There are open questions about the chemical form of iodine, but even small fractions of I_2-gas can lead to a non-negligible dose due to I-129 release.

- There might be a small release of I_2-gas even without a contact of the canister with water, if a container fails mechanically. In this case it is highly scenario dependent whether there exists an additional gas stream to transport the radionuclides.

According to the results obtained in this project, the release of gaseous radionuclides from a repository for high level waste in salt has to be considered in the safety assessment, but is not considered to be an issue that could jeopardize the concept of nuclear waste disposal in salt, since additional measures are available to reduce the potential consequences of gaseous radionuclide release. These are for example to consider gas storage areas in the repository to delay potential gas release from the repository. Open questions and uncertainties remain on which an eye has to be kept on, like the distribution of the radioactive inventory in the different compartments and their release rates.

4   Two phase flow in the near field

The transport of gases in the repository mine has not been regarded in detail in previous long-term safety assessments for nuclear waste repositories for high-level waste in salt formations[51]. The final report of the research project ISIBEL /TEC 08/ states as one open issue requiring further R&D work in the field of performance assessment that:

"*It should be investigated whether the formation and behaviour of gases in a final repository for HLW need to be considered in more detail in the safety assessment models. So far, the accumulation of gas in a segment and the release of gas from a segment have been considered in the concept only in a very simplified form. The transport of gases between the mine workings cannot be calculated explicitly but is given implicitly as a boundary condition that is determined by prior calculation using external codes. Before conceptual models for the transport of gases can be developed, the volume of gas formation in a final repository for high-level radioactive waste needs to be determined. It is possible that the effects of gases in the final repository are negligible so that the development of a computer code could be unnecessary.*"

The two preceding chapters of this report have shown that:

−   Some gas production is likely to occur by corrosion or degradation of emplaced metallic or organic material, even if there is no inflow of external waters. There is sufficient water available in the repository coming either coming from the host rock or the materials emplaced to start the gas generation processes.

−   A small fraction of radioactive gases may be present or produced in the spent fuel containers. In case of container failure, the radioactive gases can be dispersed into the larger amount of non-radioactive gases in the mine.

−   In case of gases being released from the repository into the geosphere, a potential radioactive fraction of the gases may contribute significantly to the expected annual radiation exposure.

Due to the given findings, a potential relevance of the gas flow for the repository system evolution and the long-term safety cannot be excluded a priori. Therefore, the gas

---

[51] Some remarks regarding the procedure in previous safety assessments are given in chapter 5.

flow in the repository mine and its potential interaction with the fluid flow has to be investigated in the safety assessment.

The work presented in this chapter was performed to decide whether the gas flow should be implemented in a future version of the long-term assessment code used at GRS and if yes, in which way; does one have to regard two-phase flow models, or may highly simplified abstracted models suffice. The investigation is done on the basis of numerical simulations for two generic examples. The interaction between the gas flow and the fluid flow is assessed

1. during the inflow phase of the fluid through the shaft (case 1, see section 4.1) and

2. through a low-permeable geotechnical drift sealing (case 2, see section 4.2).

The numerical simulations were carried out by applying the widely accepted van Genuchten two-phase flow theory. A very brief introduction to the theory of two phase flow is given in Annex A.2. Four different codes were taken into consideration to perform the simulations. The list of codes considered and the arguments to finally choose TOUGH2 as numerical code are shortly listed in Annex A.3.

4.1 Case 1: Inflow through the shaft

The first test case considers the inflow of water from the overburden into an initially air filled repository mine. A schematic layout of the regarded repository is shown in figure 4.1.
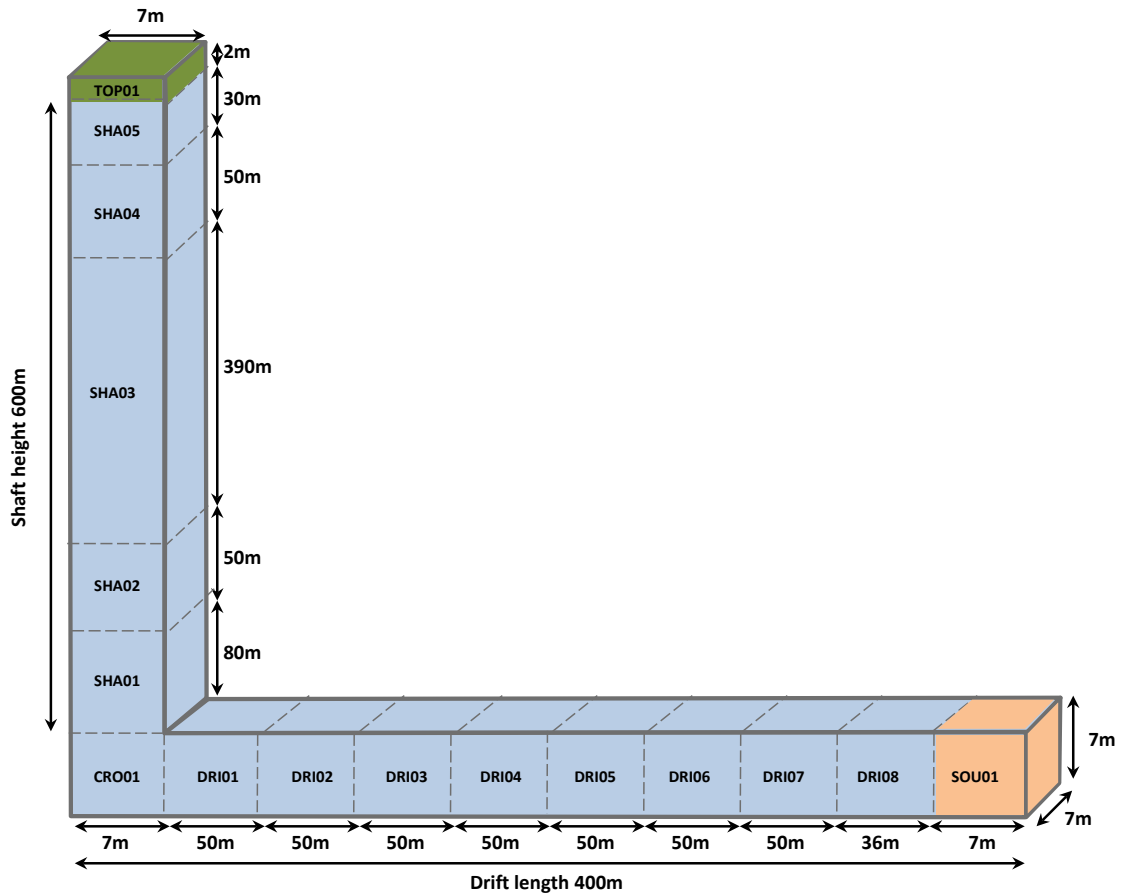
Fig. 4.1 Schematic picture of the layout of the low discretized model of case 1 (not to scale)

The repository model is highly simplified and consists of one shaft of 600 m depth and an access drift of 400 m length. For the simulation with TOUGH2, the shaft is discretized into five segments of variable length, while the drift is discretized into nine segments, most of them 50 m in length. Above the top of the shaft, a saturated overburden is assumed resulting in a hydrostatic pressure of 3 MPa at the shaft top. This corresponds to an overburden thickness of 300 m if fresh water is assumed. Therefore, the actual level of the access drift is about 900 m below ground.

For the repository mine, the model assumes salt grit at the state of full compaction as backfill throughout the repository with constant and uniform material parameters. The porosity is taken as 0.01 with a corresponding permeability of $1 \cdot 10^{-19}$ m^2. The permeability is in accordance to the PSE-law /STO 85/ for the porosity-permeability dependence of salt grit, if an exponent of five and a prefactor of $1 \cdot 10^{-9}$ m^2 is used. The material parameters for the two-phase flow are chosen accordingly to the parameters given in /KRO 09/ and resulting from experiments documented in /CIN 06/ which were performed on commercially available table salt. It has to be noted that it is questionable, whether the data from those experiments are valid for the salt grit which is used for backfill in a repository. However, since no other data is available up to date of this report, this data is used.

Two different variants are regarded, with and without gas production from corrosion. In both cases, the repository is initially filled with air at a pressure of 0.13 MPa. In case of variant b, an additional gas production of $1 \cdot 10^{-8}$ kg·s^{-1} is assumed in the rightmost segment of the access drift (segment SOU01). Since air is assumed as gas in the simulations, this gas production rate corresponds to a gas amount of about 10 moles per year. This value is at the lower end of the bandwidth expected for the gas production rate under realistic conditions in a repository for high level waste in salt (see also section 3.2). The most important model parameters are summarized in table 4.1. The TOUGH2 input file for simulation 1b is listed in Annex A.4.

Under the conditions described, the expected evolution in the repository mine is as follows: water is flowing into the repository mine through the shaft, driven by the hydrostatic pressure at the shaft top. Since the pore space is gradually occupied by the water, the gas is compressed and the pressure in the mine is slowly rising. If the local gas pressure in a partly saturated segment exceeds the gas entry pressure of a fully saturated neighbour segment, the gas is entering and transported through the according segment by two phase flow. In that way, the gas is step by step transported through the drift, into the shaft and finally exits the repository at the top of the shaft.

The final situation at the end of the inflow phase depends on the fact whether there is gas production on not. If there is no gas production, it is expected that virtually all of the gas will be either dissolved in the water or displaced from the mine by the inflowing water. This results in a full saturated state throughout the repository mine, with the exception of some small amount of air that might be trapped at the dead end of the drift at a pressure of the local hydrostatic pressure plus the gas entry pressure.

If there is gas production, it is expected, that in steady state, the gas flow through the repository is constant throughout the repository and equals the gas production rate. The saturation stays below full saturated state and is locus-dependent, but time-independent. The actual final saturation level at each position in the mine mainly depends on the porosity, the gas production rate, the permeability and the local hydrostatic pressure.

Tab. 4.1   Model parameters for case 1

General parameters		Value
Density of salt grit	[kg·m^{-3}]	2 165
Porosity of salt grit	[-]	0,01
Permeability of salt git	[m^2]	1E-19
Density of solution	[kg·m^{-3}]	1 000
Volume of the repository mine	[m^3]	49 000
Pore volume in the mine	[m^3]	490

Van Genuchten two phase flow parameters		
m	[-]	0,73
θ_{lr}	[-]	0,18
θ_s	[-]	1,0
θ_{gr}	[-]	1E-3
α	[MPa^{-1}]	2E-5

Initial and boundary conditions		
Gas production rate	[kg·s^{-1}]	0, resp. 1E-8
Hydrostatic pressure at shaft top	[MPa]	3
Initial gas pressure	[MPa]	0.13
Initial liquid saturation	[-]	0.001

For a complete listing of the input file see Annex A.4

4.1.1   Variant 1a: No gas production

The first variant of case 1 investigates the inflow behaviour into the initially air filled mine without an additional gas production. Figure 4.2 shows the saturation and the pressure in the repository versus the position for different times. The position is given

relative to the lower left corner of the model (segment CRO01). Distances in the drift are given as positive distance, while the height in the shaft is given as negative value. At the top of the shaft (position = -604.5 m), the saturation is constant 1 and the pressure is 3 MPa. At the beginning (t = 0), the saturation is 0.01 and the pressure is 0.1 MPa in the rest of the mine.

With increasing time, the saturation increases in the mine due to the water inflow. Until 100 000 years, the shaft is still not fully saturated and the water front reaches about 150 m into the access drift. Accordingly, the pressure monotonously decreases from the maximum value of 3 MPa at the top of the shaft down to low values of 0.5 MPa more than 125 m into the drift. After one million years, the shaft and most of the drift is completely saturated. Only in the last 100 m of the drift, the saturation is slightly below 100 %. The pressure linearly increases from the top to the bottom of the shaft in accordance with the height of the water column. In the drift, the pressure is nearly constant.

Figure 4.3 shows the temporal evolution of the saturation and the pressure for selected segments. The water inflow is reaching the drift after about 80 000 years and nearly all drift segments are completely saturated after 200 000 years. Only the last segment shows a very slow increase in saturation after 200 000 years and the process is still not complete after one million years. The pressure, however, is nearly constant after 200 000 years in all segments.

The results of the two phase flow simulations with TOUGH2 were compared to results obtained from simulations using the code LOPOS which only regards single phase fully saturated flow /BUH 99/. The model for the LOPOS simulation was set up with the same discretization as shown in figure 4.1. The pressure boundary condition and the material parameters for permeability and density are chosen in the same way as in the TOUGH2 model. Figure 4.4 shows the comparison of the calculated pressures in selected segments. A reasonably good agreement was achieved between the two-phase flow TOUGH2 results and the single phase LOPOS results. The results from the TOUGH2 simulation generally show an early rise of the pressure, which is related to the pressure in the gas phase due to the compression of the air. This effect is not regarded in the LOPOS simulation. Other obvious differences are the results for the pressure in each segment at very late times, which are the steady-state values. This difference is a model artefact that is due to the different position in the segments were the pressure values are calculated by the respective programmes and is therefore re-

lated to the height of the respective segment. Consequently, the largest difference is found for the 390 m high segment SHA03. As stated above, this difference is only of technical reason and does not compromise the consistency of the results. The actual saturation of the segments and the point in time, when the full saturation of each segment is reached is almost the same in both simulations.

Therefore, it can be stated that in this case, the displacement of the air from the mine by the inflowing water obviously does not hinder the water inflow considerably. If there is no additional gas production, the single phase flow simulations as performed with LOPOS yield sufficient well results. Some differences may occur for dead end parts of the mine, where air is trapped. The situation changes, if the initial gas pressure in the mine is significantly higher than the assumed value of 0.1 MPa. Gas pressures higher than the atmospheric pressure are expected due to the convergence of the mine and the compaction of the salt grit. When emplaced, the salt grit has an initial porosity of about 30 %. Compacted down to 1 %, the gas pressure in the pore space is consequently expected to rise up to 3 MPa, if no gas is flowing out of the mine.

The effect of higher initial gas pressures on the two-phase flow process can be studied in figure 4.5. This figure shows the result of four variation simulations with TOUGH2 for initial gas pressures of 0.1, 1.1, 2.1 and 3.1 MPa, respectively. It is clearly obvious, that the higher the initial gas pressure, the more the water inflow is hindered and the later the fluid pressure rises in each segment. Also the point in time at which the full saturation in each segment is reached is considerably delayed by the initial gas pressure.

LOPOS is not able to reproduce this effect in a similar way. The higher initial pressure results in a decrease of the effective hydraulic gradient at the shaft top. Therefore, an initial pressure of 3.1 MPa results in the inflow to stop completely. The fluid is not able to enter a gas filled segment at the same pressure level in the single phase simulation. If the initial pressure is 2.1 MPa, some inflow occurs also in the LOPOS model, as is shown in figure 4.6, but the results do not very well compare to the results obtained with TOUGH2.

For gas pressures which are low compared to the hydraulic pressure, the effect of hindrance of the fluid inflow can be neglected. However, if the gas pressure is higher, the actual local gas pressures and the two phase flow processes have to be taken into account.
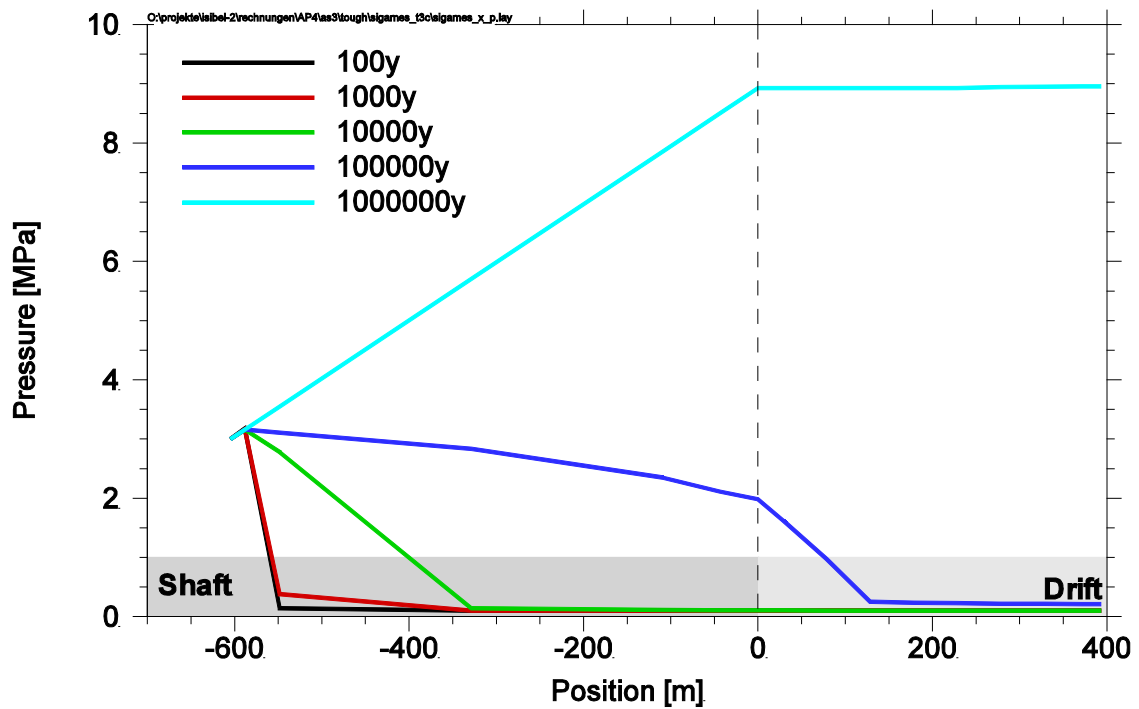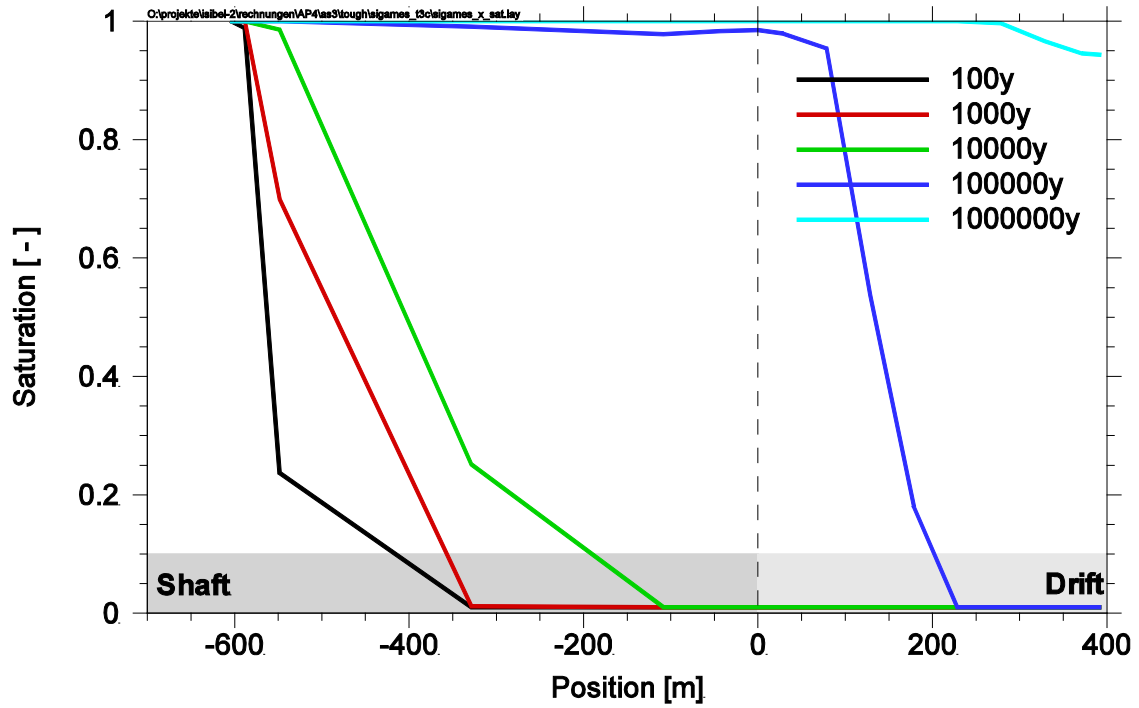
Fig. 4.2 Saturation and pressure along the shaft and drift for selected times

The position is given as distance to segment CRO01, where negative values denote vertical distance (height) in the shaft and positive values denote horizontal distance in the drift
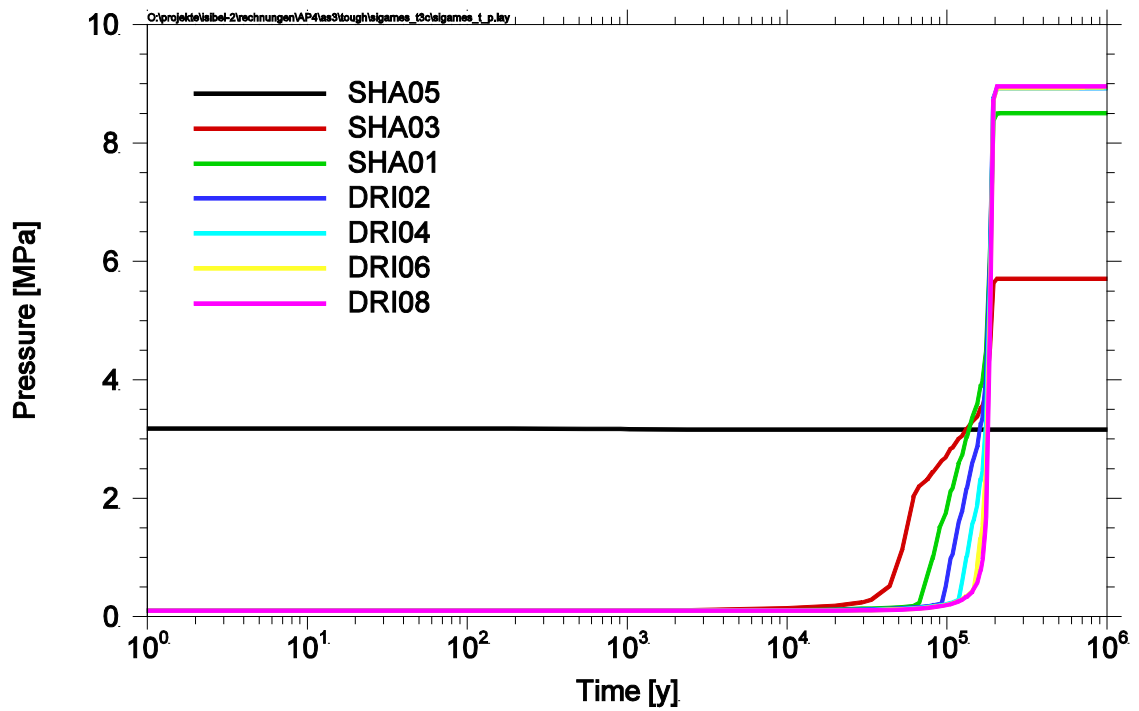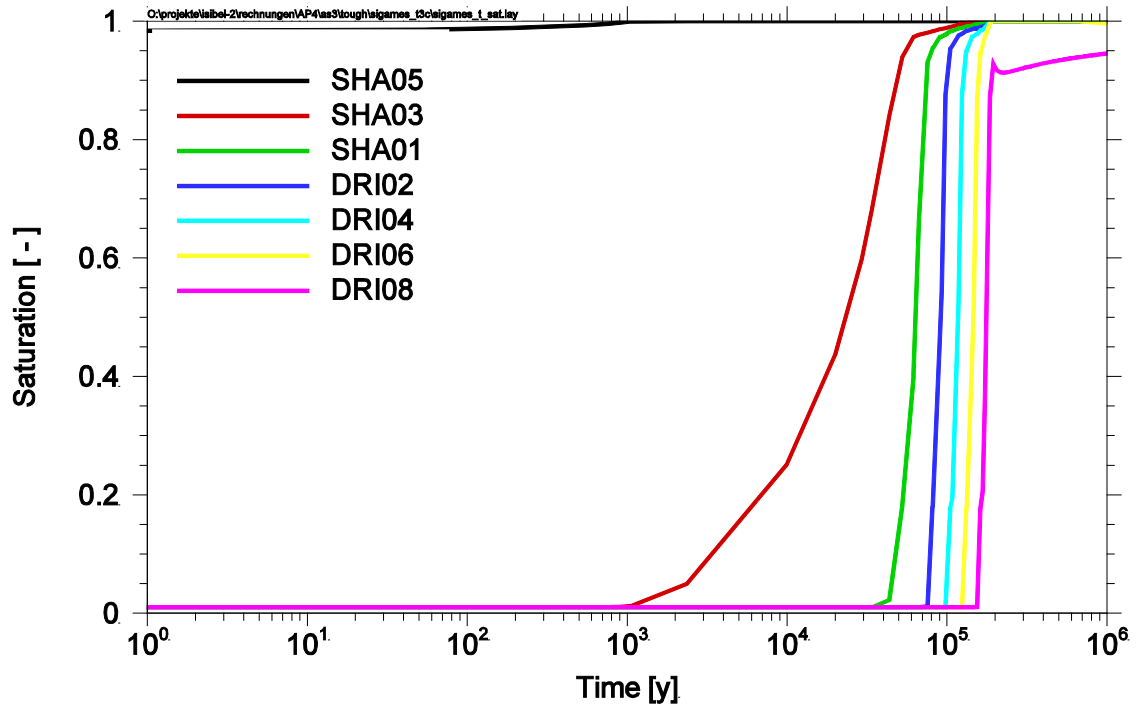
Fig. 4.3 Evolution of saturation and pressure versus time for selected segments
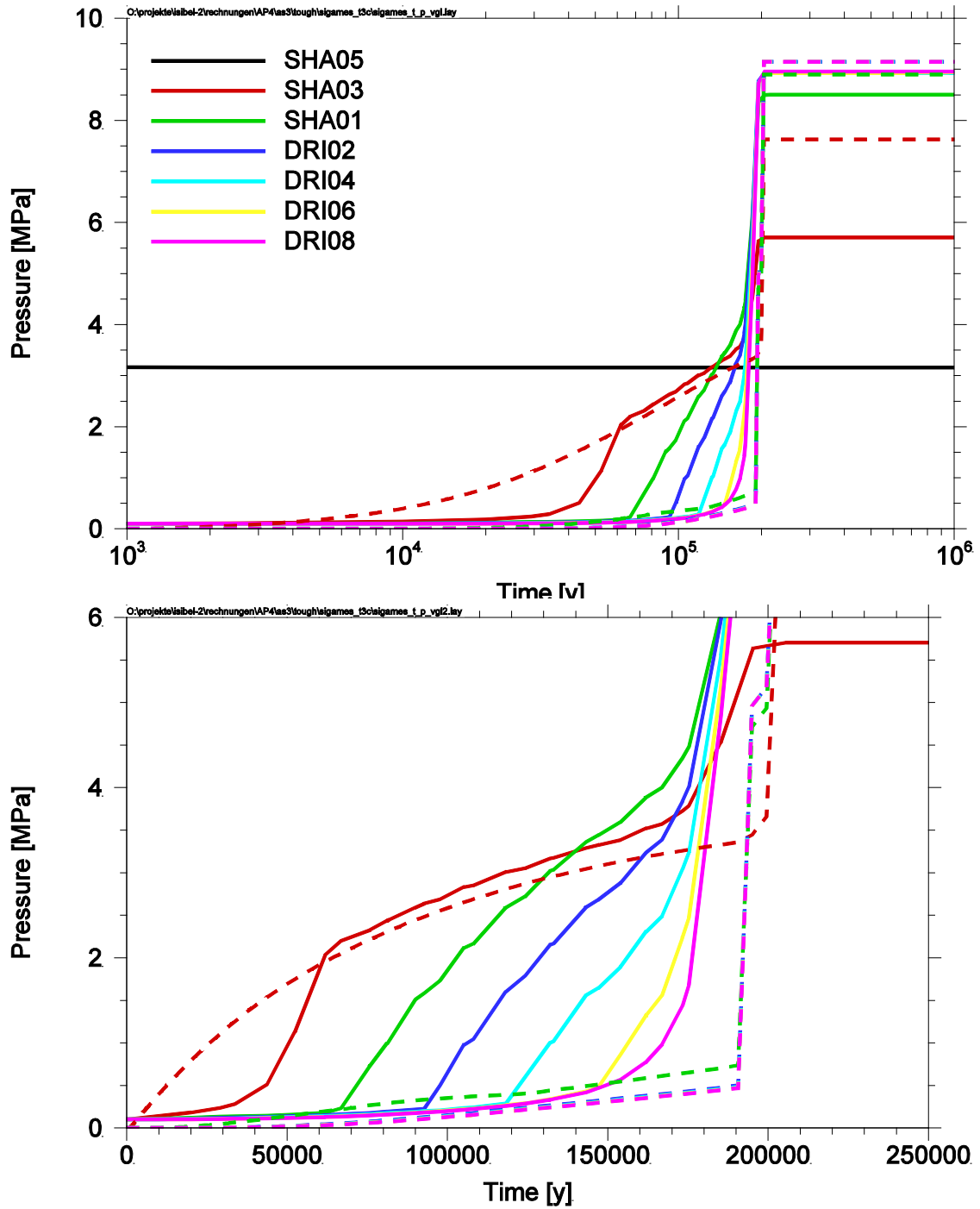
Fig. 4.4   Evolution of pressure versus time for selected segments from two and single phase flow simulations

The lower figure is a detail of the upper using a linear x-axis.

solid lines: two-phase gas/liquid flow simulation with TOUGH2

dashed lines: single phase liquid flow simulation with LOPOS
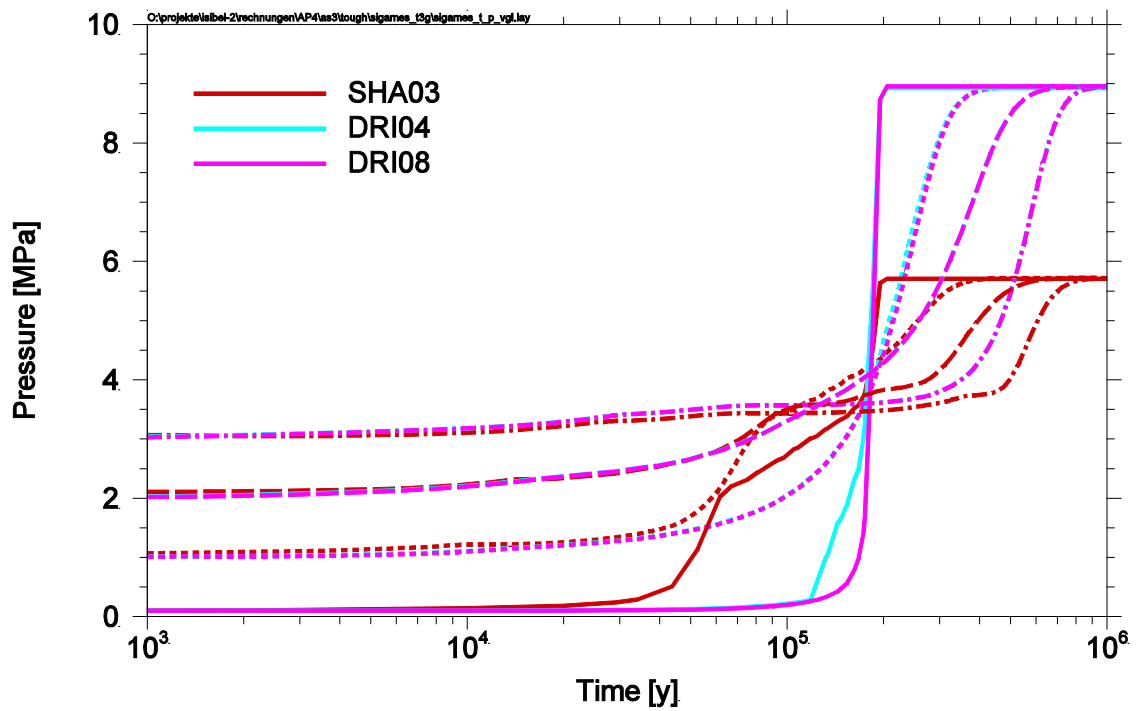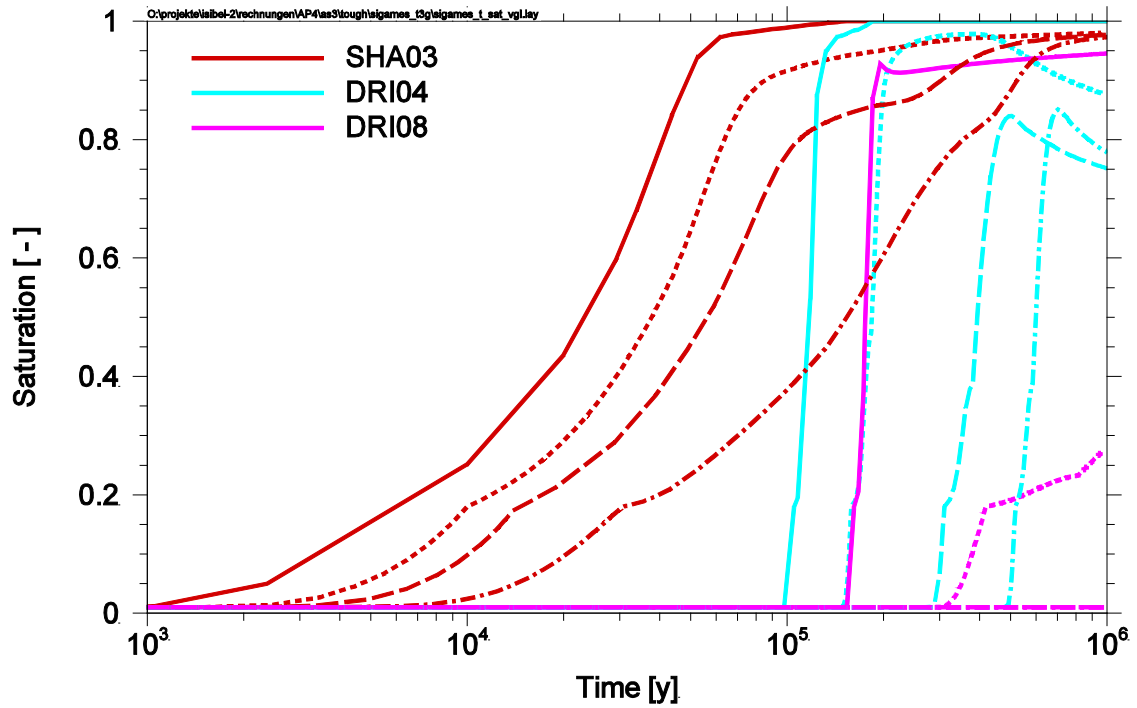
Fig. 4.5   Evolution of saturation and pressure versus time for selected segments and for different initial gas pressures

solid lines:	0.1 MPa (see figure 4.3)
dotted lines:	1.1 MPa
dashed lines	2.1 MPa
dash-dot lines	3.1 MPa
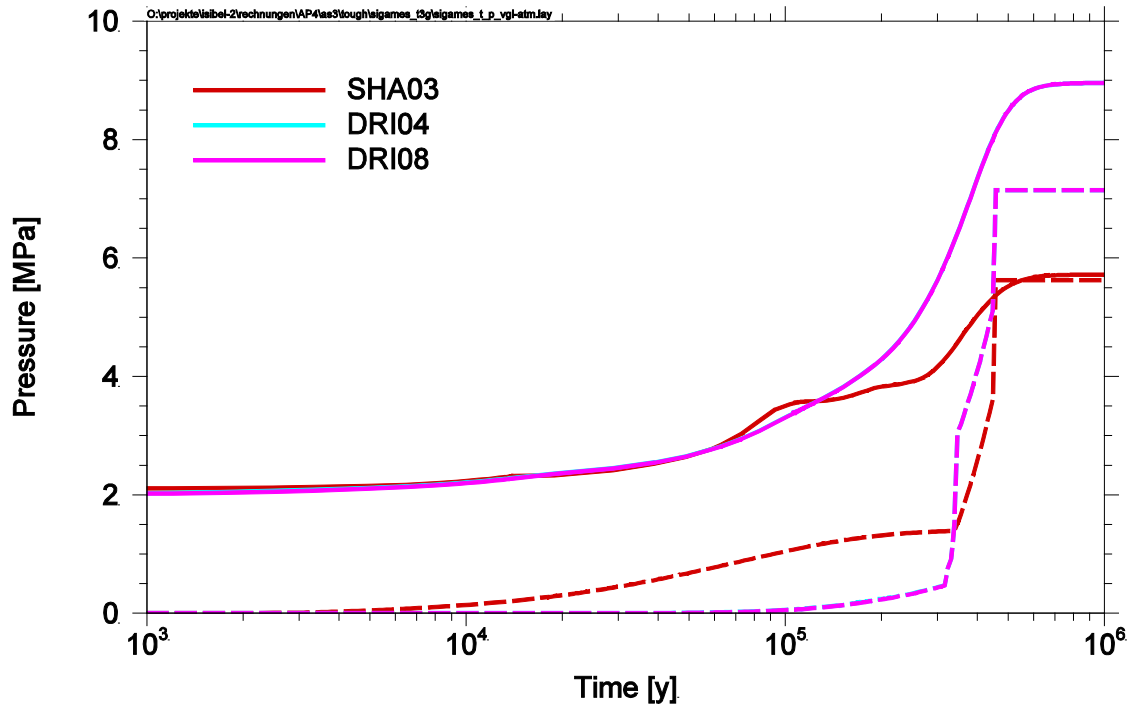
Fig. 4.6   Evolution of pressure versus time for selected segments from two and single phase flow simulations for a higher initial pressure of 2.1 MPa

solid lines: two-phase gas/liquid flow simulation with TOUGH2
dashed lines: single phase liquid flow simulation with LOPOS

4.1.2   Variant 1b: Gas production

The second variant of case 1 investigates the inflow behaviour into the initially air filled mine with an additional constant gas production of about 10 moles per year in the rightmost segment of the drift (SOU01). The gas production is assumed to start directly at the beginning of the period under investigation.

Figure 4.7 shows the saturation and the pressure in the repository versus the position for different points in times. Significant differences can be recognized to the variant without gas production. Even for early times, the increasing pressure from the gas production at the end of the drift is clearly visible. After about 40 000 years, the pressure is more or less the same throughout the repository mine. At the end of the simulation time, the pressure shows a linear increase in the shaft in the same way as in the variant without gas production. With gas production however, the pressure also increases along the access drift due to the gas pressure. The saturation does not reach the fully

saturated state throughout the mine. While in the shaft, the saturation rises to values around 70 %, the saturation in most part of the drift remains below 5 % until the end.

Figure 4.8 shows the temporal evolution of the saturation and the pressure for selected segments. Especially from the temporal evolution of the pressure, it is visible that the system is not yet in steady state after one million years. It is interesting to see that the system reaches a semi stable state at around 100 000 years (lower figure in 4.8), where the pressure is rather constant throughout the mine for several 100 000 years, until the pressure significantly rises again at about 400 000 years. The same effect can be seen in figure 4.9, which shows in the lower part the gas flow versus time for selected segments. After about 100 000 years, the system is close to the steady state with regard to the gas flow. The gas entering the drift in segment SOU1 is transported through the mine from segment to segment with nearly the same rate and finally leaves the mine at the shaft top. Later, changes in the pressure regime result from comparably small changes in the gas flow to settle the steady state which is reached approximately after two million years, which is not depicted in the figures.

Two points in time are of special interest with regard to the long-term safety. These are first of all, the time when the outflow of gases from the mine starts and second, when the outflow from the mine reaches the same rate than the production rate. From figure 4.9 these two points in time can be determined to be about 50 000 and 100 000 years. The reason why these two points in time are of interest is the potential release of radioactive gases. The first point in time is when radioactive gases may be potentially released to the geosphere. Radioactive gases with a short half-life compared to this timespan are subject of a notable radioactive decay in the mine. After the second point in time, one can easily estimate the travel time of the gases in the repository mine, i. e. the retention of gases, by dividing the gas production rate by the gas volume in the mine. For the presented simulation, the amount of gases in the mine at stead-state is 260.7 m^3 corresponding to a mean water saturation in the mine of 46.7 %. The mass of gas is about 23 150 kg. With a gas production rate of 0.315 $kg \cdot a^{-1}$, this results to a mean travel time of the gas in the mine of about 73 000 years.

Depending on the radionuclides present in the gas phase, a late release of the gases from the mine and a long travel-time in the mine might be preferable since the radioactivity of the radionuclides is reduced by radioactive decay. This is especially true for the potential volatile radionuclide C-14 which has a half-life of 5 730 years. For C-14, a

travel time of 70 000 years would result in a reduction in activity by more than three orders of magnitude.

However, the time span until the first release is significantly depending on the gas production rate and the volume in the mine, i. e. the repository concept. Figure 4.10 shows as example the gas flow for a simulation in which the porosity in the whole mine is reduced by a factor of 10 compared to the simulation presented before, and hence is 1 per mil. The same result is derived, if the gas production rate is increased by a factor of 10. The change of the according parameter value in the simulation results in the first gas release from the repository to occur already after 5 000 years and in a mean travel time of the gases in the mine of 7 300 years. These timespans are by a factor of 10 shorter than given above and therefore are of very high influence on potential releases C-14. Since gas production rate and the backfill porosity are such sensitive parameters for the simulation results, the gas flow in the repository has to be determined specifically for each repository concept. The uncertainty of the simulation can have a high impact on the uncertainty of the calculated potential radionuclide flows from the repository in some cases.

It was tested, whether the influence of the gas flow can be regarded in the LOPOS code in terms of very highly abstracted models using decoupled flow in both phases. The two approaches used were

−   the assumption of a perfectly mobile gas (resulting in instantaneous balance of the gas pressure throughout the mine) and

−   the use of an adopted relative permeability for the fluid phase as a function of the saturation degree.

Both approaches did not at all lead to a satisfying approximation of the TOUGH2 results (see also figure 4.11).

As stated before, the issue of the gas transport and the potential release of volatile radionuclides are issues to be considered with regard to the long-term safety of a high level waste repository in salt. There is expected to be a high sensitivity of the model results on the repository concept like on the pore space available for gas storage and on the material parameters. Therefore, it is recommended to consider the gas transport in the repository mine in the long-term safety assessment code in future performance assessments and to use an appropriate two-phase flow model approach for the gas flow.
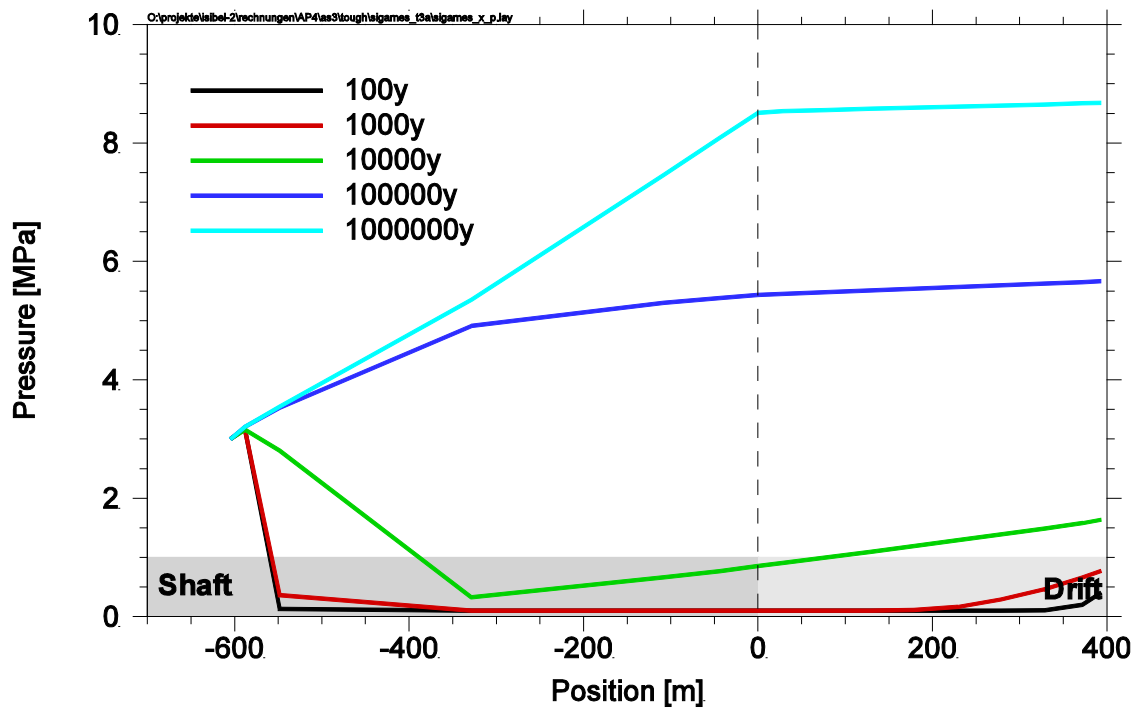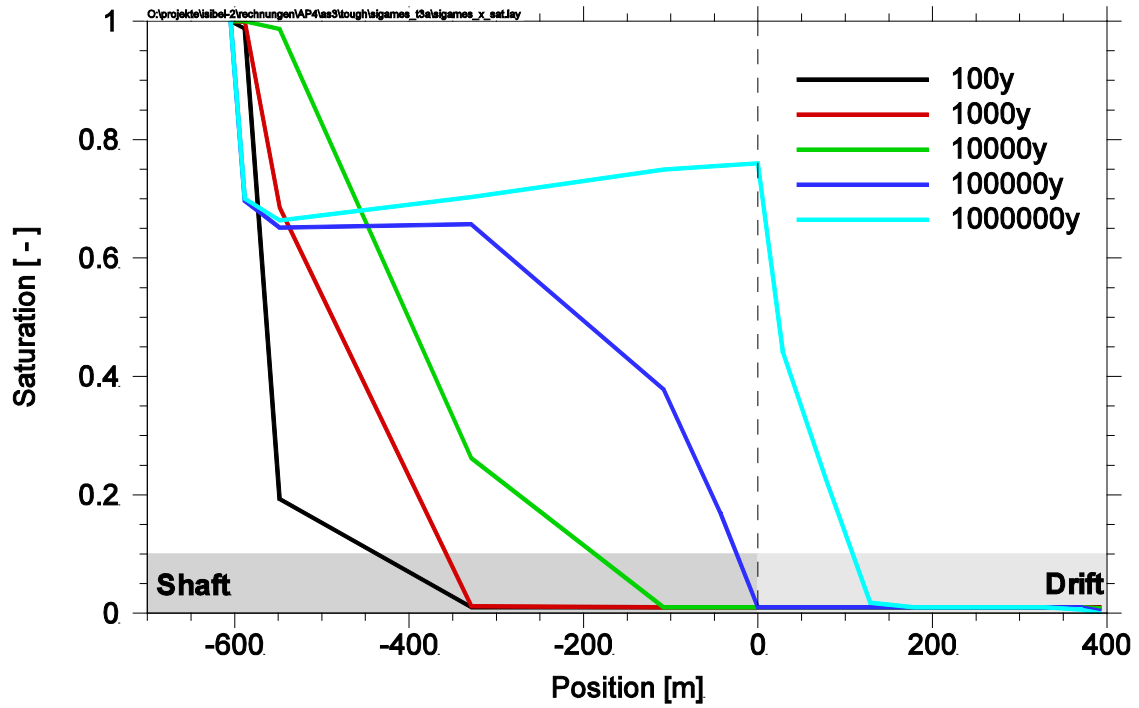
Fig. 4.7 Saturation and pressure along the shaft and drift for selected times.

The position is given as distance to segment CRO01, where negative values denote vertical distance (height) in the shaft and positive values denote horizontal distance in the drift.
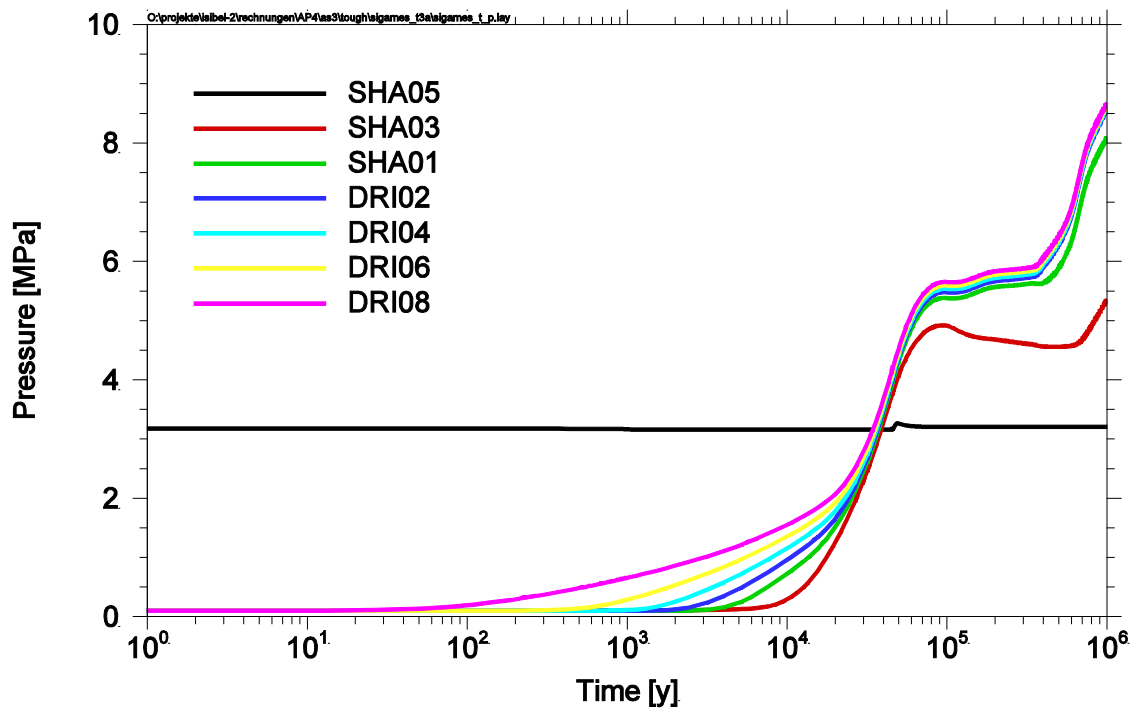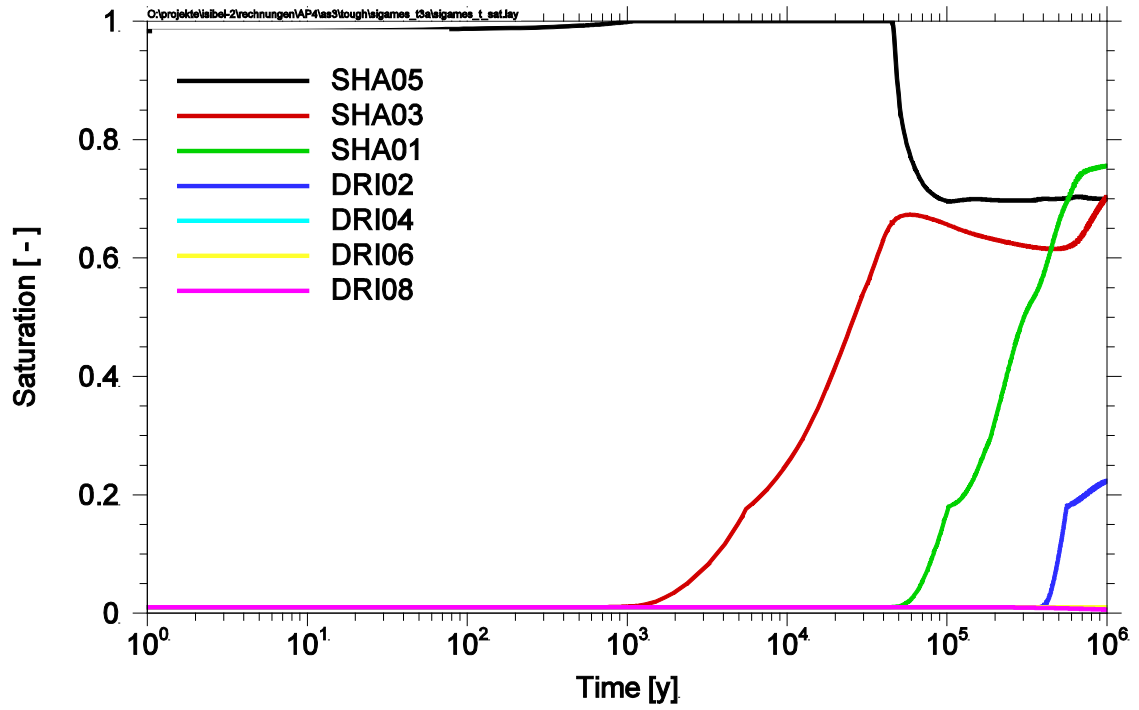
Fig 4.8   Evolution of saturation and pressure versus time for selected segments
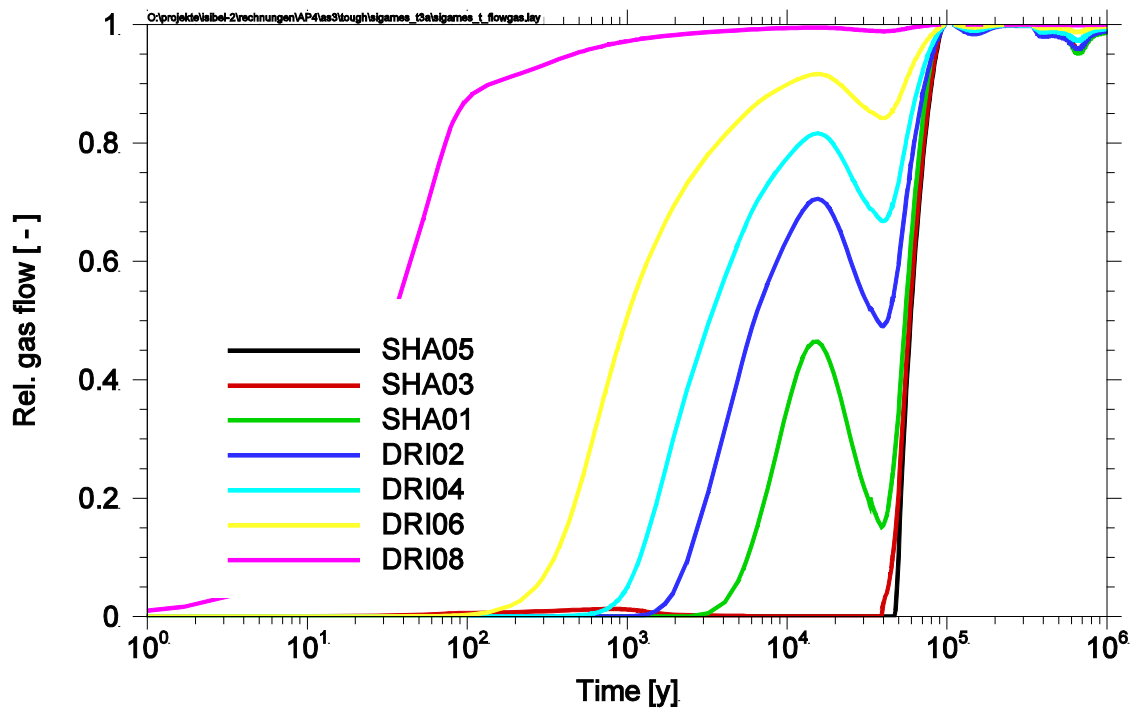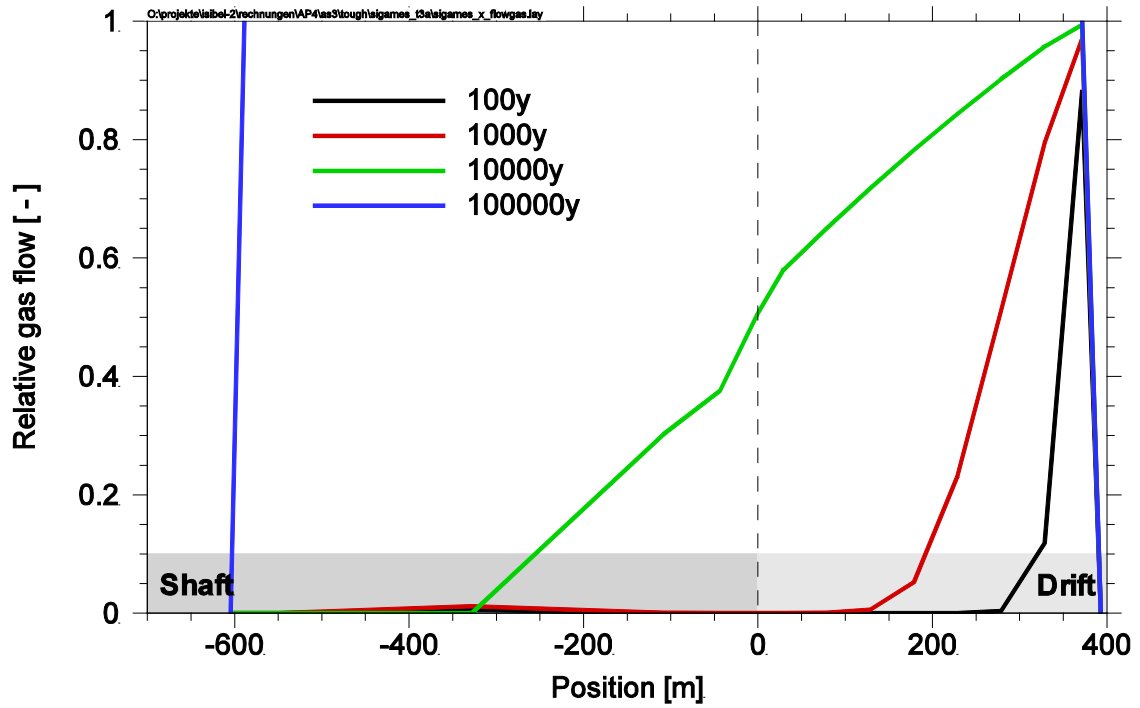
Fig. 4.9 Gas flow normalized on the gas production rate versus position and versus time
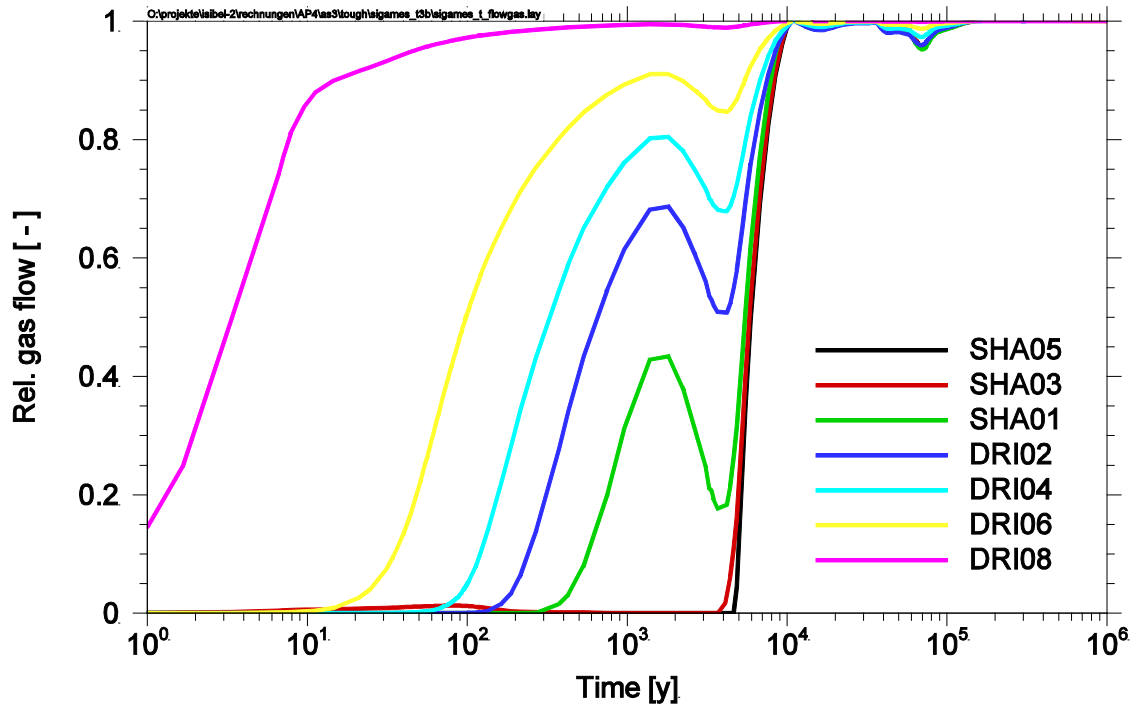
Fig. 4.10   Gas flow normalized on the gas production rate versus time.

Compared to the lower part of figure 4.9, the porosity is reduced by a factor of 10.
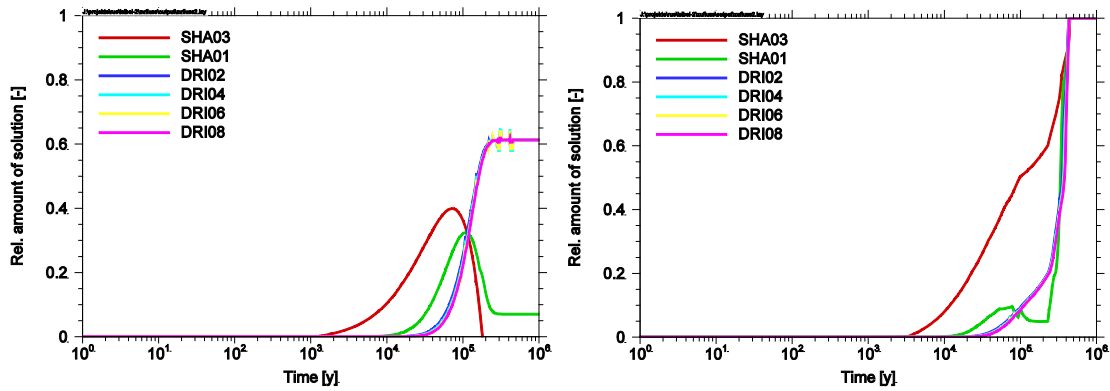
Fig. 4.11   Results from simulations with decoupled gas/liquid phenomena with LOPOS.

left: infinite mobile gas approach
right: use of adapted "relative" permeability

4.1.3 Variant 1c: Gas production, increased model resolution

The discretization of the model used in the simulations presented before is rather coarse and consists of only 15 elements. To test the influence of the discretization of the model on the results, another model was set up with the same geometry, but which uses a uniform grit consisting of 285 segments, each 3.5 m in height and 7 m in width. A schematic view of the model is shown in figure 4.12.
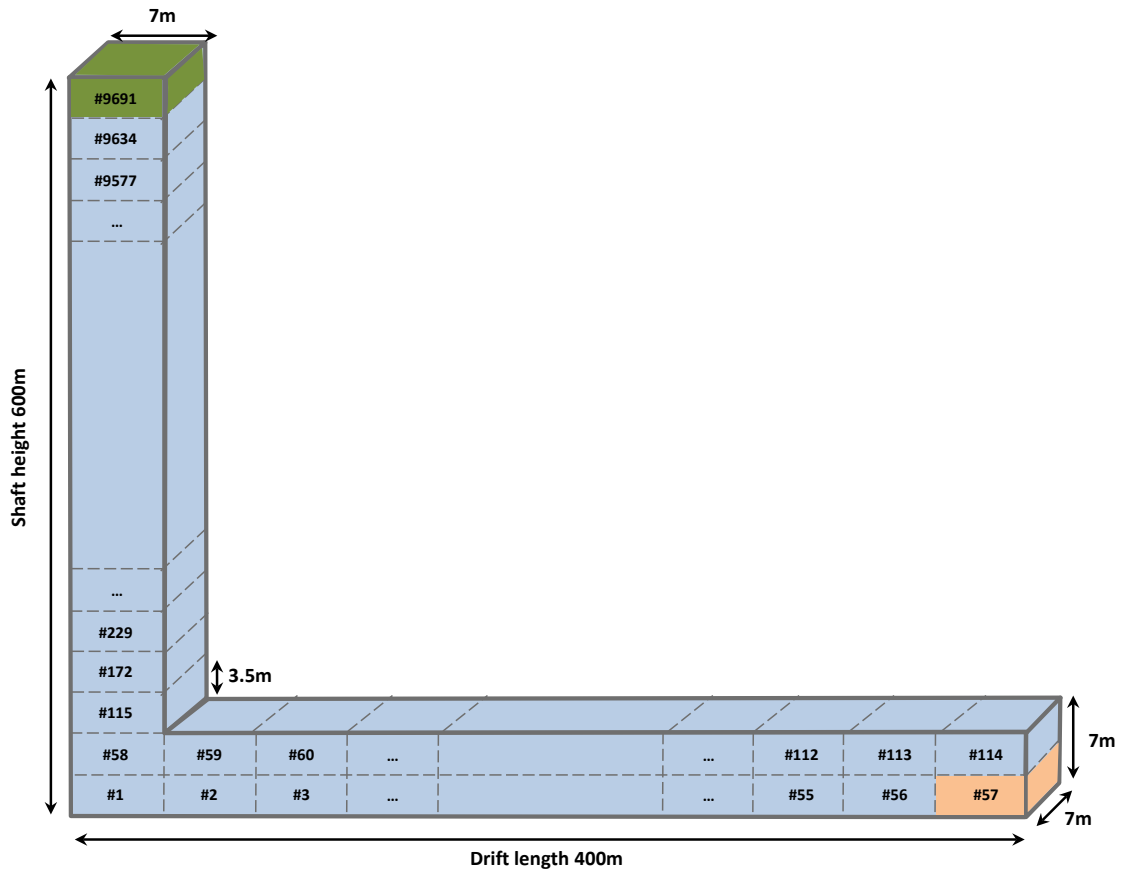
Fig. 4.12   Schematic picture of the layout of the highly discretized model of case 1 (not to scale)

The comparison of the results of the higher discretized model with the low discretized model is shown in figure 4.13. The agreement between both models is reasonably good for 10 000 years. For earlier times the higher discretized model yields a higher saturation and for later times a lower saturation compared to the low discretized model. These differences in the drift are mainly due to the different vertical averaging in the low discretized vs. the high discretized model. The general agreement is satisfactory

enough to state that the low discretized approach as it would be used in a performance assessment model like LOPOS is sufficient to model the gas flow.
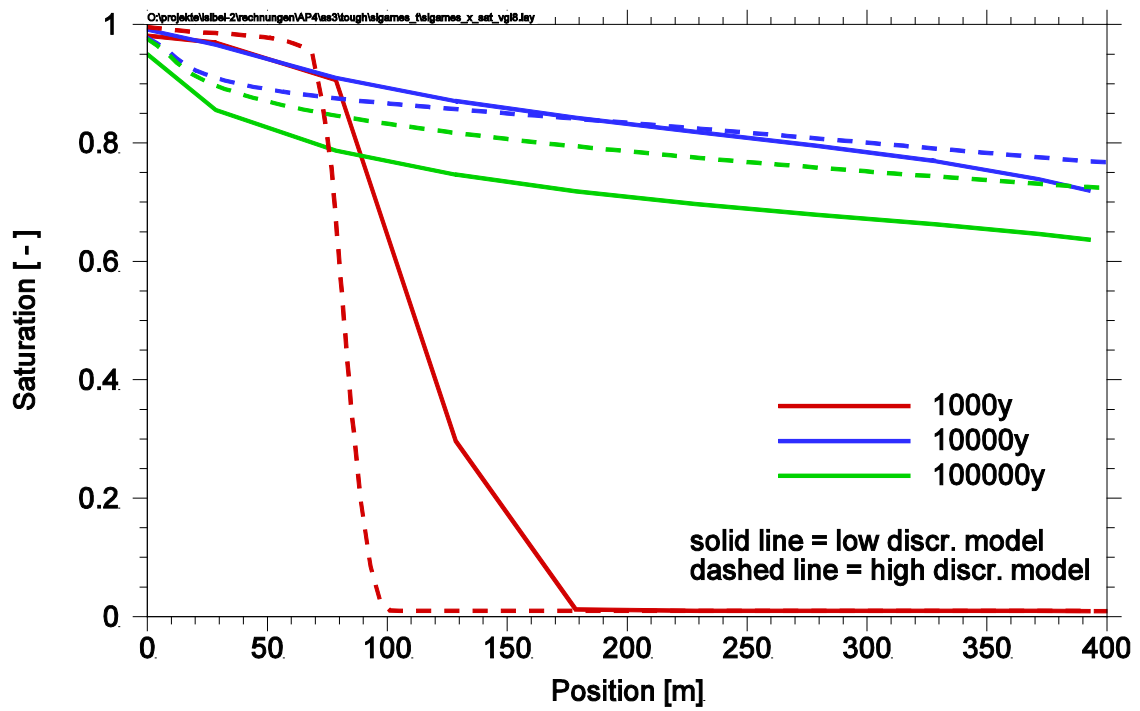
Fig. 4.13 Comparison of the saturation along the drift in the high and low discretized models for different times

4.2 Case 2: Flow through a low permeable sealing

The second test case investigates the inflow of water through an initially air filled drift, which is backfilled with salt grit. The drift has a length of 400 m and has a cross-section of 8x8 m. In the middle of the drift, there is a drift sealing of 40 m in length. A schematic layout of the regarded repository is shown in figure 4.14. For the simulation with TOUGH2, the drift is discretized into 100 segments in horizontal direction and 4 segments in vertical direction. Each segment is 4 m in length and 2 m in height. At the left end of the drift (segments #1, #101, #201 and #301, coloured in green in figure 4.14), a constant hydrostatic pressure is assumed.
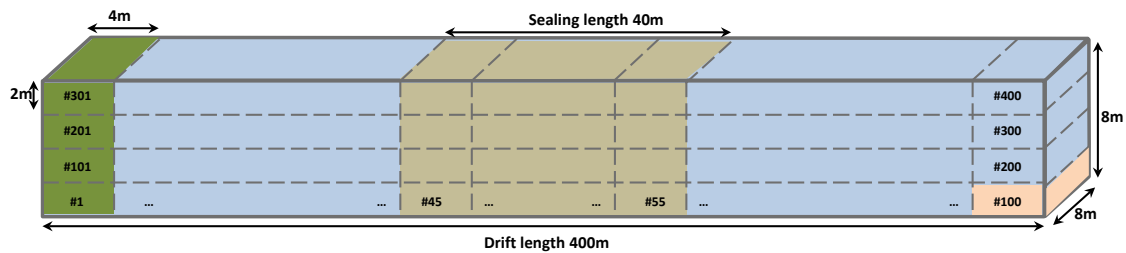
Fig. 4.14 Schematic picture of the layout of the model of case 2 (not to scale)

Four different variants are regarded, each of them considering different boundary conditions. Three variants are considering different hydrostatic pressures, which are 1, 3 and 9 MPa. This corresponds to an actual hydrostatic pressure level at the access drift of about 100, 300 and 900 m water column height, if fresh water is assumed. The right end of the drift is assumed to be closed reflected by a no-flux boundary condition in the model.

The first variant does not consider any gas production, but only the displacement of the air in the drift. The three other variants all consider gas production at the right end of the drift (segment #100, coloured in red in figure 4.14). The gas production rate is $1 \cdot 10^{-8}$ ks·s^{-1} which corresponds to about 10 moles per year. While the water enters the drift at the left hand side, the gas is produced and enters the drift at the other side and both phases have to bypass each other.

The repository system is assumed to be in an early stage of evolution; the salt grit backfill is not yet at the state of full compaction, but still has a porosity of 10 % and a permeability of $1 \cdot 10^{-15}$ m^2. For the sealing, also a porosity value of 10 % is assumed, but a permeability value of $1 \cdot 10^{-18}$ m^2, three orders of magnitude lower than in the

backfill. As in case 1, the material parameters for the two-phase flow are chosen accordingly to the parameters given in /KRO 09/. It has to be noted again that it is questionable whether this data are valid for salt grit as used for backfill in a repository. An overview of the model parameters is given in table 4.2. The input file for the TOUGH2 simulation for variant d is listed in Annex A.5.

Tab. 4.2   Model parameters for case 2

General parameters		Salt grit	Sealing
Density	[kg·m^{-3}]		2 165
Porosity	[-]		0,1
Integral permeability	[m^2]	1E-15	1E-18

Two phase flow parameters (van Genuchten)		
m	[-]	0,73
θ_{lr}	[-]	0,18
θ_s	[-]	1,0
θ_{gr}	[-]	1E-3
α	[MPa^{-1}]	2E-5

Boundary conditions		
Variant a		
Gas production rate	[kg·s^{-1}]	0
Hydrostatic pressure	[MPa]	3
Variant b		
Gas production rate	[kg·s^{-1}]	1E-8
Hydrostatic pressure	[MPa]	3
Variant c		
Gas production rate	[kg·s^{-1}]	1E-8
Hydrostatic pressure	[MPa]	1
Variant d		
Gas production rate	[kg·s^{-1}]	1E-8
Hydrostatic pressure	[MPa]	9

The results of the TOUGH2 simulations for all four variants are shown in figures 4.15 to 4.18 as 2D cross sections through the drift showing the gas saturation distribution. Blue

colours denote liquid, while red colours denote gas. For each variant, four pictures are presented showing saturation distributions at different time steps with increasing time from the figure in the upper left to the one in the lower right. Except for one variant, the points in time are 10, 100, 10 000 and 100 000 years. The position of the drift seal is indicated by vertical dashed lines.

For the first point in time shown, one can see in all variants that the fluid is flowing through the drift as a steep front. The steepness of the front seems to be the higher, the higher the hydrostatic pressure at the left boundary. These observations are in agreement with the ones obtained from the modelling with HYDRUS 2D in a previous project /RUE 10/. As soon as the front enters the drift sealing, the steepness even increases. The principal behaviour until this point in time is more or less the same for all variants, except that the flow velocity is different depending on the hydrostatic pressure at the left boundary.

The flow behaviour of the water dramatically changes as soon as the water front leaves the drift seal and enters the part of the model area to the right of the drift. The drift seal acts as a hydraulic throttle; the water does not move as a sharp front, but more or less fills the right hand part of the model from the bottom to the top (e. g. right blue part in figure 4.14). Until 10 000 years one can see for all variants, except variant c, that the gas is held back on the right hand side of the drift seal, but after 100 000 years, the gas has entered and partly desaturated also the upper part of the drift seal.

The variant d, considering gas generation and a high hydraulic pressure at the left boundary condition shows a minimum in the gas saturation to the right of the seal for a certain point in time. In this situation, the gas pressure resulting from the gas compression by the water inflow first overshoots the final steady state value and relieves again. This effect is most notable in the upper right picture in figure 4.18, representing a simulation time of 10 000 years, when the drift right to the seal is nearly saturated. For later times (see lower right picture representing 100 000 years), the upper part of the drift to the right of the seal clearly has a lower saturation state again. This is an effect that is due to the closed end on the right hand side of the drift, resulting in trapped air which is elastically compressed until the gas flow starts.

The steady state for the variants considering gas generation can be described as follows: On the right hand side of the seal, the drift shows a clear vertical gradient in the saturation state from highly saturated at the bottom to lower saturated at the top. The

thickness of the fully saturated part at the bottom of the drift is the higher, the higher the hydrostatic pressure at the left end boundary condition. The same applies more or less to the part of the drift to the left of the seal, but the lower saturated part at the top of the drift is always much thinner than on the right hand side. In the seal there is a transition zone from the conditions at left to the one at the right hand side.

The evolving flow patterns during the inflow phase and the saturation distributions in the steady state are quite complex and result from the interaction of the liquid and the gaseous phase. A correct description of these distributions can only be achieved if two-phase flow is considered in the model.
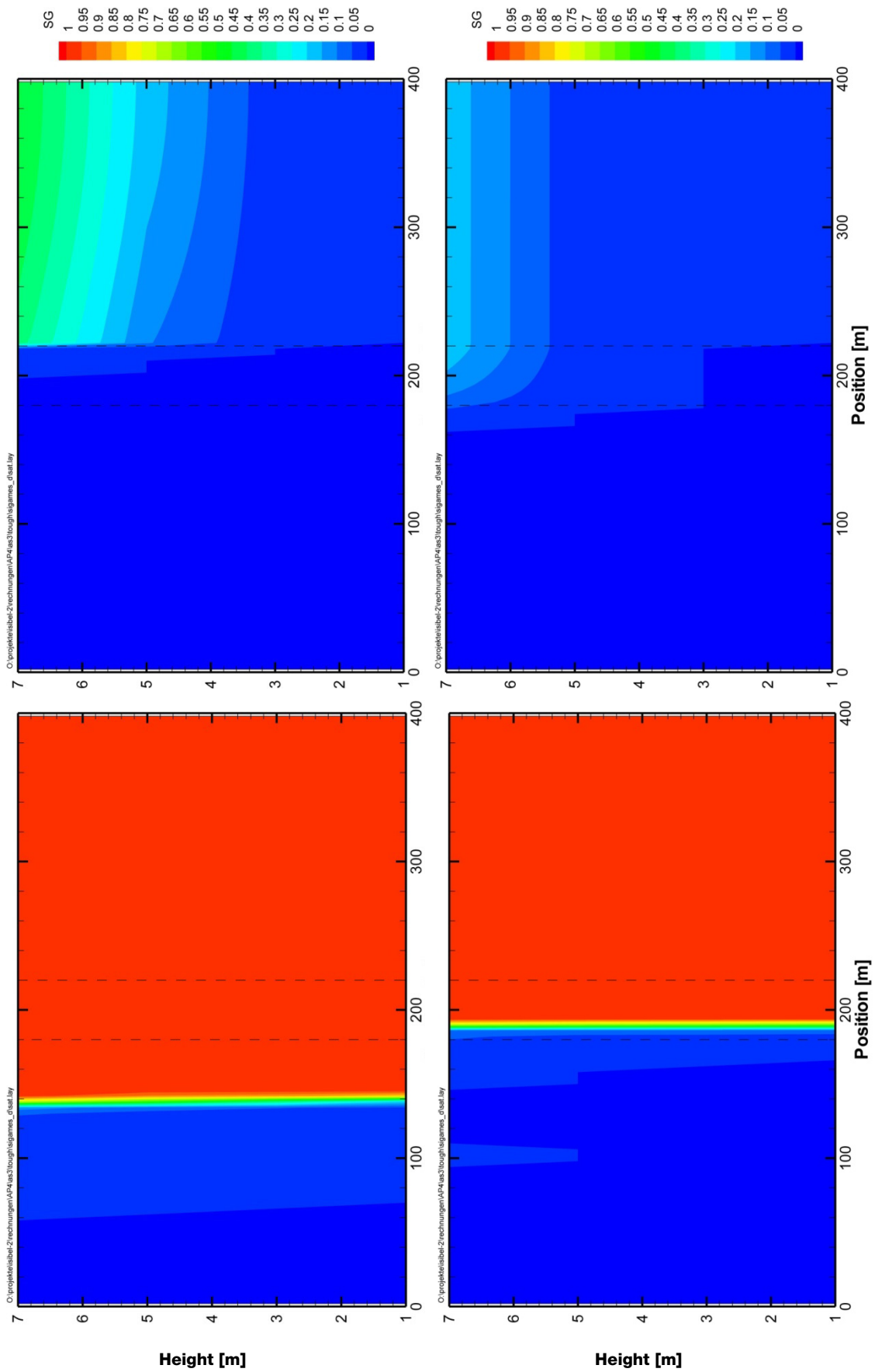
Fig. 4.15 Saturation of gas after about 10^1, 10^2, 10^4 and 10^5 years in variant a
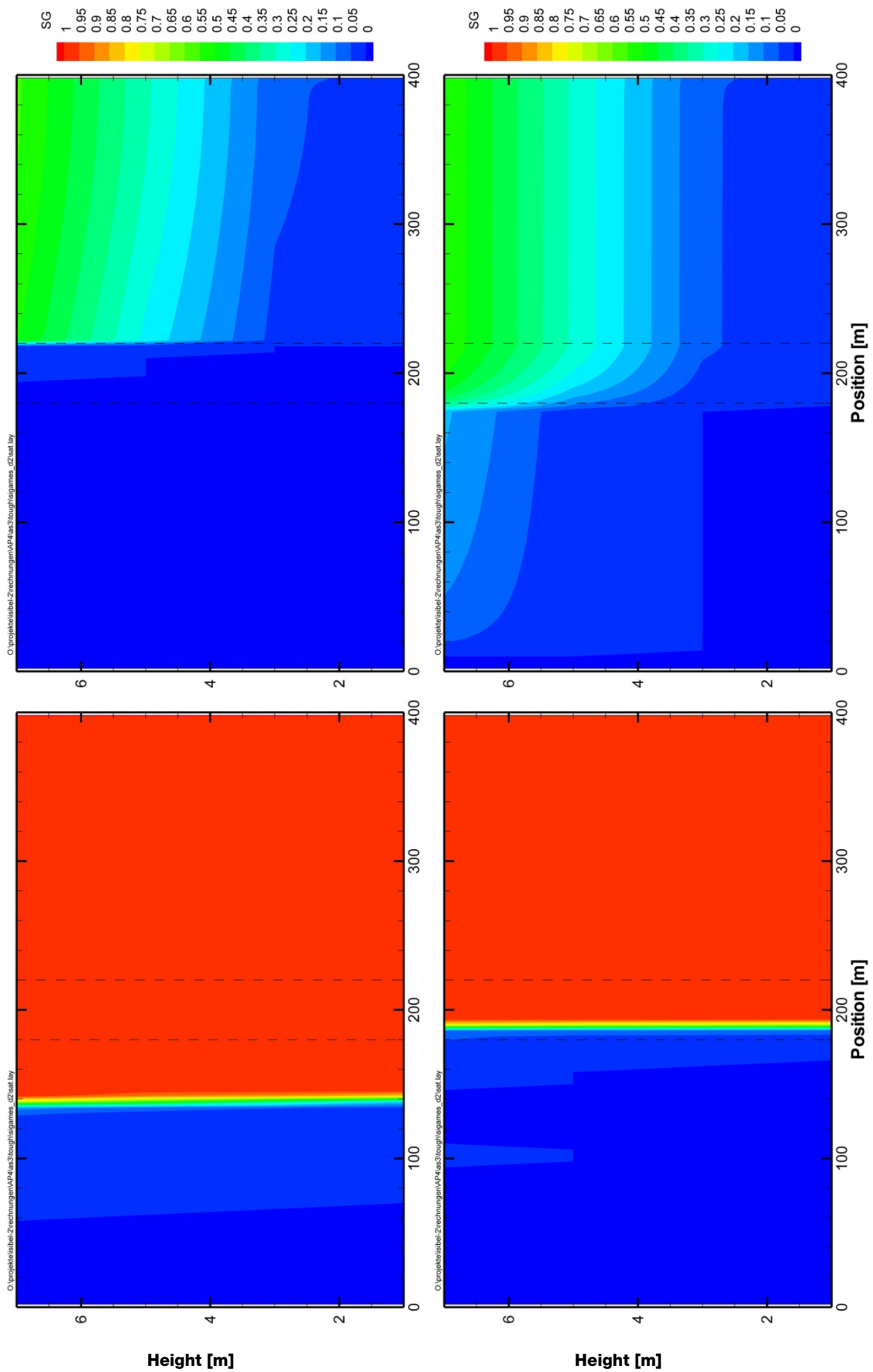
Fig. 4.16 Saturation of gas after about 10^1, 10^2, 10^4 and 10^5 years in variant b
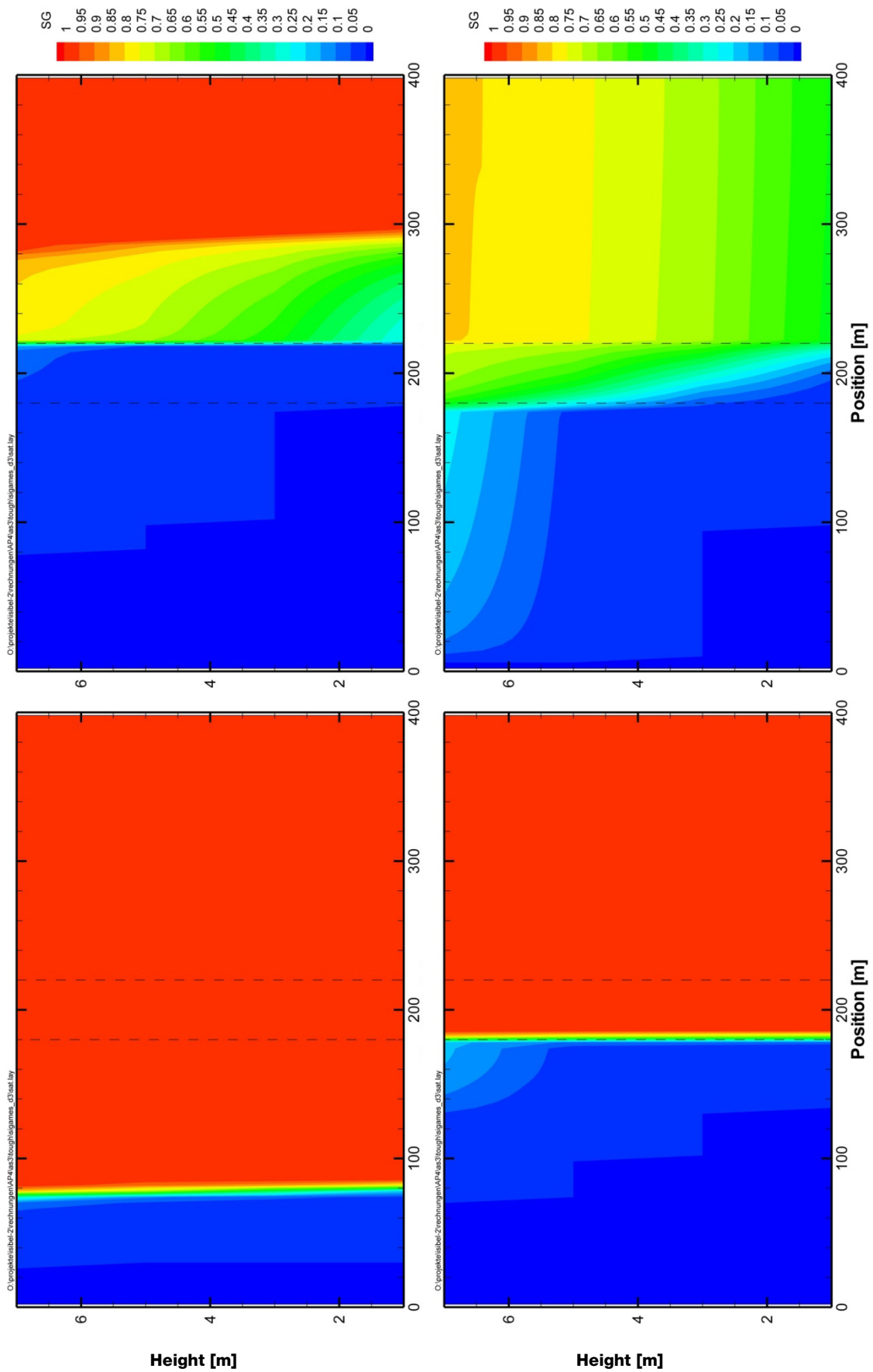
Fig. 4.17   Saturation of gas after about 10^1, 10^2, 10^4 and 10^5 years in variant c

83
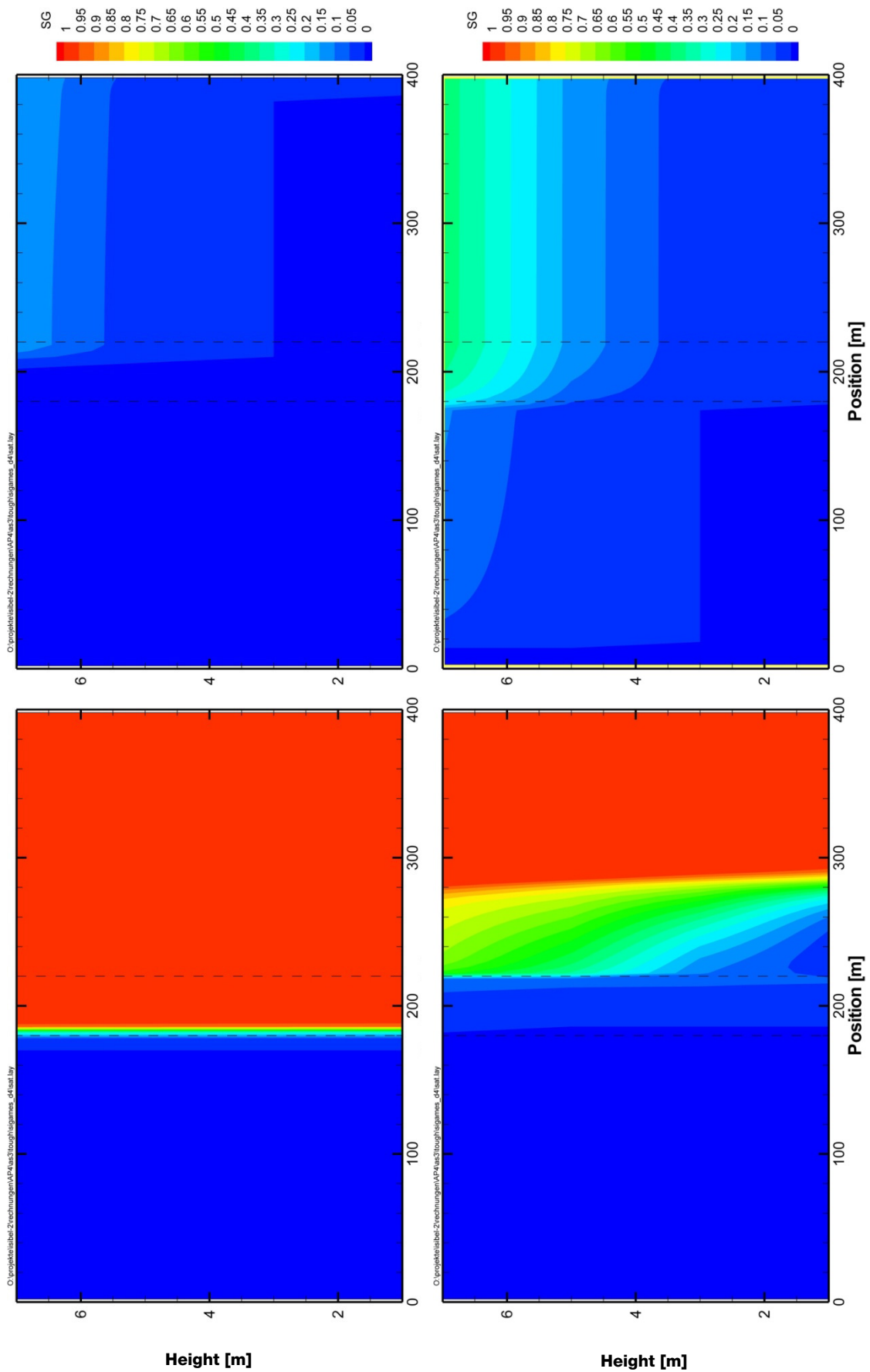
Fig. 4.18 Saturation of gas after about 10^1, 10^3, 10^4 and 10^5 years in variant d

4.3 Résumé

After closure of a repository mine, the remaining spaces are initially filled with air. As soon as water is entering the mine this is a two-phase system, where the movement of one phase usually results also in a movement on the other phase. Neither the movement of gas, nor its interaction with the liquid has been considered in detail in the previous performance assessments for high-level waste repositories in salt. Gaseous radionuclides might contribute to the potential radiation exposition in the biosphere (see chapter 1); therefore, a more detailed consideration of the gas transport in the performance assessment model is preferred in the future.

In this chapter, the need for two-phase flow models in performance assessments to estimate the fluid and gas transport in the near field of a repository for high-level waste in salt was investigated on the basis of two selected generic examples, each with different variants. From the simulations presented, the following conclusions are drawn:

-   In case of no additional gas production, but initially air present at atmospheric pressure, displacement of air only slightly influences liquid transport. Single flow simulations with LOPOS describe the fluid flow in most cases sufficiently well. However, in case of higher gas pressures, the liquid flow is hindered significantly by the gas flow and the use of a two-phase flow model is inevitable to describe the fluid flow correctly.

-   If gas generation occurs, liquid and gas flow are influencing each other significantly and the coupled transport should be regarded by two-phase flow.

-   The simulated result of the gas flow is highly depending on the repository concept like on the pore space available for gas storage and the material parameters. Therefore, a detailed modeling of the two-phase flow phenomena should be regarded, since too abstracted estimations might lead to unpredictable deviations from the actual behavior.

-   The use of low discretized models on the basis of segments as used in integrated PA models seems to be sufficient to yield acceptable results.

In summary, it can be concluded that the use of a full two-phase flow model according to the van Genuchten approach is preferable to describe fluid flow in future performance assessments of high-level waste repositories in salt and should be implemented in the next version of the near-field code for salt.

5   Conclusions for integrated performance assessment

The following chapter shortly summarises the results presented in this report from the perspective of integrated performance assessment. One of the reasons, why the presented work was initiated is that the German safety requirements issued in 2010 /BMU 10/ have fundamental impact on the way how gas production and -transport have to be considered in the long-term safety assessment of a high level waste repository in salt due to a paradigm shift that goes along with these safety requirements. At first, this issue is shortly explained in the following three paragraphs.

Long-term-safety assessments performed for high level waste repositories until the year 2000, e. g. /BUH 91/, considered as main scenario a worst case, where the repository mine is flooded shortly after the beginning of the post-operational phase by an inflow from the overburden because of a failure of the geological barrier. The scenario further assumed that the brine gets contaminated from the contact with the radioactive waste and is subsequently displaced from the mine by convergence of the salt rock and gas production. After leaving the mine, the contaminated brine is diluted in the ground water flow in the overburden and finally leads to a potential radiation exposure if the ground water is used for food production or as drinking water. In these safety assessments, it was furthermore always assumed that the gaseous radionuclides are completely dissolved in the liquid phase and transported with the groundwater. No explicit gas pathway was considered. To model the influence of the gas production on the brine flow by displacement, only gas production rates were needed. These can be derived from corrosion rates of the affected material. Therefore, a large amount of laboratory experiments was performed to measure the corrosion rates for different materials and for different types of brines at different temperatures, e. g. /SMA 95/, /SMA 99 and SMA 02/.

The AKEnd (Arbeitskreis Endlagerung), which was a group of experts to develop a new site selection procedure, invented the new concept of the so called "Einschlusswirksamer Gebirgsbereich" (ewG) /AKE 02/ which is a part of the host rock and that ensures the containment of the waste. This concept is also found in the safety requirements for repositories for high level waste in Germany /BMU 10/. According to the safety requirements, the safety concept is based on the containment of the radionuclides in the ewG and therefore only allows for negligible radionuclide fluxes at the ewG boundary. The safety requirements allow for a simplified long-term radiological statement without

modeling the dispersion in the overburden, if the radionuclide release at the ewG boundary is proved to be below a given limit.

One of the safety requirements states that for probable developments the integrity of the ewG has to be demonstrated for the whole reference period of 1 Million of years. Since salt itself is impermeable for water flow, this requirement excludes the scenario of a host rock failure that has been regarded in the safety assessments before. For a licensable repository, this leaves scenarios where an inflow of water from the overburden only occurs through the sealed shaft and drifts which results in very low inflow rates. Therefore, it is expected that for long timeframes, the porespace in the repository mine is not fully saturated and there does not exist a continuous pathway of water filled pores from the waste to the ewG boundary. Consequently, no release of dissolved radionuclides occurs during that timeframe, but the radionuclide transport through the gas phase is a potential alternative radionuclide release pathway. Since the ewG is part of the host rock, the ewG boundary where the radionuclide fluxes will have to be assessed for the radiological statement are those points, where the ewG intersects the drifts or shafts of the repository mine.

The information given in this report has led to the following conclusions about the potential release of radionuclides through the gas pathway:

− Even if there is no inflow of external waters into the mine, there is some gas production expected to occur in the repository due to corrosion of container material from water disposed of with the backfill and inflowing from the host rock during the thermal phase.

− The amount of gases in the repository, which are trapped air and gas generated by corrosion and degradation processes, exceed the storage capacity for gases in the repository if not dedicated gas storage areas might be foreseen in the repository concept. Consequently, an outflow of gases from the repository is expected to occur.

− If there are failed containers for spent fuel, radioactive gases might be released from the containers into the gas space of the backfill and subsequently transported together with the gas flow of non-radioactive gases.

− The travel time of the gases in the mine does highly depend on the boundary conditions like gas production rate and gas volume in the mine. Measures to reduce

the potential consequences of gaseous radionuclide release could consider gas storage areas in the repository to delay potential gas release from the repository.

Since radionuclides fluxes at the ewG boundary cannot be ruled out a priori and the gases are not completely dissolved due to lack of fluids, fluxes of radionuclides in the gas phase are to be assessed at ewG boundary. In contrast to the safety assessments performed before, it cannot be assumed that the volatile radionuclides are completely dissolved in the liquid phase and transported together with the brine.

Since the distance between the emplacement areas and the ewG boundary, where the radionuclide fluxes are assessed, is rather low, an uncertainty in the travel time for radionuclides might result in a comparably high uncertainty of the determined radionuclide fluxes. Therefore, an appropriate model for the gas transport in the mine is necessary. Besides the need for more sophisticated models in integrated performance assessment, a lack of knowledge was identified in this report in the following fields to accomplish this task:

- Gas transport:

    - Gas permeability of salt grit backfill at a low porosity, i. e. at high compaction state.

    - Two-phase flow parameters of compacted salt grit.

- Source term of volatile radionuclides

    - Effectiveness of the conversion of C-14 in oxide films into gaseous form, if only water vapor is present.

    - Fraction of iodine present as I_2 under repository conditions in the gap of spent fuel elements.

The knowledge in these fields has to be improved either to reduce conservatism or to be able to perform realistic gas transport simulations at all.

References

/ANT 71/ Anthony, T.R.; Cline, H.E.: Thermal Migration of Liquid Droplets through Solids. Journal of Applied Physics, 42/9, pp. 3380-3387, 1971.

/ANT 73/ Anthony, T.R.; Cline, H.E.: The stability of migrating droplets in solids. Acta Metallurgica, Vol. 21/2, pp. 117-122, 1973.

/AKE 02/ Arbeitskreis Auswahlverfahren Endlagerstandorte (AkEnd): Auswahl-verfahren für Endlagerstandorte – Empfehlungen des AkEnd Bonn, 2002.

/AVV 90/ Allgemeine Verwaltungsvorschrift zu § 45 Strahlenschutzverordnung: Er-mittlung der Strahlenexposition durch die Ableitung radioaktiver Stoffe aus kerntechnischen Anlagen oder Einrichtungen (21. Februar 1990). Bundes-anzeiger, 42. Jg. Nummer 64a, 1990.

/BEC 09/ Becker, D.-A.; Buhmann, D.; Mönig, J.; Noseck, U.; Rübel, A.; Spießl, S.: Endlager Morsleben, Sicherheitsanalyse für das verfüllte und verschlosse-ne Endlager mit dem Programmpaket EMOS. Planfeststellungsverfahren zur Stilllegung des Endlagers für radioaktive Abfälle Morsleben. Verfah-rensunterlage P 278, Bundesamt für Strahlenschutz (BfS), Salzgitter, 2009. *(http://www.bfs.de/de/endlager/endlager_morsleben/stilllegung/genehmigungsverfa hren/verfahrensunterlagen_eram.html, Oct. 01. 2012)*

/BFS 02/ Bundesamt für Strahlenschutz: Vorkommen salinarer Lösungen im Erkundungsbergwerk Gorleben sowie in einigen Bereichen des Salzstocks Gorleben (Lösungsverzeichnis Gorleben). Bundesamt für Strahlenschutz, 9G/HE/RB/0014/01, 2002. *(http://www.bfs.de/de/endlager/erkundungsbergwerk_ gorleben/geologie/loesungsverzeichnis_gorleben.html, Oct. 01. 2012)*

/BMU 01/ Bundesministerium für Umwelt, Naturschutz und Reaktorsicherheit: Be-kanntmachung der Dosiskoeffizienten zur Berechnung der Strahlenexposi-tion. RSII1-11413/28, Bonn, 2001.

/BMU 10/ Bundesministerium für Umwelt, Naturschutz und Reaktorsicherheit: Sicherheitsanforderungen an die Endlagerung wärmeentwickelnder radio-aktiver Abfälle. BMU, Stand: 30. September 2010.

/BOL 08/ Bollingerfehr, W.; Filbert, W.; Pöhler, M.; Tholen, M.; Wehrmann, J.: Über-prüfung und Bewertung des Instrumentariums für eine sicherheitliche bewertung von Endlagern für HAW – ISIBEL – AP1.2 – Konzeptionelle Endlagerplanung und Zusammenstellung des endzulagernden Inventars. TEC-20-2008-AP, DBE Technology, Peine, 2008.

/BOR 08/ Bornemann, O.; Behlau, J.; Fischbeck, R.; Hammer, J.; Jaritz, W.; Keller, S.; Mingerzahn, G.; Schramm,M.: Standortbeschreibung Gorleben Teil 3 – Ergebnisse der über- und untertägigen Erkundung des Salinars. Geologisches Jahrbuch Reihe C, Band C 73, E. Schweizerbart'sche Verlagsbuchhandlung, Stuttgart.

/BRA 68/ Bradshaw, R.L.; Sanchez, F.: Brine Migration Studies. Health Physics Division Annual Progress Report, ORNL-4316, p. 32, Oak Ridge National Laboratory, Oak Ridge, 1968.

/BUH 91/ Buhmann, D.; Nies, A.; Storck, R.: Analyse der Langzeitsicherheit von Endlagerkonzepten für wärmeerzeugende radioaktive Abfälle. GSF Forschungszentrum für Umwelt und Gesundheit GmbH, GSF 27/91, Neuherberg, 1991.

/BUH 99/ Buhmann, D.: Das Programmpaket EMOS. Ein Instrumentarium zur Analyse der Langzeitsicherheit von Endlagern. Gesellschaft für Anlagen- und Reaktorsicherheit (GRS) mbH, GRS-159, Braunschweig, 1999.

/BUH 09/ Buhmann, D.; Grupa, J.; Hart, J.; Hirsekorn, R.-P.; Ionescu, A.; Lerch, C.; Rübel, A.; Schneider, A.; Schröder, T.J.: Report on the benchmarks on rock salt. PAMINA Deliverable D4.1.1, 2009. *(http://www.ip-pamina.eu/downloads/ pamina4.1.1.pdf, Oct. 01. 2012)*

/CIN 06/ Cinar, Y., Pusch, G., Reitenbach, V.: Petrophysical and Capillary Properties of Compacted Salt. Transport in Porous Media (2006) 64: 199-228, Springer, 2006.

/CLI 72/ Cline, H.E., Anthony, T.R.: The Migration of Liquid Droplets in Solids. Journal of Crystal Growth, Vol. 13/14, pp. 790-794, 1972.

/CRA 79/ Crank, J.: The Mathematics of Diffusion. Oxford University Press, Oxford, 1979.

/CUS 97/ Cussler, E.L.: Diffusion – Mass transfer in fluid systems. Cambridge University Press, Cambridge, 1997.

/DAV 79/ Davis, W.: Carbon-14 production in nuclear reactors. in: Carter,M. et al.: Management of Low-Level Radioactive Waste. p. 151, Pergamon Press, New York, 1979.

/DEL 97/ De Las Cuevas, C.: Pore structure characterization in rock salt. Engineering Geology 47, pp. 17-30, 1997.

/DEN 97/ Deng, B.; Campbell, T.J.; Burris, D. R.: Hydrocarbon formation in metallic iron/water systems. Environmental Science & Technology, Vol. 31, No. 4, pp. 1185-1190, 1997.

/EC 82/ Commission of the European Communities: Seminar on iodine removal from gaseous effluents in the nuclear industry - Vol I. 21-24 September 1981, Mol (Belgium), V/5283/82-EN,FR,DE, European Commission, Luxembourg, 1982.

/FRI 00/ Friedrich, A.J.: Selbstdiffusion von Wasser im intergranularen Raum von Steinsalz. Diplomarbeit, Institut für Umweltphysik, Ruprecht-Karls-Universität, Heidelberg, 2000.

/GEN 80/ Van Genuchten, M. Th.: A Closed-form Equation for Predicting the Hydraulic Conductivity of Unsaturated Soils. Soil Science Society of America Journal, Vol. 44, no.5, pp. 892-898, 1980.

/GEV 81/ Gevantman, L.H. (ed.): Physical Properties Data for Rock Salt. National Bureau of Standards Monograph 167, Washington, 1981.

/GRA 00/ Grambow, B.; Loida, A.; Martínez-Esparza, A.; Díaz-Arocas, P.; Pablo, J.; Paul, J.L.; Marx, G.; Glatz, J.P.; Lemmens, K.; Ollila, K.; Christensen, H.: Source term for performance assessment of spent fuel as a waste form. EUR 19140, European Commission, Luxemburg, 2000.

/HAD 80/   Hadley, G.R.; Faris, G.W.: Revised Theory of Water Transport in Rock Salt. Sandia National Labatories, SAND80-2398, Albuquerque, 1980.

/HAD 81/   Hadley, G.R.: Salt Block II: Brine Migration Modeling. Sandia National Labatories, SAND81-0438, Albuquerque, 1981.

/HAD 82/   Hadley, G.R.: Theoretical Treatment of Evaporation Front Drying. International Journal of Heat and Mass Transfer, Vol. 25(10), pp. 1511-1522, 1982.

/HAN 96/   Hanson, R.S.; Hanson, T.E.: Methanotrophic bacteria. Microbological Reviews 60 (2), pp. 439-471, 1996.

/HEL 98/   Helmig, R.; Class, H.; Huber, R.; Sheta, H.; Ewing, J.; Hinkelmann, R.; Jakobs, H.; Bastian, P.: Architecture of the Modular Program System MUFTE-UG for Simulating Multiphase Flow and Transport Processes in Heterogeneous Porous Media. Mathematische Geologie, Vol. 2, 1998.

/HOH 79a/ Hohlfelder, J.J.: Measurement of Water Lost From Heated Geologic Salt. Sandia National Labatories, SAND79-0462, Albuquerque, 1979.

/HOH 79b/ Hohlfelder, J.J.; Hadley, G.R.: Laboratory Studies of Water Transport in Rock Salt. Sandia National Labatories, SAND79-1519, Albuquerque, 1979.

/HOH 80/   Hohlfelder, J.J.: Salt Block II: Description and Results. Sandia National Labatories, SAND79-2226, Albuquerque, 1979.

/ICRP 68/ Evaluation of Radiation Doses to Body Tissues from Internal Contamination due to Occupational Exposure. ICRP Publication 10, Pergamon Press, Oxford, 1968.

/ICRP 89/ Age-dependent Doses to Members of the Public from Intake of Radionuclides: Part 1. ICRP Publication 56, Pergamon Press, Oxford, 1989.

/ICRP 96/ Age-dependent Doses to Members of the Public from Intake of Radionuclides: Part 5. ICRP Publication 72, Pergamon Press, Oxford, 1996.

/JEN 79/   Jenks, G.H.: Effects of Temperature, Temperature Gradients, Stress, and Irradiation on Migration of Brine Inclusions in a Salt Repository, ORNL-5526, Oak Ridge National Laboratory, Oak Ridge, 1979.

/JOC 80/   Jockwer, N.: Die thermische Kristallwasserfreisetzung des Carnallits in Abhängigkeit von der absoluten Luftfeuchtigkeit. Kali und Steinsalz, Vol. 8, p. 55- 58, 1981.

/JOC 81a/   Jockwer, N.: Untersuchungen zu Art und Menge des im Steinsalz des Zechsteins enthaltenen Wassers sowie dessen Freisetzung und Migration im Temperaturfeld endgelagerter radioaktiver Abfälle. Thesis, TU Clausthal, 1981.

/JOC 81b/   Jockwer, N.: Die thermische Kristallwasserfreisetzung des Polyhalits und Kieserits in Abhängigkeit von der absoluten Luftfeuchtigkeit. Kali und Steinsalz, Vol. 4, p. 126-128, 1981.

/JOH 05/   Johnson, L.H.; Ferry, C.; Poinssot,C.; Lovera, P.: Spent fuel radionuclide source-term model for assessing spent fuel performance in geological disposal. Part I: Assessment of the instant release fraction. Journal of Nuclear Materials 346, pp. 56–65, 2005.

/JOH 97/   Johnson, L.H.; Tait, J.C.: Release of segregated radionuclides from spent fuel. TR 97–18, SKB, Stockholm, 1997.

/KEE 05/   Keesmann, S.; Noseck, U.; Buhmann, D.; Fein, E.; Schneider, A: Modell-rechnungen zur Langzeitsicherheit von Endlagern in Salz- und Granitforma-tionen. GRS-206, GRS, Braunschweig, 2005.

/KON 94/   van Konynenburg, R.A.: Behavior of carbon-14 in waste packages for spent fuel in a tuff repository. Waste Management, Vol. 14 No.5, pp. 363-383, 1994.

/KOP 90/   Kopp, D., Münzel, H.: Release of volatile carbon-14 containing products from Zircaloy. Journal of Nuclear Materials 173, pp. 1-6, 1990.

/KRO 09/ Kröhn, K.P.; Stührenberg, D.; Herklotz M.; Heemann, U.; Lerch, C.; Xie, M.: Restporosität und -permeabilität von kompaktierendem Salzgrus-Versatz. Gesellschaft für Anlagen- und Reaktorsicherheit (GRS) mbH, GRS-254, Braunschweig, 2010.

/KUE 99/ Kühle, Th.; Graefe, V.; Hirsekorn, R.P.: Zweiphasenfluss-Modell-rechnungen zur Berücksichtigung der Gasproduktion in Endlagern und Modellansätze für Langzeitsicherheitsanalysen. GRS-158, GRS, Braunschweig, 1999.

/KUP 00/ Kupfer, A.: Radiochemische Korrosionsuntersuchungen an Urandioxid und Cladding-Materialien von Kernbrennstoffen in praxisrelevanten Salzlaugen als Beitrag zur direkten Endlagerung. Dissertation FU-Berlin, 2000. *(http://www.diss.fu-berlin.de/diss/receive/FUDISS_thesis_342, Oct. 01. 2012)*

/LAM 80/ Lambert, S.: Mineralogical Aspects of Fluid Migration in the Salt Block II Experiment. Sandia National Labatories, SAND79-2423, Albuquerque, 1980.

/LAR 13/ Larue, J.; Baltes, B.; Fischer, H.; Frieling, G.; Kock, I.; Navarro, M.; Seher, H.: Radiologische Konsequenzenanalyse, Bericht zum AP 10, Vorläufige Sicherheitsanalyse für den Standort Gorleben. Gesellschaft für Anlagen- und Reaktorsicherheit (GRS) mbH, GRS-289, Köln, 2013.

/LEW 96/ Lewis, S.; Holness, M.: Equilibrium halite-H_2O dihedral angles: High rock-salt permeability in the shallow crust? Geology 24, pp. 431–434, 1996.

/MCC 87/ McCauley, V.S.; Raines, G.E.: Expected Brine Movement at Potential Nuclear Waste Repository Salt Sites. Office of Nuclear Waste Isolation, ONWI-654, Columbus, 1987.

/MOE 12/ Mönig, J., Buhmann, D., Rübel, A., Wolf, J., Baltes, B.: Grundzüge des Sicherheits- und Nachweiskonzepts. Vorläufige Sicherheitsanalyse für den Standort Gorleben. Gesellschaft für Anlagen- und Reaktorsicherheit (GRS) mbH, GRS-277, Köln, 2012.

/MOR 01/ Moreno, L.: Project SAFE: Gas related processes in SFR. R 01-11, SKB, Stockholm, 2001.

/NAG 02/   Jahmson, L.H.; McGinnes, D.F.: Partitioning of radionuclides in Swiss power reactor fuels. NTB 02-07, Nagra, Wettingen, 2002.

/NCRP 85/ Carbon-14 in the Environment. NCRP Publication 81, National Council on Radiation Protection and Measurement, Bethesda, 1985.

/NOH 04/   Noshita, K.: Fundamental Study of C-14 Chemical Form under Irradiated Condition. in: Johnson, L.H. & Schwyn, B.: Proceedings of a workshop on the release and transport of C-14 in repository environments. NIB 04-03, Nagra, Wettingen, 2004.

/NOS 09/   Noseck, U.; Becker, D.; Fahrenholz, C.; Fein, E.; Flügge, J.; Kröhn, K.-P.; Mönig, J.; Müller-Lyda, I.; Rothfuchs, T.; Rübel, A.; Wolf, J.: Assessment of the long-term safety of repositories - Scientific basis. Gesellschaft für Anlagen und Reaktorsicherheit (GRS) mbH, GRS-237, Braunschweig, 2009.

/OLA 80/   Olander, D.R.; Machiels, A.J.; Yagnik, S.: Thermal Gradient Migration of Brine Inclusions in Salt. Office of Nuclear Waste Isolation, ONWI-208, Columbus, 1980.

/OLA 84/   Olander, D.R.: A Study of Thermal-Gradient-Induced Migration of Brine Inclusions in Salt: Final Report. Office of Nuclear Waste Isolation, ONWI-538, Columbus, 1984.

/PAR 70/   Parsly, L.F.: Design Considerations of Reactor Containment Spray Systems. Part IV. Calculation of Iodine-Water Partition Coefficients ORNL-TM-2412, Part IV. ORNL, Oak Ridge, 1970.

/PEI 11/   Peiffer, F.; McStocker, B.; Gründler, D.; Ewig F.; Thomauske, B.; Havenith, A.; Kettler, J.: Abfallspezifikation und Mengengerüst - Basis Ausstieg aus der Kernenergienutzung (Juli 2011). Gesellschaft für Anlagen und Reaktorsicherheit (GRS) mbH, GRS-278, Köln, 2011.

/POI 05/   Poinssot, C.; Ferry, C.; Lovera, P.; Jegou, C.; Grtas, J.-M.: Spent fuel radionuclide source term model for assessing spent fuel performance in geological disposal. Part II: Matrix alteration model and global performance. Journal of Nuclear Materials 346, pp.66-77, 2005.

/POT 02/   Potthoff, S.; Perau, E.: Parameteridentifikation bei Zweiphasen-Strömungen – Theorie und Numerik. Bauhaus-Universität Weimar, Schriftenreihe Geotechnik, Heft 08, Weimar, 2002.

/PRO 02/   Pröhl, G.; Gering, F.: Dosiskonversionsfaktoren zur Berechnung der Strahlenexposition in der Nachbetriebsphase von Endlagern nach dem Entwurf der Allgemeinen Verwaltungsvorschriften zu §47 Strahlenschutzverordnung in Anlehnung an die Vorgehensweise im Rahmen des Planfeststellungsverfahrens des geplanten Endlagers Konrad. Planfeststellungsverfahren zur Stilllegung des Endlagers für radioaktive Abfälle Morsleben. Verfahrensunterlage P 162 Bundesamt für Strahlenschutz (BfS), Salzgitter, 2002. *(http://www.bfs.de/de/endlager/endlager_morsleben/stilllegung/genehmigungsverfahren/verfahrensunterlagen_eram.html, Oct. 01. 2012)*

/PRU 99/   Pruess, K.; Oldenburg, C.; Moridis, G.: TOUGH2 User's Guide, Version 2.0. Lawrence Berkley National Laboratory, LBNL-43034, Berkley. *(http://esd.lbl.gov/research/projects/tough/, Oct. 01. 2012)*.

/ROD 03/   Rodwell, W.; Norris, S.: A thematic network on gas issues in safety assessment of deep repositories for radioactive waste (Gasnet). EUR 20620, European Commission, Luxemburg, 2003.

/ROE 80/   Roedder, E.; Belkin, H.E.: Thermal gradient migration of fluid inclusions in single crystals of salt from the Waste Isolation Pilot Plant site (WIPP). Scientific Basis for Nuclear Waste mangement, Vol. 2, pp. 453-464, Plenum Pub. Corp., New York, 1980.

/ROE 81/   Roedder, E.; Bassett, R.L.: Problems in determination of the water content of rock-salt samples and its significance in nuclear waste storage siting. Geology, Vol. 9, p. 525-530, 1981.

/ROE 82/   Roedder, E.; Chou, I.-M.: A critique of "brine migration in salt and its implications in the geologic disposal of nuclear waste". U.S. Geol. Survey Open File Report, 82-1131, 31 pp, 1982.

/ROT 86/ Rothfuchs, T.: Untersuchung der thermisch induzierten Wasserfreisetzung aus polyhalitischem Steinsalz unter in-situ Bedingungen – Temperaturversuch 5 im Salzbergwerk Asse. European Commission, EUR 10392, Bruxelles, 1956.

/ROT 88/ Rothfuchs, T., Wieczorek, K., Feddersen, H.K., Staupendahl, G., Coyle, A.J., Kalia, H., Eckert, J.: Brine Migration Test. Final Report. GSF-Bericht, 6/88, 1988.

/RUE 00/ Rübel, A.: Stofftransport in undurchlässigen Gesteinsschichten – Isotopenuntersuchungen im Grund- und Porenwasser. Der Andere Verlag, Osnabrück, 2000.

/RUE 04/ Rübel, A.; Noseck, U; Müller-Lyda, I.; Kröhn, K.-P.; Storck, R.: Konzeptioneller Umgang mit Gasen im Endlager. GRS-205, Gesellschaft für Anlagen und Reaktorsicherheit (GRS) mbH, Braunschweig, 2004.

/RUE 10/ Rübel, A.; Becker, D.-A.; Fein, E.; Ionescu, A.; Noseck, U.; Lauke, T.; Mönig, J.; Schneider, A.; Spießl, S.; Wolf, J.: Development of Performance Assessment Methodologies. GRS-259, Gesellschaft für Anlagen und Reaktorsicherheit (GRS) mbH, Braunschweig, 2010.

/RUE 10a/ Rübel, A.; Mönig, J: Prozesse, Modellkonzepte und sicherheitsanalytische Rechnungen für ein Endlager im Salz. GRS-A-3521, GRS mbH, Braunschweig, 2010.
(http://www.bfs.de/de/endlager/standortfindung/VerSi_proz_modell_salz.pdf, Oct. 01. 2012)

/SAN 01/ Sander, W.; Herbert, H.J.: Wassergehaltsbestimmung am Steinsalz (Erkundungssohle). Abschlußbericht für den Zeitraum 01.01.1998 - 31.12.2000. PSP Element 9G 412210-00. Gesellschaft für Anlagen- und Reaktorsicherheit (GRS) mbH, Braunschweig, 2001 (unveröffentlichter Bericht).

/SAS 04/ Sasoh, M.: The Study for The Chemical Forms of C-14 Released from Activated Metals. in: Johnson, L.H. & Schwyn, B.: Proceedings of a workshop on the release and transport of C-14 in repository environments, NIB 04-03, Nagra, Wettingen, 2004.

/SCH 86/ Schlich, M.: Simulation der Bewegung von im natürlichen Steinsalz enthaltener Feuchte im Temperaturfeld. Gesellschaft für Strahlen und Umweltforschung München, GSF-Bericht 2/86, Neuherberg, 1986

/SCO 98/ Schon, T.; Heidendael, M.: Wasserstoffbildung durch Metallkorrosion. Institut für Sicherheitsforschung und Reakttortechnik, Jül-3495, Jülich, 1998.

/SHE 82/ Shefelbine, H.C.: Brine Migration: A Summary Report. Sandia National Labatories, SAND82-0152, Albuquerque, 1982.

/SHM 10/ Schmatz, J.; Urai, J.L.: The interaction of fluid inclusions and migrating grain boundaries in a rock analogue: deformation and annealing of polycrystalline camphor-ethanol mixtures. Journal of Metamorphic Geology, 28, pp. 1-18, 2010.

/SIM 06/ Šimůnek, J.; van Genuchten, M. Th.; Šejna, M.: The HYDRUS Software Package for Simulating the Two- and Three-Dimensional Movement of Water, Heat, and Multiple Solutes in Variably-Saturated Media. Technical Manual, 2006.

/SKB 03/ Svensk Kärnbränslehantering AB: Planning report for the safety assessment SR-Can. SKB, Technical Report TR-03-08, Stockholm, 2003.

/SMA 02/ Smailos, E.; Cuñado, M.Á.; Azkarate, I.; Kursten, B.; Marx, G.: Long-Term Performance of Candidate Materials for HLW/Spent Fuel Disposal Containers. Forschungszentrum Karlsruhe, FZKA 6706, Karlsruhe, 2002.

/SMA 95/ Smailos, E.; Gago, J.A.; Azkarate, I.; Fieh, B.: Corrosion Studies on Selected Packaging Materials for Disposal of Heat-Generating Radioactive Wastes in Rock-Salt Formations. Forschungszentrum Karlsruhe, FZKA 5587, Karlsruhe, 1995.

/SMA 99/ Smailos, E.; Martínez-Esparanza, A.; Kursten, B.; Marx, G.; Azkarate, I.: Corrosion evaluation of metallic materials for long-lived HLW/spent fuel disposal containers. EUR 19112, European Commission, Luxemburg, 1999.

/SMI 93/ Smith, H. D., Baldwin, D. L.: An investigation of thermal release of carbon-14 from PWR Zircaloy spent fuel cladding. Journal of Nuclear Materials 200, pp.128-137, 1993.

/STO 85/ Storck, R.; Hossain, S.; Podtschaske, T.; Rimkus, D.; Stelte, N.; Weber, P.: Einzeluntersuchungen zur Radionuklidfreisetzung aus einem Modellsalzstock. Projekt Sicherheitsstudien Entsorgung (PSE), Abschlussbericht: Fachband 15, Hahn-Meitner Institut, Berlin, 1985.

/TAN 09/ Tanabe, H.; Nishimura, T.; Kaneko, M.; Sakuragi, T.; Nasu, Y.; Asano, H.: Characterisation of Hull Waste in Underground Condition. in: Mobile Fission and Activation Products in Nuclear Waste Disposal. pp. 207-220, NEA-6310, OECD Nuclear Energy Agency, Issy-les-Moulineaux, 2009.

/TEC 08/ Überprüfung und Bewertung des Instrumentariums für eine sicherheitliche Bewertung von Endlagern für HAW – ISIBEL. Gemeinsamer Bericht von DBE TECHNOLOGY GmbH, BGR und GRS. DBE TECHNOLOGY GmbH Peine, April 2008.

/TER 05/ Ter Heege, J.H.; De Bresser, J.H.P.; Spiers, C.J.: Rheological behaviour of synthetic rocksalt: the interplay between water, dynamic recrystallization and deformation mechanisms. Journal of Structural Geology 27, pp. 948–963, 2005.

/UPC 10/ Universitat Politéchnica de Catalunya CODE_BRIGHT User's guide 2010. *(https://www.etcg.upc.edu/recerca/webs/code_bright, Oct. 01. 2012).*

/URA 86/ Urai, J.L.; Spiers, C.J.; Zwart, H.J.; Lister, G.S.: Weakening of rock salt by water during long-term creep. Nature, 324, pp. 554-557, 1986.

/WAT 02/ Watanabe, T.; Peach, C. J.: Electrical impedance measurement of plastically deforming halite rocks at 125 °C and 50 MPa. Journal of Geophysical Research 107, pp. ECV 2-1–2-12, 2002.

/YAM 99/ Yamaguchi, I.; Tanuma, S.; Yasutomi, I.; Nakayama, T.; Tanabe, H.; Katsurai, K.; Kawamura, W.; Maeda, K.; Katao, H.; Saigusa, M.: A study on chemical forms and migration behaviour of radionuclides in hull wastes. ICEM '99 Conference Proceedings, Nagoya, Japan, 1999.

Additional references of relevance about brine migration in rock salt formations which are not cited in the text

Bradshaw, R. L.; Sanchez,F.: Migration of Brine Cavities in Rock Salt Journal of Geophysical Research, Vol. 74(17), pp. 4209 – 4212, 1969.

Cline, H.E.; Anthony, T.R.: Vaporization of liquid inclusions in solids. The philosophical magazine, Vol. 24(192), pp. 1483 –1494, 1971.

Cheung, H.; Fuller, N.E.; Gaffney, E.S.: Modeling of Brine Migration in Halite. International Symposium on Scientific Basis for Nuclear Waste Management, November 27-30, 1979, Boston, Material Research Society, proc. Symp.

Ewing, R.I.: Test of a Radiant Heater in the Avery Island Salt Mine. Sandia National Labatories, SAND81-1305, Albuquerque, 1981.

Ewing, R.I.: Preliminary Moisture Release Experiment in a Potash Mine in Southeastern New Mexico. Sandia National Labatories, SAND81-1318, Albuquerque, 1981.

Gnirk, P.S.; Krause, W.B.; Fossum, A.S.: State-of-the-Art Review of Brine Migration Studies in Salt. Sandia National Labatories, SAND81-7054, Albuquerque, 1981.

Holdoway, K.A.: Behavior of fluid inclusions in salt during heating and irradiation. In: Coogan, A.H. (ed.), 4th Symp. Salt. N. Ohio Geol. Soc., Cleveland, Vol. 1, pp. 303–312, 1974.

Hohlfelder, J.J.; Beattie, A.G.; Shefelbine, H.C.: Water Release and Mechanical Failure in Heated Geologic Salt. Sandia National Labatories, SAND81-1488, Albuquerque, 1981.

Jenks, G.H.; Claiborne, H.C.: Brine Migration in Salt and Its Implications in the Geologic Disposal of Nuclear Waste. ORNL-5818, Oak Ridge National Laboratory, Oak Ridge, 1981.

Mikhailov, M.D.: Exact solution of temperature and moisture distributions in a porous half-space with moving evaporation front. International Journal of Heat and Mass Transfer, 18/6, pp. 797-804, 1975.

Müller, E.: The migration of gas-filled brine inclusions in rock salt under a temperature gradient. Crystal Research and Technology, 20, pp. 521–526, 1985.

Neltrup, H.: Heat Gradient Induced Migration of Brine Inclusions in Rock Salt – Mathematical Treatment. Risø-M-2260, Risø National Laboratory,.Roskilde, 1980.

Nikitin, A.N.; Pocheptsova, O.A.; Matthies, S.: Aspects of the Thermal and Transport Properties of Crystalline Salt in Designing Radioactive Waste Storages in Halogen Formations. Crystallography Reports, 2010, Vol. 55, No. 3, pp. 450–457, 2010.

Novak, E.J.; McTigue, D.F.: Interim Results of Brine Transport Studies in the Waste Isolation Pilot Plant (WIPP). Sandia National Labatories, SAND87-0880, Albuquerque, 1987.

Roedder, E.: Composition of fluid inclusions. U.S. Geol. Surv., Prof. Pap. 440JJ, p. 164, 1972.

Roedder, E. and Belkin, H.E.: Migration of fluid inclusions in polycrystalline salt under thermal gradients in the laboratory and in Salt Block II (abst.). Proc. Natl. Waste Terminal Storage Program Information Meeting, 212, 361-363, 1980.

Roedder, E. and Belkin, H.E.: Petrographic study of fluid inclusions in salt core samples from Asse Mine, Federal Republic of Germany. U.S. Geol. Survey Open File Report 81-1128, 32 pp., 1981

Roedder, E.: The fluids in salt. American Mineralogist, 69, 413-439, 1984.

Schenk, O.; Urai, J. L.; Piazolo, S.: Structure of grain boundaries in wet, synthetic polycrystalline, statically recrystallizing halite – evidence from cryo-SEM observations. Geofluids 6, pp. 93–104, 2006.

Sherer, N.M. (ed.): Salt Repository Project – Proceedings of Salt Repository Project's Workshop on Brine Migration, University of California-Berkley, April 17-19, 1985. Pacific Northwest Laboratory, PNL/SRP-SA-14341, Richland, 1987.

Wilcox, W. R.: Removing Inclusions From Crystals by Gradient Techniques. Industrial and Engineering Chemistry, Vol 60, No. 3, pp. 13 – 23, 1968.

List of Figures

List of Tables

A. Appendices

A.1 LOPOS simulation of brine inflow into a repository mine

Since the availability of water is crucial for the corrosion process, the inflow of water in from the overburden to a waste repository in salt is estimated in the following using the LOPOS code. The simulation was carried out along the lines used for the VerSi project /RUE 10a/ and is briefly described in the following.
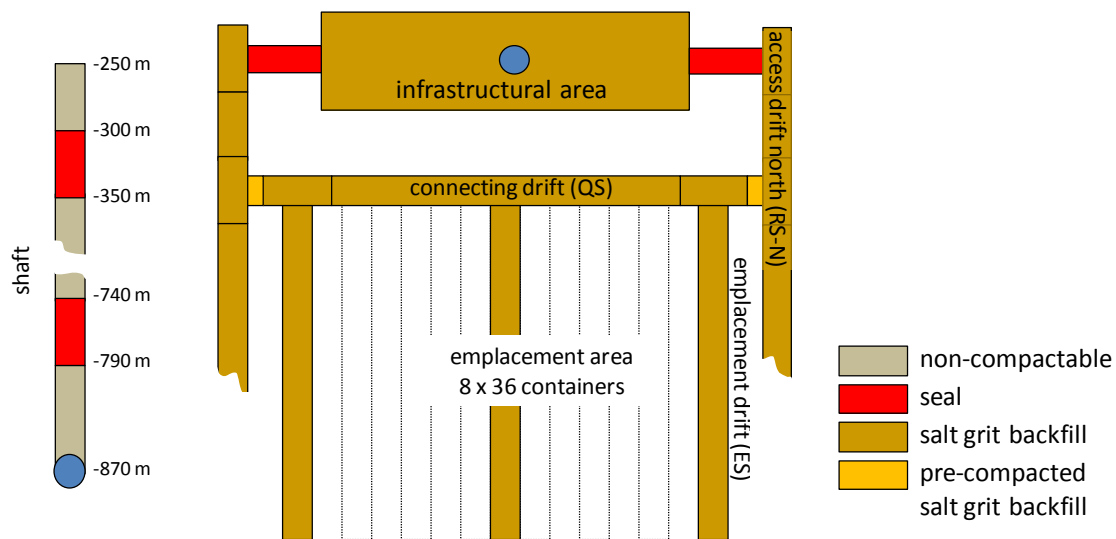
Fig. A.1   Repository layout for the modelling of the water inflow (not to scale)

Figure A.1 shows the model of the repository and its segmentation used for the modelling of the water inflow. It consists of a shaft including two shaft seals, each 50 m in length, an infrastructural area with a volume of 120 000 m^3, two access drifts and an emplacement area that includes a connecting drift and the emplacement drifts. Two drift seals of 50 m length separate the emplacement area from the infrastructural area. All drifts and the infrastructural area are assumed to be backfilled with salt grit[52] whose initial porosity of 35 % is lowered by compaction[53] until its final porosity of is reached. Immediately after repository closure, the infrastructural area holds 1 000 m^3 of solution

---

[52] One variant also accounts for non-compactible backfill in the infrastructural area.

[53] The permeability of the salt grit is assumed to be in accordance to the PSE-law /STO 85/ for the porosity-permeability dependence, with an exponent of 4.5 and a prefactor of $2 \cdot 10^{-9}$ m^2.

which is assumed to come from fluid deposits in the anhydrite. Additional fluid is intruding through the shaft at a slow rate according to the permeability of the shaft seals. Simultaneously, the fluid flows from the infrastructural area to the emplacement area. As long as the infrastructural area and the shaft are not completely filled with brine, this flow is only driven by the low hydraulic gradient of the fluid height in the infrastructural area and therefore the flow is nearly zero. The modelling is performed using realistic parameters and models given in /RUE 10a/. The essential input data of the simulation is given in table A.2. Two-phase flow mechanisms could not be modelled using the LOPOS code at the time of writing. Therefore, the impediment to the brine inflow by the gas pressure or gas outflow has not been regarded. However, two-phase flow simulations presented in chapter 0 show that this influence of the gas flow on the fluid flow is most probably not relevant as long as there is no gas production.

The most important parameter regarding the brine inflow is the minimal porosity of the salt grit backfill that can be reached by compaction. This porosity determines the long-term flow resistance of the backfill. It has to be noted that the behaviour of salt grit at low porosities is uncertain. The existence of a final porosity, where the convergence stops, clearly is a model assumption because of a lack of knowledge. Therefore, four different cases have been calculated to study the bandwidth of results. The minimal porosity of the salt grit assumed and the corresponding permeability are listed for all four cases in table A.1. The value for the permeability of the seals was set to the same value as the final permeability of the salt grit. In the fourth test case, the backfill of the infrastructural area has been regarded as a non-compactable material like gravel instead of salt-grit as in the other cases.

Tab. A.1   Simulation cases for water inflow calculation

Case	Model parameter		Calculated result	
	Minimal porosity of salt grit [%]	Corresponding permeability [m^2]	First inflow to emplacement drift [a]	Inflow to emplacement drift >0.5 l/a [a]
1	1	$2 \cdot 10^{-18}$	4 700	37 000
2	0.875	$1 \cdot 10^{-18}$	8 500	80 000
3	0.735	$5 \cdot 10^{-19}$	14 600	160 000
4	1	$2 \cdot 10^{-18}$	440 000	450 000
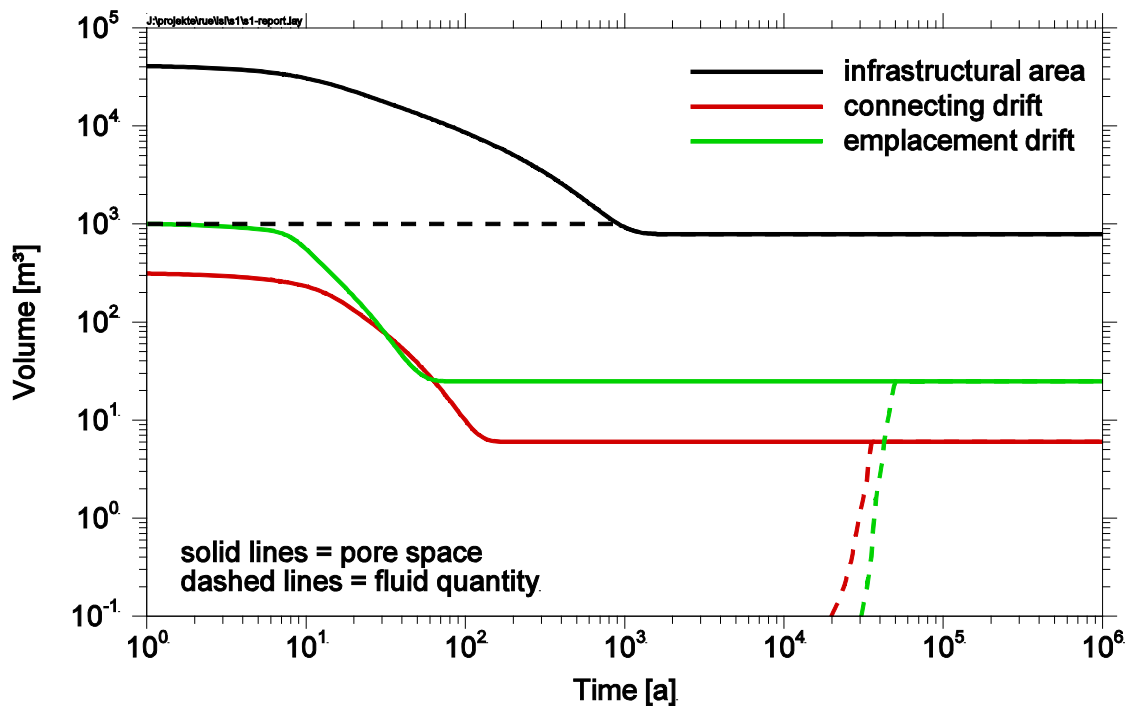
Fig. A.2 Temporal evolution of the volumes of the pore space and fluid for case 1

The result of the simulation for case 1 is plotted in figure A.2. There are 1 000 m^3 of solution in the infrastructural area from the beginning and about 0.2 m^3 are additionally flowing into the repository per year through the shaft. The inflow and the reduction of the pore space in the infrastructural area lead to its complete filling after about 900 years. After about 4 400 years, all pore space outside the drift seals is completely filled with fluid, including the shaft. The inflow rate to one of the emplacement drifts (ES-1S) versus time is plotted in figure A.3. For the case 1, the first inflow to the emplacement drift occurs after 4 700 years, but the flow rate is still extremely low. The inflow rate increases to $5 \cdot 10^{-4}$ m$^3 \cdot$a^{-1} after 37 000 years which is sufficient to provide the amount of water needed for the corrosion rate of one Pollux container per emplacement drift. The inflow rate increases to a maximum rate of $3.7 \cdot 10^{-3}$ m$^3 \cdot$a^{-1} after about 49 000 years shortly before the emplacement drift is completely filled[54]. This inflow rate would be sufficient to provide the water for the simultaneous corrosion of 7 containers per emplacement drift or for fewer containers at a higher corrosion rate.

---

[54] The consumption of water by the corrosion process is not regarded in the LOPOS calculation. Therefore, no further inflow to the emplacement drift occurs after the emplacement drift is filled and the curve ends at that point in time. Also not considered is the reduction in pore space due to the larger specific volume of the corrosion products.
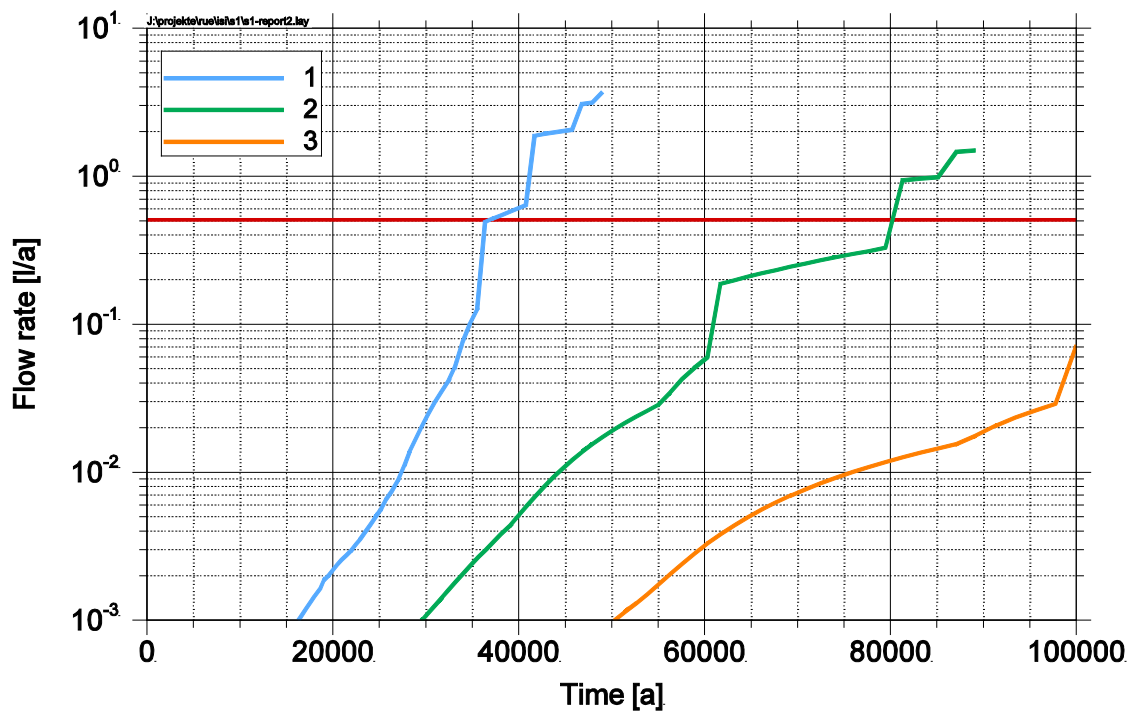
Fig. A.3   Inflow into the emplacement drift ES-1S for simulation cases 1 to 3

From these calculations it can be concluded that the corrosion of the container due to inflow of external waters does not effectively start before some 10 000 years. If NaCl-brine can be assumed and no pitting corrosion occurs, the corrosion takes about another 30 000 years until the first container fails. At least eight containers are expected to be corroded simultaneously (one for each emplacement drift), but due to the low inflow rate, a maximum of 56 containers is expected to be corroded at once (7 in each emplacement drift).

No principal difference is expected in the described behaviour if borehole disposal would be regarded as disposal option. A principal difference is only expected, for the case that borehole seals will be installed which can reliably prevent the intrusion of the water from the drifts into the subjacent boreholes. If not, container corrosion and gas production is expected to proceed in a similar way as described.

It has to be noted that the presented simulations are generic and primarily of illustrative character. Obviously, the bandwidth of the expected time until the first contact of the waste containers with external water is huge and very concept specific. Nevertheless, even for a very late contact of external waters with the waste containers, some corrosion and gas production will occur from contact with water coming from the host rock or emplaced with the waste as shown in chapter 2.

Tab. A.2   Most important input data for the LOPOS simulation

Parameter		Value
Geometrical Data		
Length of access drifts up to first emplacement area	[m]	150
Distance of access drifts	[m]	300
Cross section of northern access drift	[m²]	27
Cross section of southern access drift	[m²]	23
Length of drift seal to infrastructure area	[m]	50
Length of connecting drifts (according an angle of 120°)	[m]	335,4
Length of seals in connecting drifts	[m]	12
Cross area of connecting drifts	[m²]	23
Volume of infrastructure area	[m³]	120 000
Depth of salt dome top	[m]	250
Depth of repository	[m]	870
Length of shaft	[m]	910
Diameter of shaft	[m]	7,5
Length of shaft seals	[m]	50
Depth of upper shaft seal top	[m]	300
Depth of lower shaft seal top	[m]	740
General data		
Depth of sweet/saltwater boundary	[m]	200
Mean rock density	[kg·m-3]	2 200
Sweetwater density	[kg·m-3]	1 000
Saltwater density	[kg·m-3]	1 200
Temperature at repository level	[K]	311
Geothermal gradient	[K·m-1]	0,018
Rock pressure at repository level	[MPa]	18,8
Fluid pressure at repository level	[MPa]	9,8
Convergence data		
Reference convergence rate	[a^{-1}]	0,01
Factor convergence rate in infrastructure area	[-]	0,05
Reference porosity	[-]	0,3
Activation energy	[K^{-1}]	6 400

Parameter		Value
Factor in porosity permeability law	[m^2]	2,0E-09
Exponent in porosity permeability law	[-]	4,5
Data for fluid flow		
Permeability drift seal	[m^2]	1,0E-19
Permeability shaft seal	[m^2]	1,0E-19
Permeability of non-compactable backfill	[m^2]	1,0E-14
Starting porosity of salt grit	[-]	0,35
Starting porosity of connecting drift seal	[-]	0,1
Amount of water in infrastructure area	[m^3]	1 000
Viscosity of saturated salt water	[Pa·s]	1,7E-03
Temperature data according to curve in figure A.4		**Curve Nr.**
Access drift next to emplacement area		3
Connecting drift		8
Emplacement drift		18
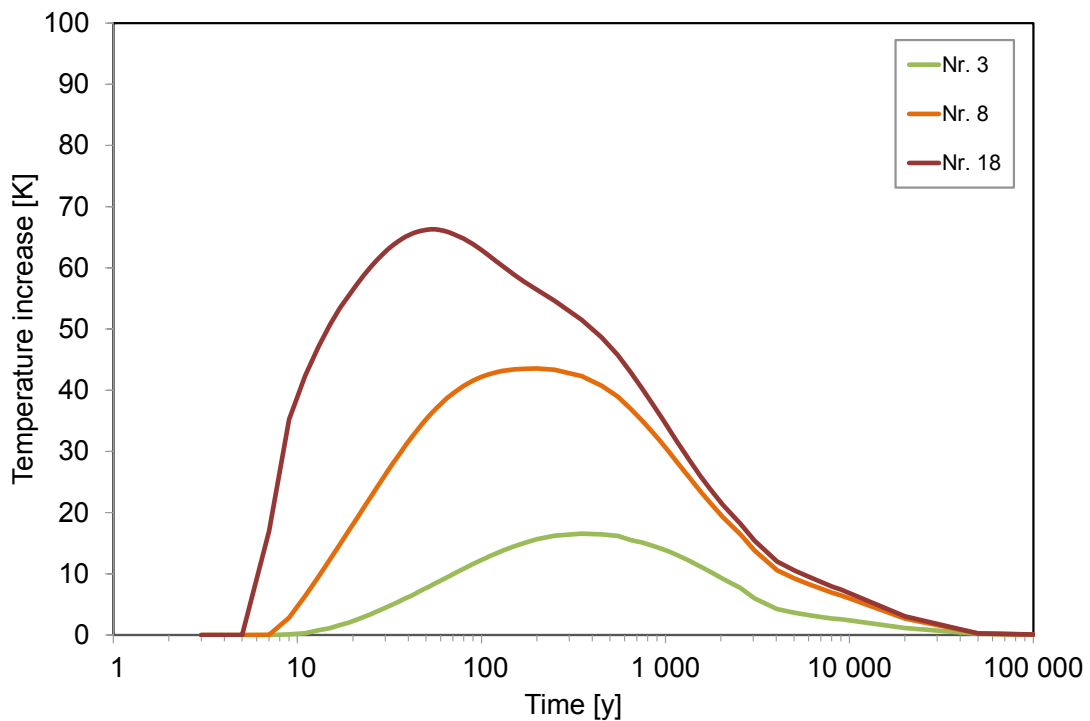
Fig. A.4   Temperature increase versus time at different repository locations

A.2   Two-phase flow model

The numerical simulations on the gas and fluid flow in the repository mine, presented in chapter 4, were carried out by applying the widely accepted van Genuchten two-phase flow theory using the numerical code TOUGH2. A very brief introduction to the theory of two phase flow is given in the following. The text is taken from the previously published report /NOS 09/.

The flow in partially saturated porous media, called two-phase flow, is a common phenomenon in soil physics and can be described by the Darcy-Buckingham equation, which extends Darcy's law for flow in saturated porous media with a term taking into account the dependence of the permeability from the saturation state

$$\mathbf{v} = -\frac{k(\theta)}{\mu}\nabla\Psi \qquad\qquad (A.1)$$

and furthermore, the equation of continuity describes the flow caused by the change in the state of saturation

$$\frac{\partial\Psi}{\partial t} = -\nabla\mathbf{v} \qquad\qquad (A.2)$$

It denotes

$\mathbf{v}$ Darcy velocity,

$k(\theta)$ permeability as a function of the water content,

θ volumetric water content, i. e. saturation,

μ dynamic viscosity and

ψ suction pressure/capillary pressure.

The crucial point in equation B.1 is the dependence of the permeability from the degree of saturation, which is usually material dependent and has to be determined from experiments. For a lot of porous media, however, curves for this dependency have been determined in soil sciences. Different theoretical models exist to parameterise the permeability as a function of the degree of saturation using a small set of model parameters. Common parameter models are the ones by Richards, Brooks-Corey and Mualem-van Genuchten.

The model used in most of the studies for two-phase flow in porous media is the one by Mualem and van Genuchten. This model describes the behaviour of the unsaturated porous media by two different functions which are given in the following according to the notation in /POT 02/. The first dependency describes the permeability of the unsaturated porous media in relation to the one of the saturated media (relative gas permeability) as a function of the saturation θ:

$$k(\theta) = k_s \left(\frac{\theta - \theta_r}{\theta_s - \theta_r} \right)^{1/2} \cdot \left(1 - \left(1 - \left(\frac{\theta - \theta_r}{\theta_s - \theta_r} \right)^{\frac{n}{n-1}} \right)^{1-\frac{1}{n}} \right)^2 \tag{A.3}$$

The second one describes the saturation θ as a function of the suction pressure ψ for the case of $\psi \geq 0$

$$\theta(\psi) = \theta_r + \frac{\theta_s - \theta_r}{\left(1 + (\alpha\psi)^n \right)^{1-\frac{1}{n}}} \tag{A.4}$$

in which denotes

θ	volumetric water content
θ_s	water content at saturation
θ_r	residual pore water saturation
k_s	permeability at saturation
α	reciprocal of the apparent gas-entry pressure
n	model parameter to be fitted on experimental data. The parameter n used in /POT 02/ depends from the parameter m used in van Genuchten's notation /GEN 80/ by $m = 1 - 1/n$.

The pore space often cannot be completely filled by water during the re-saturation (residual gas saturation). This effect is sometimes also accounted for with a parameter θ_g where $\theta_g = 1 - \theta_s$. It is usually observed that a critical gas saturation or emergence point in the pore space has to be reached before a continuous gas flow is possible. One characteristics of the model by van Genuchten is the assumption that the suction pressure is vanishing for the saturated state of the medium, i. e. in this case it is $\psi = 0$ and $\theta(\psi) = \theta_s$. As a consequence of this assumption no capillary pressure exists in this model, but small desaturation can occur already below the apparent gas-entry pressure, even if it is rather small.

A.3 Computer codes for two-phase flow simulations

The following list shows the four computer codes that were taken into consideration to perform the two-phase flow simulations presented in chapter 4. The list also gives positive (+) or negative (-) arguments which at the time of writing influenced the decision about which code was finally used:

- TOUGH2 Version 2.0 /PRU 99/:

  + Widely used in the long-term safety assessment community

  + Source code available in the IAEA code library

  + Comprehensive documentation

  − No user friendly user interface

  − No support

- CODE_BRIGHT Version 3 /UPC 10/:

  + Allows to additionally consider rock mechanics issues

  + Commercial user interface including post processing available

  + Poor numeric stability for solely two-phase flow problems, i. e. program abortion due to non converging solutions

  + Poor documentation of numerics

- HYDRUS 2D/3D /SIM 06/:

  + Code was already used in previous project /RUE 10/

  + Commercial product with support

  + Graphical interface with post processing

  + Source code not available

  + Does not allow to consider gas production

- MUFTE UG 1.0 /HEL 98/

  + Code was already used in previous project /KUE 99/

  + No user friendly user interface

  + Poor documentation.

A.4   TOUGH2 input file for simulation 1 variant b

The following listing gives the input file for the TOUGH2 module EOS7 used for the two-phase flow simulation of the investigated case 1 in variant b (see section 4.1).

```
TOUGH2 simulation case 1 variant b
ROCKS----1----*----2----*----3----*----4----*----5----*----6----*----7----*----8
Salz   3  2165.0      0.01  1.0E-19   1.0E-19   1.0E-19      2.0    1000.0
         0.0      0.0      2.0      0.0      0.0
      7            0.73     0.18      1.0     0.001
      7            0.73     0.18   2.0E-510000000.0      1.0
Rand   3  2165.0       0.5  1.0E-14   1.0E-14   1.0E-14      2.0    1000.0
         0.0      0.0      2.0      0.0      0.0
      2            1.0
      1            0.0      0.0      1.0

SELEC----1----*----2----*----3----*----4----*----5----*----6----*----7----*----8
      2




MULTI----1----*----2----*----3----*----4----*----5----*----6----*----7----*----8
      3    3    2    6

START----1----*----2----*----3----*----4----*----5----*----6----*----7----*----8

PARAM----1-MOP* 12345678901234567890l234----*----5----*----6----*----7----*----8
 8 29999        1000000100000  03 000    0
         0.0  3.15E12    100.0  3.15E10                  9.81      4.0      1.0
     1.0E-5      1.0                1.0      1.0

SOLVR----1----*----2----*----3----*----4----*----5----*----6----*----7----*----8
3  Z1   O0        0.1    1.0E-6

ELEME----1----*----2----*----3----*----4----*----5----*----6----*----7----*----8
SOU01        Salz  3.43E02      49.0      1.0    389.5     -3.5      0.0
DRI08        Salz  1.764E03     49.0      1.0    368.0     -3.5      0.0
DRI07        Salz  2.450E03     49.0      1.0    325.0     -3.5      0.0
DRI06        Salz  2.450E03     49.0      1.0    275.0     -3.5      0.0
DRI05        Salz  2.450E03     49.0      1.0    225.0     -3.5      0.0
DRI04        Salz  2.450E03     49.0      1.0    175.0     -3.5      0.0
DRI03        Salz  2.450E03     49.0      1.0    125.0     -3.5      0.0
DRI02        Salz  2.450E03     49.0      1.0     75.0     -3.5      0.0
DRI01        Salz  2.450E03     49.0      1.0     25.0     -3.5      0.0
CRO01        Salz  3.43E02      49.0      1.0     -3.5     -3.5      0.0
SHA01        Salz  3.92E03      49.0      1.0     -3.5     40.0      0.0
SHA02        Salz  2.450E03     49.0      1.0     -3.5    105.0      0.0
SHA03        Salz  1.911E04     49.0      1.0     -3.5    325.0      0.0
SHA04        Salz  2.450E03     49.0      1.0     -3.5    545.0      0.0
SHA05        Salz  1.470E03     49.0      1.0     -3.5    585.0      0.0
TOP01        Rand      0.0      49.0      1.0     -3.5    601.0      0.0

CONNE----1----*----2----*----3----*----4----*----5----*----6----*----7----*----8
CRO01DRI01              1      3.5     25.0     49.0      0.0
DRI01DRI02              1     25.0     25.0     49.0      0.0
DRI02DRI03              1     25.0     25.0     49.0      0.0
DRI03DRI04              1     25.0     25.0     49.0      0.0
DRI04DRI05              1     25.0     25.0     49.0      0.0
DRI05DRI06              1     25.0     25.0     49.0      0.0
DRI06DRI07              1     25.0     25.0     49.0      0.0
DRI07DRI08              1     25.0     25.0     49.0      0.0
DRI08SOU01              1     25.0      3.5     49.0      0.0
CRO01SHA01              2      3.5     40.0     49.0     -1.0
SHA01SHA02              2     40.0     25.0     49.0     -1.0
SHA02SHA03              2     25.0    195.0     49.0     -1.0
SHA03SHA04              2    195.0     25.0     49.0     -1.0
SHA04SHA05              2     25.0     15.0     49.0     -1.0
SHA05TOP01              2     15.0      1.0     49.0     -1.0

GENER----1----*----2----*----3----*----4----*----5----*----6----*----7----*----8
```

```
SOU01    1                  0    COM3    1.0E-8      0.0

INCON----1----*----2----*----3----*----4----*----5----*----6----*----7----*----8
SHA01
          101300.0               0.0              10.99             25.0
SHA02
          101300.0               0.0              10.99             25.0
SHA03
          101300.0               0.0              10.99             25.0
SHA04
          101300.0               0.0              10.99             25.0
SHA05
          101300.0               0.0              10.99             25.0
CRO01
          101300.0               0.0              10.99             25.0
DRI01
          101300.0               0.0              10.99             25.0
DRI02
          101300.0               0.0              10.99             25.0
DRI03
          101300.0               0.0              10.99             25.0
DRI04
          101300.0               0.0              10.99             25.0
DRI05
          101300.0               0.0              10.99             25.0
DRI06
          101300.0               0.0              10.99             25.0
DRI07
          101300.0               0.0              10.99             25.0
DRI08
          101300.0               0.0              10.99             25.0
SOU01
          101300.0               0.0              10.99             25.0
TOP01
         3000000.0               0.0               0.0             25.0

ENDCY
```

A.5   TOUGH2 input file for simulation 2 variant d

The following listing gives the input file for the TOUGH2 module EOS7 used for the two-phase flow simulation of the investigated case 2 in variant d (see section 4.2). Due to the large number of 400 segments, resulting in an input file of about 2000 lines, some lines were omitted if the pattern is obvious. The position of the omitted lines is indicated in the listing.

```
TOUGH2 simulation case 2 variant d
ROCKS----1----*----2----*----3----*----4----*----5----*----6----*----7----*----8
SG       3   2165.0      0.1  1.0E-15   1.0E-15  1.0E-15      2.0    1000.0
       0.0      0.0      2.0      0.0       0.0
       7            0.73     0.18      1.0     0.001
       7            0.73      0.1  2.0E-510000000.0      1.0
AB       3   2165.0      0.1  1.0E-18   1.0E-18  1.0E-18      2.0    1000.0
       0.0      0.0      2.0      0.0       0.0
       7            0.73     0.18      1.0     0.001
       7            0.73      0.1  2.0E-510000000.0      1.0
Rand     3   2165.0      0.1  1.0E-15   1.0E-15  1.0E-15      2.0    1000.0
       0.0      0.0      2.0      0.0       0.0
       7            0.73     0.18      1.0     0.001
       7            0.73      0.1  2.0E-510000000.0      1.0

SELEC----1----*----2----*----3----*----4----*----5----*----6----*----7----*----8
    2



MULTI----1----*----2----*----3----*----4----*----5----*----6----*----7----*----8
    3    3    2    6
START----1----*----2----*----3----*----4----*----5----*----6----*----7----*----8

PARAM----1-MOP* 123456789012345678901234----*----5----*----6----*----7----*----8
 8 29999      100000000000001  03 000   0
       0.0  3.15E12    100.0  3.15E10                9.81      4.0       1.0
     1.0E-5      1.0                1.0      1.0

SOLVR----1----*----2----*----3----*----4----*----5----*----6----*----7----*----8
3  Z1   O0      0.1   1.0E-6
ELEME----1----*----2----*----3----*----4----*----5----*----6----*----7----*----8
     2         SG      64.0      0.0      1.0      6.0      1.0      4.0
     3         SG      64.0      0.0      1.0     10.0      1.0      4.0
     4         SG      64.0      0.0      1.0     14.0      1.0      4.0
     5         SG      64.0      0.0      1.0     18.0      1.0      4.0
     6         SG      64.0      0.0      1.0     22.0      1.0      4.0
     7         SG      64.0      0.0      1.0     26.0      1.0      4.0
     8         SG      64.0      0.0      1.0     30.0      1.0      4.0
     9         SG      64.0      0.0      1.0     34.0      1.0      4.0
    10         SG      64.0      0.0      1.0     38.0      1.0      4.0
    11         SG      64.0      0.0      1.0     42.0      1.0      4.0
    12         SG      64.0      0.0      1.0     46.0      1.0      4.0
    13         SG      64.0      0.0      1.0     50.0      1.0      4.0
    14         SG      64.0      0.0      1.0     54.0      1.0      4.0
    15         SG      64.0      0.0      1.0     58.0      1.0      4.0
    16         SG      64.0      0.0      1.0     62.0      1.0      4.0
    17         SG      64.0      0.0      1.0     66.0      1.0      4.0
    18         SG      64.0      0.0      1.0     70.0      1.0      4.0
    19         SG      64.0      0.0      1.0     74.0      1.0      4.0
    20         SG      64.0      0.0      1.0     78.0      1.0      4.0

: following 70 lines omitted

    91         SG      64.0      0.0      1.0    362.0      1.0      4.0
    92         SG      64.0      0.0      1.0    366.0      1.0      4.0
    93         SG      64.0      0.0      1.0    370.0      1.0      4.0
    94         SG      64.0      0.0      1.0    374.0      1.0      4.0
```

95	SG	64.0	0.0	1.0	378.0	1.0	4.0
96	SG	64.0	0.0	1.0	382.0	1.0	4.0
97	SG	64.0	0.0	1.0	386.0	1.0	4.0
98	SG	64.0	0.0	1.0	390.0	1.0	4.0
99	SG	64.0	0.0	1.0	394.0	1.0	4.0
100	SG	64.0	0.0	1.0	398.0	1.0	4.0
102	SG	64.0	0.0	1.0	6.0	3.0	4.0
103	SG	64.0	0.0	1.0	10.0	3.0	4.0
104	SG	64.0	0.0	1.0	14.0	3.0	4.0
105	SG	64.0	0.0	1.0	18.0	3.0	4.0
106	SG	64.0	0.0	1.0	22.0	3.0	4.0

⋮ following 282 lines omitted

390	SG	64.0	0.0	1.0	358.0	7.0	4.0
391	SG	64.0	0.0	1.0	362.0	7.0	4.0
392	SG	64.0	0.0	1.0	366.0	7.0	4.0
393	SG	64.0	0.0	1.0	370.0	7.0	4.0
394	SG	64.0	0.0	1.0	374.0	7.0	4.0
395	SG	64.0	0.0	1.0	378.0	7.0	4.0
396	SG	64.0	0.0	1.0	382.0	7.0	4.0
397	SG	64.0	0.0	1.0	386.0	7.0	4.0
398	SG	64.0	0.0	1.0	390.0	7.0	4.0
399	SG	64.0	0.0	1.0	394.0	7.0	4.0
400	SG	64.0	0.0	1.0	398.0	7.0	4.0
1	Rand	0.0	0.0		2.0	1.0	4.0
101	Rand	0.0	0.0		2.0	3.0	4.0
201	Rand	0.0	0.0		2.0	5.0	4.0
301	Rand	0.0	0.0		2.0	7.0	4.0

CONNE----1----*----2----*----3----*----4----*----5----*----6----*----7----*----8						
1	2	1	2.0	2.0	16.0	0.0
2	3	1	2.0	2.0	16.0	0.0
3	4	1	2.0	2.0	16.0	0.0
4	5	1	2.0	2.0	16.0	0.0
5	6	1	2.0	2.0	16.0	0.0
6	7	1	2.0	2.0	16.0	0.0
7	8	1	2.0	2.0	16.0	0.0
8	9	1	2.0	2.0	16.0	0.0
9	10	1	2.0	2.0	16.0	0.0
10	11	1	2.0	2.0	16.0	0.0
11	12	1	2.0	2.0	16.0	0.0
12	13	1	2.0	2.0	16.0	0.0
13	14	1	2.0	2.0	16.0	0.0
14	15	1	2.0	2.0	16.0	0.0
15	16	1	2.0	2.0	16.0	0.0
16	17	1	2.0	2.0	16.0	0.0
17	18	1	2.0	2.0	16.0	0.0
18	19	1	2.0	2.0	16.0	0.0
19	20	1	2.0	2.0	16.0	0.0
20	21	1	2.0	2.0	16.0	0.0

⋮ following 320 lines omitted

391	392	1	2.0	2.0	16.0	0.0
392	393	1	2.0	2.0	16.0	0.0
393	394	1	2.0	2.0	16.0	0.0
394	395	1	2.0	2.0	16.0	0.0
395	396	1	2.0	2.0	16.0	0.0
396	397	1	2.0	2.0	16.0	0.0
397	398	1	2.0	2.0	16.0	0.0
398	399	1	2.0	2.0	16.0	0.0
399	400	1	2.0	2.0	16.0	0.0
1	101	2	1.0	1.0	32.0	-1.0
2	102	2	1.0	1.0	32.0	-1.0
3	103	2	1.0	1.0	32.0	-1.0
4	104	2	1.0	1.0	32.0	-1.0
5	105	2	1.0	1.0	32.0	-1.0
6	106	2	1.0	1.0	32.0	-1.0
7	107	2	1.0	1.0	32.0	-1.0
8	108	2	1.0	1.0	32.0	-1.0
9	109	2	1.0	1.0	32.0	-1.0
10	110	2	1.0	1.0	32.0	-1.0

⋮ following 280 lines omitted

```
290  390                          2     1.0     1.0     32.0    -1.0
291  391                          2     1.0     1.0     32.0    -1.0
292  392                          2     1.0     1.0     32.0    -1.0
293  393                          2     1.0     1.0     32.0    -1.0
294  394                          2     1.0     1.0     32.0    -1.0
295  395                          2     1.0     1.0     32.0    -1.0
296  396                          2     1.0     1.0     32.0    -1.0
297  397                          2     1.0     1.0     32.0    -1.0
298  398                          2     1.0     1.0     32.0    -1.0
299  399                          2     1.0     1.0     32.0    -1.0
300  400                          2     1.0     1.0     32.0    -1.0

GENER----1----*----2----*----3----*----4----*----5----*----6----*----7----*----8
  1 0    1                0    COM3   1.0E-8      0.0

INCON----1----*----2----*----3----*----4----*----5----*----6----*----7----*----8
     1
           9000000.0               0.0               0.0             25.0
     2
            101300.0               0.0             10.99             25.0
     3
            101300.0               0.0             10.99             25.0
     4
            101300.0               0.0             10.99             25.0
     5
            101300.0               0.0             10.99             25.0
     6
            101300.0               0.0             10.99             25.0
     7
            101300.0               0.0             10.99             25.0
     8
            101300.0               0.0             10.99             25.0
     9
            101300.0               0.0             10.99             25.0
    10
            101300.0               0.0             10.99             25.0

⋮ following 178 lines for 89 segments omitted

   100
            101300.0               0.0             10.99             25.0
   101
           9000000.0               0.0               0.0             25.0
   101
            101300.0               0.0             10.99             25.0

⋮ following 574 lines for 287 segments omitted

   390
            101300.0               0.0             10.99             25.0
   391
            101300.0               0.0             10.99             25.0
   392
            101300.0               0.0             10.99             25.0
   393
            101300.0               0.0             10.99             25.0
   394
            101300.0               0.0             10.99             25.0
   395
            101300.0               0.0             10.99             25.0
   396
            101300.0               0.0             10.99             25.0
   397
            101300.0               0.0             10.99             25.0
   398
            101300.0               0.0             10.99             25.0
   399
            101300.0               0.0             10.99             25.0
   400
            101300.0               0.0             10.99             25.0

ENDCY
```